Production of mannooligosaccharides from pineapple pulp and pine sawdust using *Aspergillus niger* derived Man26A and determination of their prebiotic effect

A thesis submitted in fulfilment of the requirements for the degree of

Master of Science

in

Biochemistry

at

Rhodes University

By

Nosipho Hlalukana

ORCID: 0000-0001-9273-1537

May 2022

Supervisor: Prof. B.I. Pletschke

Co-supervisor: Dr. S. Malgas

Abstract

Lignocellulosic biomass is the most abundant source of renewable biomass on earth. Lignocellulosic biomass consists of cellulose, hemicelluloses and lignin. These can be used as a source of renewable fuel as well as other value-added products . Mannans are part of the hemicellulose fraction of lignocellulosic biomass and are the major hemicellulosic polysaccharide fraction in softwoods, where they are found as galactoglucomannans and as glucomannans. Mannans are also found in hardwoods in the form of glucomannans. Mannans can be enzymatically hydrolysed using endo-mannanases to produce of short chain mannooligosaccharides (MOS). MOS have received significant attention for their prebiotic properties, as they promote the growth of probiotic bacteria, which have positively affects on gut health. This study focused on the production of prebiotic MOS from lignocellulosic biomass waste (LBW) and an evaluation of the prebiotic potential of the produced MOS.

An *Aspergillus niger* derived endo-mannanase, Man26A, was fractionated and biochemically analysed. Purified Man26A had a fold purification of 1.25 and a yield of 41.1%. SDS-PAGE analysis of the enzyme revealed that it had a molecular weight of 46 kDa. The pH and temperature optima of Man26A were determined and the pH optimum was found to be pH 4.0 (but the enzyme displayed high activity over a broad acidic pH range, with up to 90% of the activity retained between pH 3.0 and 7.0). The temperature optimum was 50°C. The enzyme was shown to have the highest specific activity on locust bean gum (52.27 U/mg) and ivory nut mannan (57.25 U/mg), compared to guar gum (29.07 U/mg), which indicated that it was affected by the substitution pattern of the mannans. Man26A produced MOS of different diversity on model mannan substrates, where the MOS produced were mannobiose, mannotriose, and mannotetraose for ivory nut mannan, mannobiose, mannotriose, mannotetraose, and mannopentaose and MOS with a higher degree of polymerisation for locust bean gum, and mannobiose, mannotriose, mannotetraose, mannopentaose, and mannohexose and MOS with a higher degree of polymerisation for guar gum, as determined by thin layer chromatography (TLC) and high-performance liquid chromatography (HPLC).

Pretreatment and characterisation of pineapple pulp (PP) and pine sawdust (PSD) was conducted, and the impact of the pretreatment procedures was analysed using Megazyme sugar kits, thermogravimetric analysis (TGA), Fourier-transform infrared spectroscopy (FTIR), and microscopic analysis using scanning electron microscopy (SEM) and light microscopy. Compositional analysis of the carbohydrates present in both substrates revealed that they had

a glucan content of 36.41 and 50.47% for untreated PP and PSD, respectively. Their respective mannan content was 6.74 and 11.59% and was deemed sufficient for the production of MOS via enzymatic hydrolysis. TGA analysis revealed that untreated and sodium chlorite-acetic acid delignified samples decomposed at approximately the same time, and had a negligible ash content at 600°C, while delignified plus phosphoric acid swollen substrates decomposed at a faster rate, but had a residual ash content at 600°C. FTIR analysis of the substrates revealed slight changes in the structures of untreated and pretreated samples. SEM analysis of PP and PSD showed a change in the morphology of the substrates with subsequent pretreatment steps. Histochemical analysis for lignin for PP and PSD showed successful delignification upon pretreatment. Untreated and sodium chlorite delignified PP and PSD released low amounts of reducing sugars compared to delignified + phosphoric acid swollen substrates. The delignified + phosphoric acid swollen substrates were used for further experiments.

MOS produced from delignified and phosphoric acid swollen (Del + PAS) PP and PSD at 0.1 mg/ml enzyme loading and 80 mg/ml (8% (w/v)) substrate concentration, ran between mannose and mannobiose and between mannobiose and manotriose on TLC, with low concentrations of MOS running between mannotetraose and mannopentaose. HPLC analysis of the MOS revealed that Del + PAS PP produced mannose to mannohexose, while Del + PAS PSD produced mannose, mannobiose, and mannotetraose. The MOS were analysed using FTIR, to determine whether the MOS produced contained any acetyl groups, which were present for Del + PAS PSD at 1706 cm^{-1}. The MOS were stable at different pHs, and at temperatures below 200°C. The MOS were also found to be stable in a simulated gastrointestinal environment, in the presence of bile salts and digestive enzymes.

The prebiotic effect of the MOS derived from Del + PAS PP and PSD was evaluated. MOS had a proliferative effect on probiotic bacteria (*Lactobacillus bulgaricus*, *Bacillus subtilis* and *Streptococcus thermophilus*). The production of short chain fatty acids (SCFAs) was evaluated on TLC, where no SCFAs were observed on the plate. The effect of MOS on the adhesion ability of bacteria revealed that they do not positively influence the adhesion of probiotic bacteria. The antioxidant activities of 1 mg/ml MOS produced from both substrates were determined to be approximately 15% using the ABTS radical scavenging assay, compared to a radical scavenging activity of 45% for the 0.02 mg/ml gallic acid standard. This study demonstrated that biomass waste could be used to produce prebiotic MOS, which play a positive role in gut ecology and provide health benefits.

Table of Contents

List of Figures

List of Tables

List of abbreviations

°C	Degree Celsius
ABTS	2,2-azinobis-(3-ethylbenzothiazoline-6-sulfonate)
BSA	Bovine serum albumin
DNS	3,5-Dinitrosalicylic acid
DPPH	1,1-diphenyl-2-picrylhydrazyl
DTG	Derivative Thermogravimetry
EC	Enzyme Commission number
FTIR	Fourier-transform infrared spectroscopy
g	Gram
g	Gravity
G	α-galactosyl-mannose
GG	Guar gum
GH	Glycoside hydrolase
h	Hour
HPLC	High performance liquid chromatography
INM	Ivory nut mannan
kDa	Kilo Daltons
KG	Konjac gum
l	Litre
LB	Lignocellulosic biomass
LBG	Locust bean gum
LBW	Lignocellulosic biomass waste
Man26A	Mannanase 26A

mg	Milligram
MG	α-6^1-galactosyl-mannobiose
MGG	α-6^2-6^1-di-galactosyl-mannotriose
MGGM	α-^{63}-6^2-di-galactosyl-mannotetraose
MGGMM	α-6^4-6^3-di-galactosyl-mannopentaose
MGMM	α-6^3-galactosyl-mannotetraose
min	Minute
ml	Millilitre
mM	Millimolar
MMG	α-6^1-galactosyl-mannotriose
NDO	Non-digestible oligosaccharide
nm	Nanometer
OD	Optical density
PP	Pineapple pulp
PSD	Pine sawdust
SD	Standard deviation
SDS	Sodium dodecyl sulphate
SDS-PAGE	Sodium dodecyl sulphate polyacrylamide gel electrophoresis
TEMED	N, N, N', N'-tetramethylethylenediamine
TGA	Thermogravimetric analysis
U	Units of enzyme activity
v	Volume
VAP	Value added product
w	Weight

µg	Microgram
µl	Microlitre
µM	Micromolar
µmol	Micromole

List of research outputs

Publications in peer-reviewed journals

i. Magengelele, M., Hlalukana, N., Malgas, S., Rose, S., Van Zyl, W.E., and Pletschke, B. (2021). Production and *in vitro* evaluation of prebiotic mannooligosaccharides prepared with a recombinant *Aspergillus niger* endo-mannanase, Man26A. *Enzyme and Microbial Technology*. 150, 109893.

ii. Hlalukana, N., Magengelele, M., Malgas, S., Pletschke, B. (2021). Enzymatic conversion of mannan-rich plant waste biomass into prebiotic mannooligosaccharides. *Foods*. 10(9), 2010.

Acknowledgements

I would like to take this opportunity to thank the following people:

Prof. B.I. Pletschke, my supervisor, for affording me the opportunity to undertake this research, for your patience and enthusiasm. I will surely miss your “dad jokes”.

Dr. S. Malgas, my co-supervisor. Your mentorship throughout this project is greatly appreciated.

The members of ESP-Bioproducts. Thank you to Mihle Magengelele for crawling so that I may be able to run. Tariro Sithole, for availing the “social corner” and for always being a great sounding board. To Chantal Daub, one of the kindest people I have ever met. From our days as Honours students being afraid to talk in the lab, to finding our feet together, nice times. To Blessing Mabathe, Lithalethu Mkabayi, and Lebogang Ramatsui for your valuable input. To Happyness Mzimkhulu-Ncoyi for the conversations in the lab. Thank you to everyone for always being ready to listen. I cannot imagine being part of a better group.

Thank you to the Biochemistry and Microbiology Department.

I would like to thank my family for their continued support, especially in the past year. I would not have made it this far without it. Thank you especially to my parents, T. Mjwara and M. Hlalukana, my sister Lindiwe Mjwara, my aunt Mrs N. Shabalala, and to the whole Hlalukana clan (nibaningi). I love you guys very much.

To my friends, thank you all for being there for me. Special mention to Khanyisile Ngcongco, the Robin to my Batman, Jonathan to my David. I found a sister in you and will forever cherish your presence in my life. Akhona Ngqinambi, it always amazes me when I look back and see how much we have grown from the first time we met. Thank you for your wisdom that you always readily share. I love you two so much.

And finally, I would like to thank the National Research Foundation (NRF) and the Council for Scientific and Industrial Research (CSIR) for funding my research project.

Chapter 1: General introduction and literature review

1.1. Introduction

A large portion of the world's economy is derived from unsustainable practices, most of which rely on non-renewable resources (Khan et al., 2015). Over the past few years, there has been a growing interest in developing sustainable economic practices that have minimal impact on the environment (Yamabhai et al., 2014). Fossil fuels have been used to the detriment of the environment for many years, but recent developments have focused on using renewable energy sources to drive economic outputs (Duque-Acevedo et al., 2020; Khan et al., 2015). An economy that relies onrenewable resources for development is known as a bioeconomy, a termcoined by the Biomass Research and Development Board in 2001 (Duque-Acevedo et al., 2020; Khan et al., 2015). The agricultural, forestry, and food processing industries are some of the major role players in the bioeconomy (Khan et al., 2015). The South African bioeconomy concept is based on using biotechnological processes for the production of large-scale industrial outputs, which will lead to increased economic outputs that will enable South Africa to compete in the global market (Khan et al., 2015; DST, 2013).

Identifying and quantifying useful starting materials for generating value-added products from renewable resources is the first step. Waste materials are generated in large quantities from agricultural and forestry activities (Van Dyk et al., 2013), and these hold promise for use as precursors of value-added products synthesis. South Africa is one of the leading countries in producing ozone depleting substances, such as methane and CO_2, mainly due to the fossil fuels that are burnt for energy production, but also due to burning of waste in landfills (Ugwu and Enweremadu, 2020). Lignocellulosic biomass waste (LBW) encompasses agricultural and forestry residues, fruit processing waste and waste from processing from other food residues (Cho et al., 2020). There is increasing interest in using biomass as a starting material for value-added products, which provides a solution to the pollution problem caused by biomass. The carbohydrate and non-carbohydrate fractions of LBW can potentially be converted into commercial products (Cho et al., 2020). Processes such as the enzymatic degradation of cellulose can be used to produce fermentable sugars for the production of bioethanol (Haq et al., 2021; Rezania et al., 2020; Bååth et al., 2018). There has also been an increasing interest in the beneficiation of the hemicellulosic fraction to produce beneficial oligosaccharides that have been shown to be important for animal health, due to their beneficial effects on the

intestinal microflora (Cano et al., 2020; Gutierrez-Macias et al., 2017). These hemicellulose-derived oligosaccharides find applications in animal husbandry and in aquaculture (Bååth et al., 2018).

1.2. Lignocellulosic biomass

Lignocellulose is the most abundant biomass available on the planet - it consists of cellulose, hemicellulose and lignin, that are in close association (Dahmen et al., 2018; Sathitsuksanoh et al., 2012; Moreira and Filho, 2008). Cellulose makes up most of the lignocellulosic component, consisting of approximately 40–55% dry weight. On the other hand, the hemicellulosic component comprises approximately 20–40% of biomass in dry weight and varies between softwoods and hardwoods, with hardwoods having a higher xylan content and softwoods having a higher mannan content (Dahmen et al., 2018; Malgas et al., 2015b; Otieno and Ahring, 2012). Lignocellulose holds great potential for producing several commodities, such as fuels, feedstocks and other value-added chemicals (Moreira and Filho, 2008).

Lignocellulosic biomass waste (LBW) offers an attractive option for producing value-added products, because of its abundance, renewability and low cost (Otieno and Ahring, 2012). Using LBW to produce value-added products is also attractive because its usage does not affect food security, nor does it interfere with other industries (Ahorsu et al., 2018). The sugars obtained from the cellulosic and hemicellulosic fractions can be used as precursors for replacing of fossil fuels and food-based feedstocks (Rusanen et al., 2019). LBW can be obtained from forestry and agricultural residues, municipal waste and grasses (Zhu et al., 2009). Currently, in South Africa, food wastes are disposed of in landfills, which increases pollution and contributes to the emission of ozone depleting gases, such as methane (Ugwu and Enweremadu, 2020). It is estimated that one third of the food produced per annum goes to waste, and only approximately 10% of it is recycled (Ugwu and Enweremadu, 2020).

The conversion of lignocellulosic biomass (LB) and LBW into value-added products is limited by its recalcitrance to enzymatic degradation (Rusanen et al., 2019; Sathitsuksanoh et al., 2012). Several factors influence resistance to enzymatic hydrolysis of LB, such as the presence of lignin, its particle size and cellulose crystallinity (Van Dyk et al., 2013). Pretreatment steps can overcome the recalcitrance prior to enzymatic hydrolysis (Jagtap et al., 2017; Sathitsuksanoh et al., 2012). Most pretreatment strategies used involve the removal of lignin to create holocellulose, which is more amenable to processes such as enzymatic degradation of the biomass (Álvarez et al., 2016). Delignification also affects the crystallinity of cellulose,

which makes the holocellulose more accessible to the enzymes (Álvarez et al., 2016). Pretreatment, which involves the delignification process, is depicted in Figure 1.1 below.

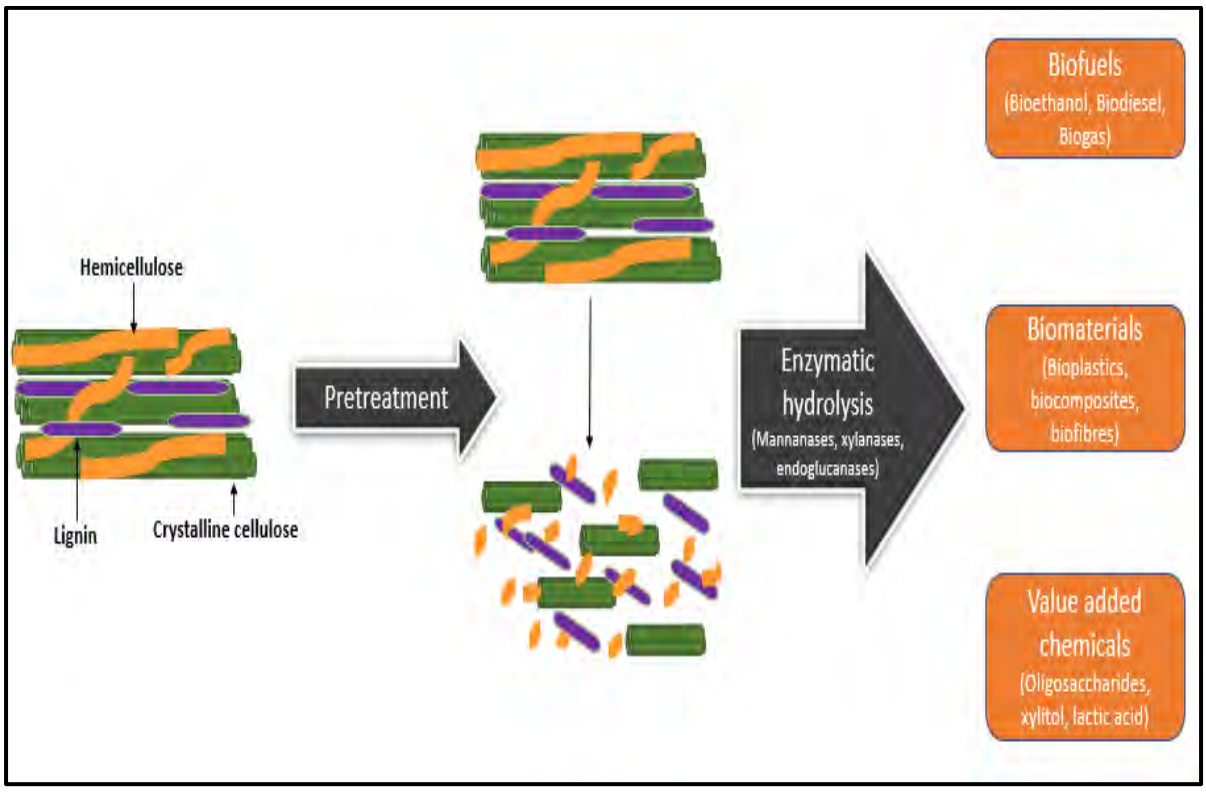

Figure 1.1: Illustrative summary of the conversion of lignocellulosic biomass waste into value-added products. Adapted from Østby et al. (2020) and Amorim et al. (2019).

Various types of pretreatment strategies exist to overcome biomass recalcitrance. The major pretreatment technologies used in large-scale industries include acid, alkaline, steam explosion, hydrothermal pretreatment, wet oxidation, and methods based on using ionic liquids and organic solvents (Østby et al., 2020). Acid hydrolysis is one of the oldest existing pretreatment methods (Østby et al., 2020). The acid hydrolysis conditions for different polymers vary because of their difference in structure (Cano et al., 2020). Some polysaccharides, like pectin, require only dilute acid pretreatment, while cellulose may require pretreatment with stronger acids due to its rigidity and crystallinity (Cano et al., 2020). Acid pretreatment has been reported to exhibit high efficiency for the removal of lignin and hemicellulose (Zhu et al., 2017). Alkali pretreatments are known to be effective in lignin removal (Moodley et al., 2020). They are non-invasive and do not cause harm to the environment (Moodley et al., 2020; Sewsynker-Sukai et al., 2020). An example of an alkali pretreatment method is sodium hydroxide (NaOH) (Moodley et al., 2020). A disadvantage of alkali pretreatments is the high cost associated with using this method (Sewsynker-Sukai et al., 2020). Steam explosion (SE)

is a more economical pretreatment method (Beig et al., 2021). SE requires temperatures ranging from 160 - 200°C and pressures ranging from 5 – 50 atm (Amin et al., 2017). Steam explosion is more effective on hardwoods and agricultural residues compared to softwoods (Amin et al., 2017). Wet oxidation uses oxygen to oxidize the biomass, with water often used to wet the biomass (Sewsynker-Sukai et al., 2020). Wet oxidation produces more inhibitory products compared to SE (Sewsynker-Sukai et al., 2020). Ionic liquid pretreatment is environmentally friendly, has high thermal stability, and does not release toxic or explosive gases (Soltanian et al., 2020; Han et al., 2020). The drawback to using ionic liquids is their high cost, long processing times, and the need for their recovery (Soltanian et al., 2020; Han et al., 2020).

1.2.1. Mannans

Mannans are plant polysaccharides that are found in the cell walls of plants. They constitute a large portion of the hemicellulosic component in plant cell walls, particularly in softwoods and specialised plant structures like seeds and vacuoles (Jana et al., 2021a; Srivastava and Kapoor, 2017; Moreira and Filho, 2008). Mannans mainly consist of mannose residues in their structural backbone, which are linked by β-1,4-glycosidic linkages (Jana and Kango, 2020). Mannans play a structural role in plant cell walls, and they also serve as storage polysaccharides in some plants as non-starch carbohydrate reserves (Jana et al., 2018; Srivastava and Kapoor, 2017; Moreira and Filho, 2008). Mannans have also been shown to play a role in plant metabolism as signalling molecules (Srivastava and Kapoor, 2017; Moreira and Filho, 2008). Based on the substitution of their backbones and backbone composition, mannans can be classified into four groups, namely linear mannan, glucomannan, galactomannan and galactoglucomannan (Malgas et al., 2015a; Moreira and Filho, 2008). A schematic representation of the different mannan types is represented in Figure 1.2 below.

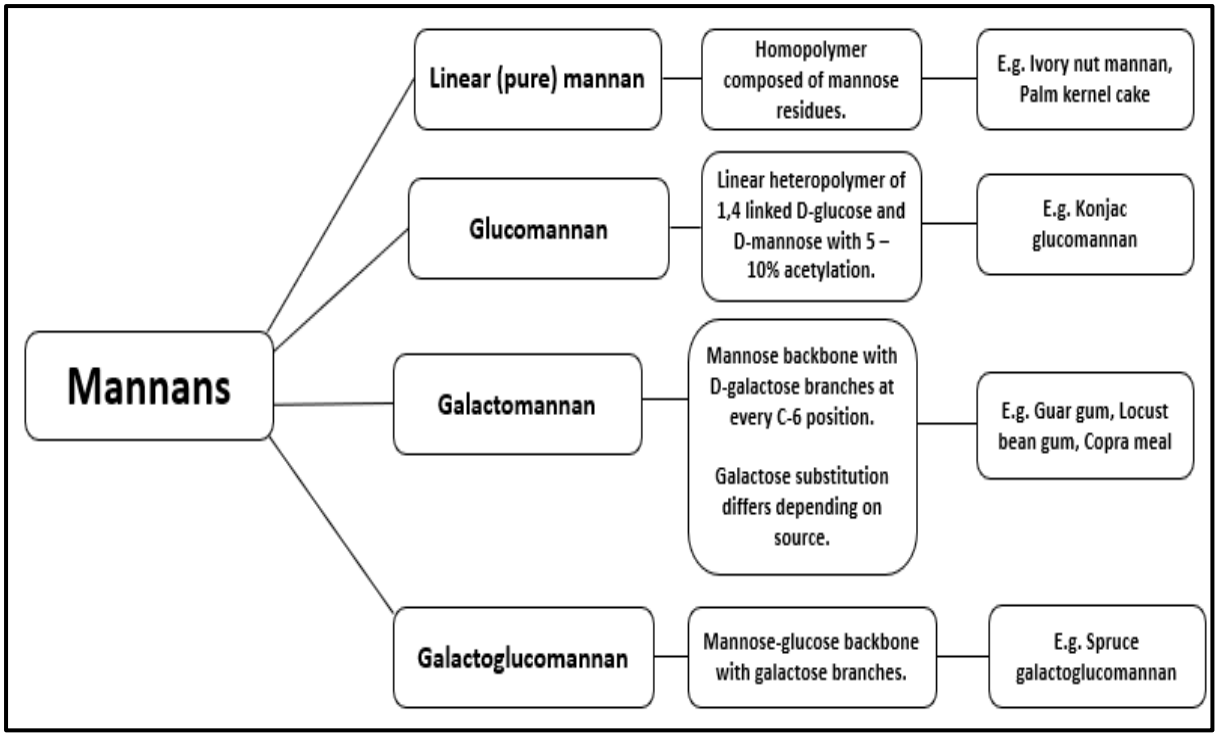

Figure 1.2: Schematic representation of the different types of mannans and examples of their sources. Adapted from Singh et al. (2018).

Linear mannan is a homopolymer that mainly consists of β-1,4-linked mannose residues. Linear mannans can be divided into either mannan I or A or mannan II or B, which is a result of a low degree (<5%) of α-1,6-galactose substitution (van Zyl et al., 2010; Moreira and Filho, 2008). Mannan A results in a polysaccharide with a degree of polymerisation (DP) of ~15, which is compressed into dense granular and crystalline structures. Mannan B is a polysaccharide with a DP of ~80 that contains microfibrils that are less dense and crystalline (van Zyl et al., 2010; Moreira and Filho, 2008). Linear mannans primarily have a structural function in plants. They are insoluble in water, which plays an important role in maintaining the structural integrity of plants (Singh et al., 2018; van Zyl et al., 2010). Examples of sources of linear mannans include ivory nut and copra meal (Yamabhai et al., 2014; van Zyl et al., 2010).

Glucomannans are linear mannans that consist of alternating β-1,4-linked mannose, which are randomly interspersed with glucose residues (Moreira and Filho, 2008). They occur inhardwood and softwood plants but are more abundant in the hardwoods (van Zyl et al., 2010). In softwoods, glucomannans often occur with a 3:1 ratio of mannose to glucose compared to hardwoods, where they occur with a 1:1.5-2 ratio (van Zyl et al., 2010; Moreira and Filho, 2008). Glucomannans in softwoods are characterised by a DP >200, while those in hardwoods

have a DP that is approximately 70 (van Zyl et al., 2010; Moreira and Filho, 2008). Glucomannans have been used commercially as gelling and thickening agents, and have also been used in the pharmaceutical industry as drug delivery agents (Yamabhai et al., 2014; An et al., 2010). An example of a glucomannan source is konjac glucomannan (KGM), which is the most widely used glucomannan (Yamabhai et al., 2014; An et al., 2010). Glucomannans can also be acetylated at the C-2, C-3, and C-6 of mannose residues (Minjares-Fuentes et al., 2018). The acetyl:mannose ratio is 1:1, and may be even higher (Minjares-Fuentes et al., 2018).

Galactomannans consist of a linear β-1,4-linked mannose backbone substituted with α-1,6-linked galactose residues at the C-6 position (Singh et al., 2018; van Zyl et al., 2010). Galactose substitution on the mannan backbone can either be ordered, randomly or block-wise, depending on the degree of substitution of the galactomannan (Malgas et al., 2015a; Jian et al., 2013). The α-1,6-linked galactose residues contribute to the higher solubility of galactomannans compared to linear mannans (van Zyl et al., 2010), which leads to them forming viscous solutions (Srivastava and Kapoor, 2017). Guar gum (GG) and locust bean gum (LBG) are considered to be the most important commercial galactomannans in food and non-food industries (Silveira and Bresolin, 2011). GG and LBG have a 2:1 and 4:1 M:G ratio, respectively (Silveira and Bresolin, 2011). They are used in the food and pharmaceutical industries as food thickeners and stabilisers, and as controlled drug release agents (Srivastava and Kapoor, 2017). Galactomannans also have applications in the cosmetic industry (Srivastava and Kapoor, 2017; Silveira and Bresolin, 2011).

Galactoglucomannan (GGM) consists of a glucomannan backbone substituted with α-1,6-linked galactose side chains (Berglund et al., 2019). GGM is the most widely available type of mannan in nature (Berglund et al., 2019; Bååth et al., 2018). The mannose residues in GGM can be acetylated at C-2 or C-3 to varying degrees, which depends on the source of the GGM (Yamabhai et al., 2014). The acetylated GGM is the major hemicellulose in softwoods and represents approximately 20% of the dry mass of woods (Bååth et al., 2018). GGM is the most complex mannan, requiring a larger repertoire of enzymes for it to be completely hydrolysed into monosaccharides (Bååth et al., 2018).

1.2.2. Mannans in lignocellulosic biomass

1.2.2.1. Pineapple waste

Pineapple (*Ananas comosus*) is a tropical plant which belongs to the family Bromeliaceae. Pineapple taste and flavour make it one of the most commercially important fruit crops (Baidhe

et al., 2021). Pineapples are grown in different parts of the world, with the most important pineapple growers being the Caribbean, Asia and Africa (specifically South Africa and Kenya) (Campos et al., 2020). Pineapple processing activities result in by-products known as pineapple pulp (PP) (Campos et al., 2020). Standard pineapple processing results in approximately 60% (w/v) of pineapple by-products being produced (Campos et al., 2020). PP comprises approximately 19% cellulose, 22% hemicellulose, 5% lignin, and 53% cell soluble matter (Malgas and Pletschke, 2020; Olver et al., 2011). The composition of PP largely depends on the variety, location, season, and the maturity of the pineapple (Baidhe et al., 2021). The PP may be composed of the crown, fruit, peel, leaves, and trimmings (Campos et al., 2019). The wastes make up approximately 30–60% of the total weight of the pineapple, and about 70% of the flesh is discarded as waste (Campos et al., 2020; Omwango et al., 2013; Ketnawa et al., 2012). One of the polysaccharides in pineapple is an acetylated mannan (Wang et al., 2015). This polysaccharide can potentially be used to produce value-added products (Hlalukana et al., 2021).

In South Africa, pineapple farming mainly occurs in the Eastern Cape province, with over three quarters of the national production, while the second highest production occurs in northern KwaZulu Natal, in the Hluhluwe District (DAFF, 2017). A total of 115 507 metric tons of pineapples were reported to be produced in South Africa in 2018/2019 (Hlalukana et al., 2021). Although there was a decline in the production of pineapples after 2006, the pineapple industry remains a viable economic activity in South Africa (Hlerema and Eiasu, 2017). South Africa, therefore, faces challenges in converting the waste into value-added products (Baidhe et al., 2021).

1.2.2.2. Pine sawdust

Pine trees are softwoods comprising of 28–31% lignin, 27–33% hemicellulose, and 41–44% cellulose as dry matter (Kruyeniski et al., 2019). Pine trees are not native to South Africa, their seeds were first planted in South Africa just over 300 years ago (Ugwu and Enweremadu, 2020; Moran et al., 2000). They are an invasive species in South Africa, competing with native plants for water and other resources (van Wilgen, 2015; Moran et al., 2000). Even so, pine has become a significant contributor to the South African economy, where it is used to produce timber products for building, furniture, and packaging (van Wilgen, 2015; Moran et al., 2000). Waste generated from pine trees, known as pine sawdust/shavings can cause environmental problems if not properly disposed of, making its valorisation as a forestry residue important (Ferreira-Santos et al., 2020; Rusanen et al., 2019).

Sawdust is obtained from the use of wood in sawmills (Rusanen et al., 2019). Traditionally, sawdust is burnt for purposes such as power generation and biomass boiler feed (Mukosha et al., 2013). Sawdust also has potential for use as a starting material for value-added products in food-based feed stocks (Rusanen et al., 2019; Mukosha et al., 2013). In South Africa, the estimated waste generated from pine tree shavings were 6 million tons a year, following their use in the recycling processes previously mentioned (Mukosha et al., 2013). Softwoods contain galactoglucomannan as the major hemicellulose (Hlalukana et al., 2021). Softwood galactoglucomannans may also contain O-acetyl groups, and are known as O-acetylgalactoglucomannans (Berglund et al., 2019). The mannans present in softwoods have potential for use in the production of value-added products (Hlalukana et al., 2021)

1.3. Mannan degrading enzymes

Lignocellulosic biomass degradation can occur via hydrolytic (cellulases, hemicellulases, etc.) and oxidative (peroxidases, laccases, etc.) enzyme activities (Baig 2020; Fillat et al., 2017). Hemicellulases are essential enzymes in the degradation of plant biomass (Moreira and Filho, 2008). Hemicellulases are either exo-hydrolases or endo-hydrolases. The former cleaves terminal glycosidic linkages and releases terminal monosaccharide units from the nonreducing end, while the latter cleave internal glycosidic bonds at random or specific points (Moreira and Filho, 2008). With a few exceptions, hemicellulases catalyse reactions through a double-displacement reaction mechanism, retaining the anomeric carbon (Moreira and Filho, 2008). A double displacement reaction mechanism is illustrated in Figure 1.3. Hemicellulases can contain specialised structures known as carbohydrate-binding modules (CBMs), which increase interaction between the enzyme and substrate, thereby increasing the enzyme's catalytic efficiency (Srivastava and Kapoor, 2017; Yamabhai et al., 2014; Moreira and Filho, 2008). Mannan degrading enzymes belong to the hemicellulase cohort but are specialised for mannan polysaccharide hydrolysis.

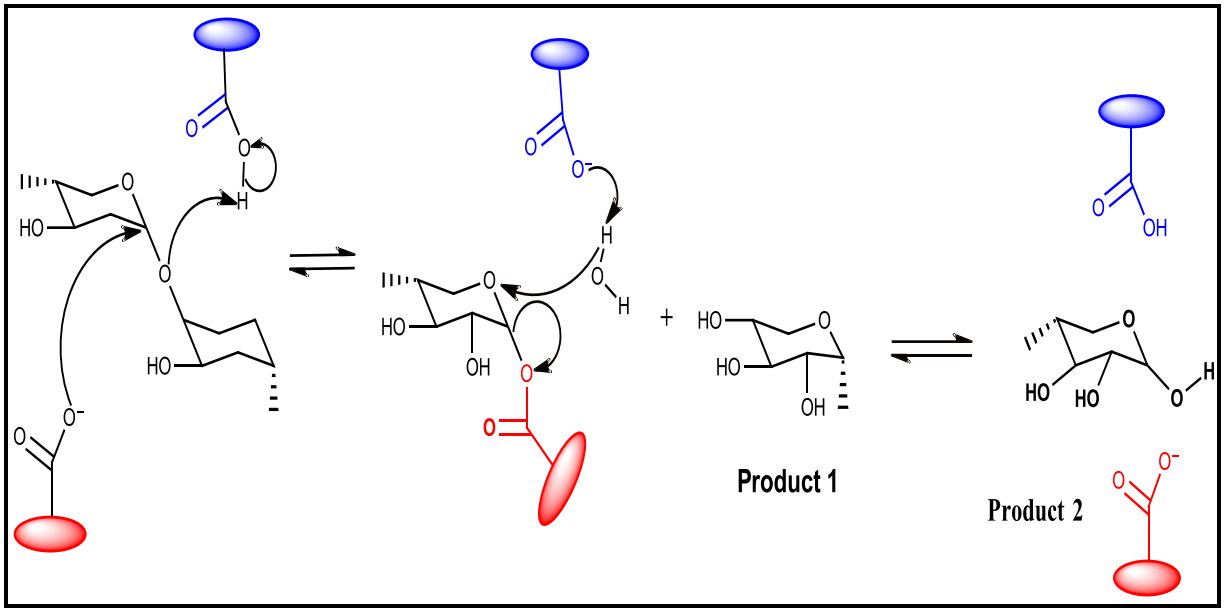

Figure 1.3: Illustration of a double-displacement reaction mechanism catalysed by hemicellulases.

The complete hydrolysis of mannans depends on the action of different mannan degrading enzymes working together (Srivastava and Kapoor, 2017; Malgas et al., 2015a; Moreira and Filho, 2008). The important enzymes required for the mannan main chain hydrolysis are endo-β-1,4-D-mannanases (EC 3.2.1.78), β-1,4-mannosidases (EC 3.2.1.25) and β-1,4-glucosidases (EC 3.2.1.21) (Yamabhai et al., 2014; van Zyl et al., 2010; Moreira and Filho, 2008). Side chain removal occurs through the action of α-1,6-galactosidases (EC 3.2.1.22) and, in some cases, acetyl mannan esterases (EC 3.1.1.6) (Yamabhai et al., 2014; Chauhan et al., 2012; Moreira and Filho, 2008).

1.3.1. Endo-β-1,4-D-mannanases

Mannanases are endo-acting mannan degrading enzymes which initiate mannan degradation by randomly cleaving the mannan backbone to produce mannooligosaccharides (MOS) (Malgas et al., 2015a; 2015b; Moreira and Filho, 2008). They are present in various organisms in nature and have been isolated from bacteria, fungi, plants, and animals, and are the most crucial of the mannan-degrading enzymes (Mano et al., 2018; Malgas et al., 2015a; Moreira and Filho, 2008). They have received much attention in industry and research for their potential applications in many industrial sectors (Dawood and Ma, 2020; Srivastava and Kapoor, 2017). The random hydrolytic action of mannanases in the mannan substrate results in the production of oligosaccharides of differing degrees of polymerisation (DP) with different substitution

patterns, which is also affected by the degree of substitution of the mannan backbone (Moreira and Filho, 2008; Dhawan and Kaur, 2007).

1.3.1.1. Structure and classification of mannanases

The majority of mannanases that have been characterised belong to the GH5 and GH26 families, with other endomannanases found in the GH families 113 and 134, where enzymes are classified into the same GH (glycosyl hydrolase) family based on their amino acid sequence similarities (Bååth et al., 2018; Sharma et al., 2018). GH5, GH26 and GH113 mannanases belong to clan GH-A of GH enzymes (Bååth et al., 2018; Sharma et al., 2018). These are grouped into the same clan based on a similar structural fold, which is the $(\beta/\alpha)_8$ TIM-barrel fold and modular architecture (Bååth et al., 2018; Sharma et al., 2018; Moreira and Filho, 2008). They catalyse reactions through a retaining double-displacement reaction mechanism, where the configuration of the anomeric carbon on the mannan substrate is retained (Bååth et al., 2018; Sharma et al., 2018; Dhawan and Kaur, 2007). GH134 mannanases are a relatively new class of enzymes characterised by a lysozyme-like fold and display an inverting reaction mechanism (Von Freiesleben et al., 2019). The $(\beta/\alpha)_8$ TIM-barrel fold is canon shaped and contains a central β-barrel composed of eight β-strands which lie parallel to each other and form a cylinder (Sharma et al*.,* 2018; Srivastava and Kapoor, 2017). These β-strands are surrounded by eight major α-helices (Sharma et al*.,* 2018; Srivastava and Kapoor, 2017). An illustration of the TIM-barrel catalytic domain is shown in Figure 1.4 below.

.

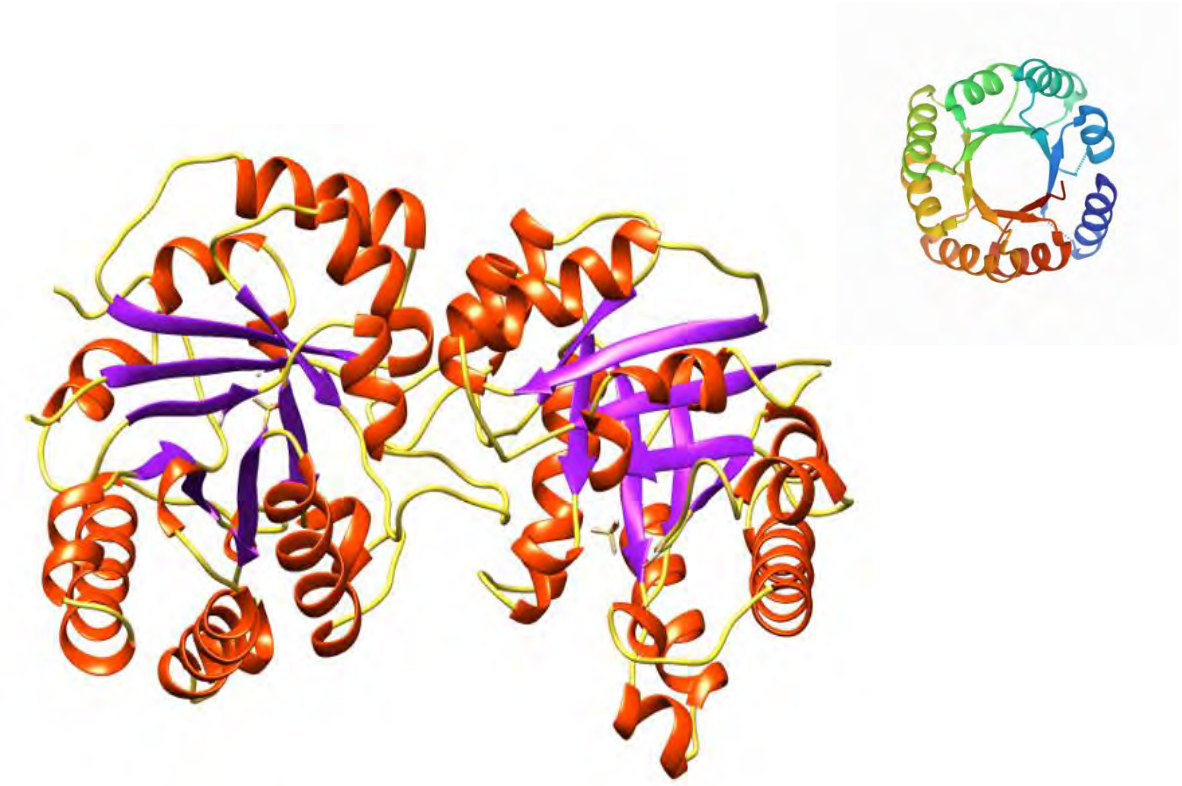

Figure 1.4: Crystal structure of the TIM-barrel canonical shaped catalytic domain (PDB ID: 3WH9). Orange – α-helices; purple – β-sheets; yellow- loops. Insert – top view of TIM-barrel catalytic domain obtained from Haung et al. (2014).

1.3.1.2. Mechanism of action of mannanases

Mannanases require at least four binding subsites for efficient hydrolysis of mannans (Chauhan et al., 2012; van Zyl et al., 2010; Dhawan and Kaur, 2007). The subsites are numbered from the non-reducing to the reducing end as -*n* to +*n* (where *n* = an integer) (Srivastava and Kapoor, 2017; van Zyl et al., 2010; Dhawan and Kaur, 2007). The cleavage site is the same for all mannanases, located between the -1 and +1 subsites, but sites for interaction with the substrate differ between mannanases (Srivastava and Kapoor, 2017; Chauhan et al., 2012; van Zyl et al., 2010). The subsites for catalysis are shown in Figure 1.5 below.

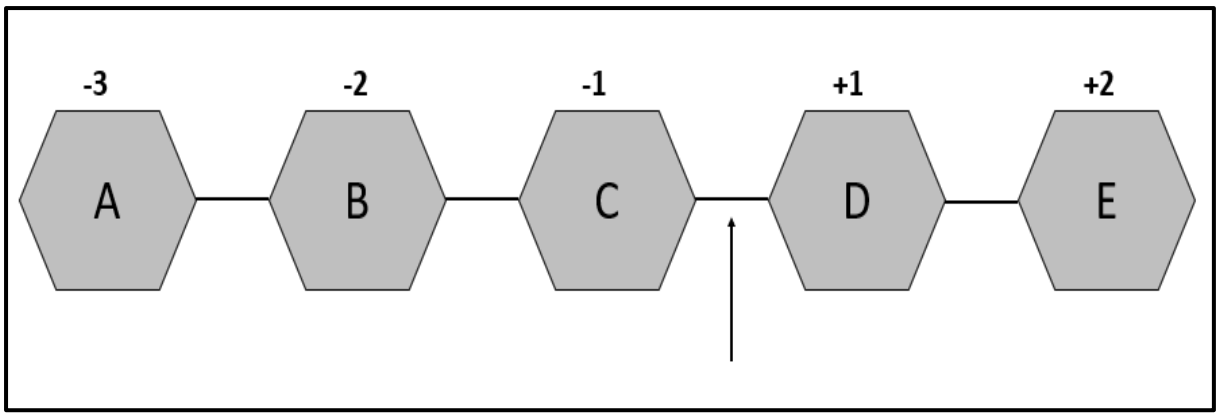

Figure 1.5: An illustration of the subsites required for mannanase catalysis on the mannan backbone. The subsites are represented by the numbers -3 to +2, A to E represents the mannan backbone, and the arrow represents the point at which mannanase cleaves the mannan backbone (Adapted from Dhawan and Kaur, 2007).

Like other hemicellulases, mannanases catalyse the hydrolysis of mannans via a double displacement reaction with retention of the anomeric carbon (Srivastava and Kapoor, 2017; Chauhan et al., 2012; van Zyl et al., 2010). Mannanases have a conserved cleft-shaped active site with two glutamic acid residues; Glu128 and Glu225 in GH5 and Glu212 and Glu320 in GH26, which were identified from the crystal structures of *Thermomonospora fusca* and *Cellvibrio japonicus* derived mannanases (Sharma et al., 2018). The reaction occurs in two steps; (1) the formation of an oligosaccharide-enzyme complex through glycosylation and (2) the release of product through the deglycosylation step (Sharma et al., 2018; Van Zyl et al., 2010). Mannanases belonging to GH5 and GH113 have been reported to exhibit transglycosylation activity (Couturier et al., 2013). To date, no transglycosylation ability has been reported for GH26 and GH134 enzymes (Couturier et al., 2013). During transglycosylation, a sugar or oligomer acts as the nucleophile instead of water, forming a higher DP oligosaccharide than the one added in the initial reaction (Sharma et al., 2018; Couturier et al., 2013; Van Zyl et al., 2010). Transglycosylation may also result in the formation of new oligomers that are not natural mannanase substrates, such as 6^1-α-D-galactosyl-β-D-mannotriose (Van Zyl et al., 2010). A transglycosylation reaction is illustrated in Figure 1.6 below.

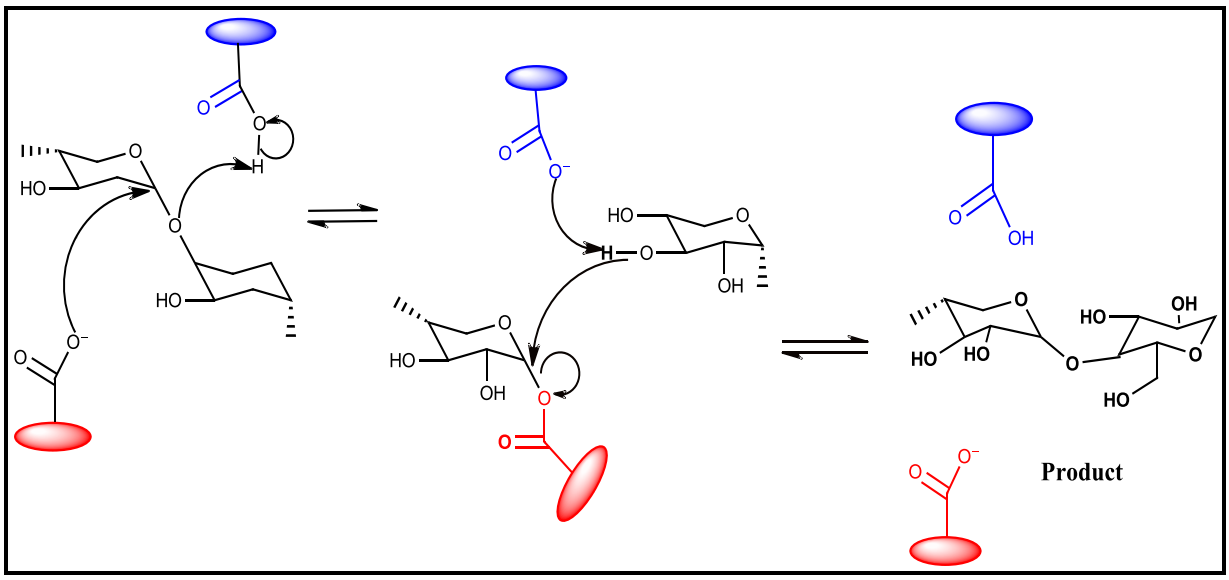

Figure 1.6: Illustration of a double displacement transglycosylation reaction mechanisms catalysed by GH5 and GH113 mannanases.

1.3.1.3. Applications of mannanases

Mannanases have also received attention in the pharmaceutical industry for their potential use as excipients (Van Zyl et al., 2010). They can be used in animal feeds, food juice clarification, paper and pulp production and bleaching, and as boosters to detergents, and bio-ethanol production (Dawood and Ma, 2020; Chauhan et al., 2012; Van Zyl et al., 2010). Mannanases have also been used as a pretreatment step for LB in the production of second generation biofuels (Yamabhai et al., 2014; Van Zyl et al., 2010). Aside from their use in producing prebiotic MOS, mannanases have applications in various industries (Yamabhai et al., 2014).

1.4. Prebiotics

The definition of a prebiotic has changed numerous times over the years. Previously, a prebiotic was described as a non-digestible carbohydrate, which, when ingested, provides health benefits to the host (Mano et al., 2018; Gibson et al., 2017; Patel and Goyal, 2012). Recently, the definition of a prebiotic has been changed to incorporate all foods that proliferate the growth of beneficial bacteria (Davani-Davari et al., 2019; Gibson et al., 2017). A prebiotic is any non-digestible food product that proliferates the growth of beneficial bacteria while inhibiting the growth of pathogenic bacteria, therefore, having an overall beneficial effect on the host's health (Jana et al., 2021a; Davani-Davari et al., 2019; Gibson et al., 2017). The previous definition of prebiotics was limited to fermentation by beneficial bacteria in the gut. However, it has recently

been noted that probiotic bacteria can ferment prebiotics outside the gut, where they can play a role in the balance of vaginal microbiota as well as in the oral cavity (Suryawanshi and Kango, 2021; Monteagudo-Mera et al., 2019; Gibson *et al*., 2017). For a food product to be considered a prebiotic, it must be resistant to digestion by host enzymes in the upper gastrointestinal (GI) tract, must only be fermented by beneficial bacteria, whereby it selectively stimulates the growth or activity of these beneficial bacteria (Davani-Davari et al., 2019; Yamabhai et al., 2014; Patel and Goyal, 2012). The most well-known and well-studied classes of prebiotics to date are non-digestible oligosaccharides (NDOs), such as inulin, fructooligosaccharides (FOS), galactooligosaccharides (GOS), isomaltooligosaccharides (IMO), xylooligosaccharides (XOS) and mannooligosaccharides (MOS) (Mano et al., 2018; Tian et al., 2017; Patel and Goyal, 2012). NDOs have a long-standing history of being considered prebiotics because they are the most likely substrates that meet the requirements of being classified as a prebiotic. They can resist digestion by GI tract resident hydrolytic enzymes (Davani-Davari *et al*., 2019; Mano et al., 2018). FOS and GOS are well established as prebiotics and are commercially available, while XOS and MOS are considered emerging prebiotics (Mano et al., 2018; Patel and Goyal, 2012).

The global prebiotic market is on the rise, and it is estimated to reach U$10.55 billion by 2025, a 12.7% increase from 2015, when prebiotics were worth over U$2.90 billion (Mano et al., 2018). The rapid rise in the prebiotic industry results from their health-promoting potential, as they may protect against colon cancer and prevent cardiovascular diseases and metabolic syndromes (Mano et al., 2018). They are also an attractive substitute for antibiotics, which can have a devastating impact on the gut microbial ecosystem (Johnson et al., 2015). A summary of the different prebiotic classes, their sources and commercial examples are seen in Figure 1.7.

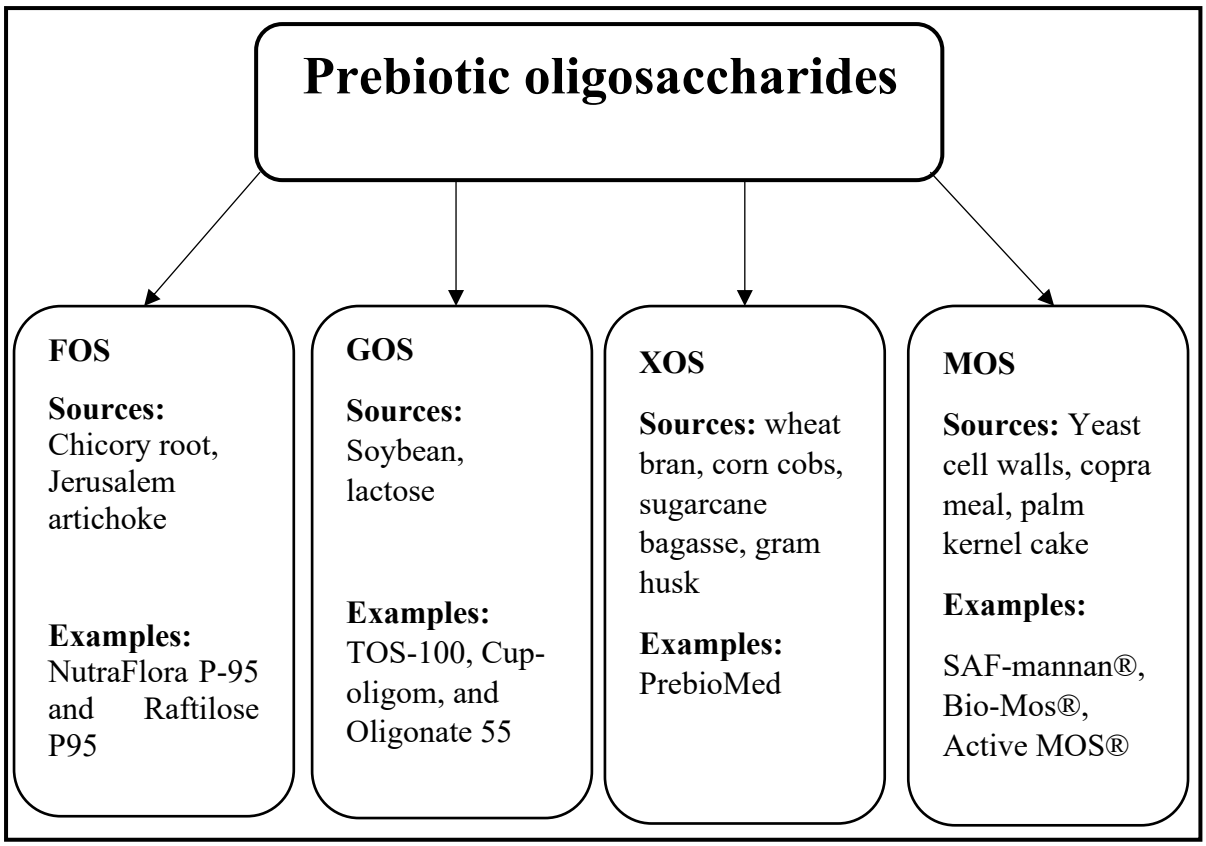

Figure 1.7: Types of prebiotic oligosaccharides, their sources and commercial examples

Fermentation of prebiotics by beneficial bacteria in the gut leads to reduced pH, hindering the growth of pathogens in the gut (Mano et al., 2018). The reduction in gut pH is said to be due to the short-chain fatty acids (SCFAs) acetate, propionate and butyrate, which are fermentation products of the beneficial bacteria (Jana et al., 2021a; Suryawanshi and Kango, 2021; Mary et al., 2019). SCFAs affect the membrane fluidity and rigidity of pathogenic bacteria because of their partial solubility of these membranes, which could lead to a change in osmotic balance, DNA synthesis and nutrient uptake in pathogenic bacteria (Jana et al., 2021a; Feng et al., 2018). Reduced luminal pH leads to protection against enteropathogens (Mano et al., 2018). Branched-chain amino acids (BCAA) (leucine, valine, and isoleucine) are specific molecular signals produced by some bacteria and their production can be influenced by prebiotic MOS (Suryawanshi and Kango, 2021; Mutaguchi et al., 2013). In addition, they have also been found to have health promoting properties (Jana et al., 2021a; Suryawanshi and Kango, 2021; Mutaguchi et al., 2013).

1.4.1. Prebiotic MOS

The potential of MOS as prebiotics has been investigated in several studies, these studies mainly focusing on lactobacilli and purified MOS (Zhang et al., 2021; Mary et al., 2019;

Srivastava et al., 2017). MOS were found to support the growth of probiotic Lactobacilli while retarding the growth of pathogenic species, such as *Escherichia coli* (Zhang et al., 2021; Mary et al., 2019; Srivastava et al., 2017). Lower DP MOS (DP 2 and DP 3) had a higher prebiotic effect on lactobacilli species compared to higher DP MOS (DP ≥ 5) (Zhang et al., 2021; Mary et al., 2019). While the growth of lactobacilli was dependent on the DP of MOS, the inhibition of pathogenic bacteria was not, as higher DP MOS were also able to inhibit pathogen growth (Srivastava et al., 2017). Several studies on crude MOS (unpurified MOS) have been conducted by Chauhan et al. (2014), Mary et al. (2019) and Jana and Kango, (2020). They showed an increase in the growth of lactobacilli in media supplemented with MOS (Jana and Kango 2020; Mary et al., 2019; Chauhan et al., 2014). Mary et al. (2019) demonstrated the difference in the prebiotic effect of purified MOS compared to the crude MOS produced from GG. They found that crude MOS had a higher prebiotic potential compared to purified MOS. However, only a limited number of studies have focused on elucidating the prebiotic potential of crude MOS and the differences in the prebiotic potential of these crude MOS compared to that of purified MOS.

1.4.2. Application of MOS in poultry farming and aquaculture

MOS have received significant attention in areas such as animal husbandry and aquaculture. Several studies have shown the beneficial effects of MOS on the growth of broiler chickens and several marine species. Forsatkar et al. (2017) investigated the effect of MOS on Zebrafish growth and behaviour and found a positive correlation between growth and MOS supplementation. The anxiety behaviour of Zebrafish was also observed to decrease with MOS supplementation, suggesting that MOS had a beneficial effect on the behaviour of Zebrafish. It was found that MOS fed broilers had a better immune response compared to broilers that were not fed with prebiotic, which reduces the need for antibiotic use (Al-Khalaifa et al., 2019). The beneficial effect of prebiotics on broilers was also observed in broilers grown under stress conditions, where supplementation with MOS improved the gut ecology of the broilers and resulted in the reduction of pathogenic bacteria (Kridtayopas et al., 2019).

1.4.3. Other bioactive properties of MOS

MOS have been reported to possess other bioactive properties in addition to their use as prebiotics, such as anti-cancer, anti-diabetic, and immunomodulatory properties (Jana et al., 2021a). Jana and Kango (2020) studied the anti-cancer activity of MOS using human colorectal adenocarcinoma cells (Caco-2), where a 74.19% decrease in cell viability was observed in the presence of MOS. Other studies on the potential of MOS as anti-cancer agents were conducted

by Suryawanshi and Kango (2021) and Zhou et al. (2018). Zheng et al. (2018) studied the anti-diabetic potential of MOS in conjunction with metformin in mice and found that mice supplemented with MOS/metformin improved the health of diabetic mice. MOS derived from guar gum, palm kernel cake, and copra meal also have proven antioxidant effects *in vitro* (Jana and Kango, 2020).

1.4.4. The effect of MOS on probiotics

Probiotics are live microorganisms that confer health benefits to the host when provided in sufficient amounts (Kimelman and Shemesh, 2019; La Fata et al., 2018; Seddik et al., 2017). Many documented studies support the use of probiotics for the prevention and treatment of infections (Nair et al., 2017). Most probiotic bacteria are Gram-positive and belong to the lactobacilli and bifidobacteria genera (Kimelman and Shemesh, 2019). Probiotic bacteria are primarily found in foods such as yoghurt and are delivered as dried cultures (Kimelman and Shemesh, 2019). Probiotics exert health benefits by indirect effects on the host or directly affect the pathogens (Nair et al., 2017). The indirect mechanisms by which probiotic bacteria inhibit the growth of pathogenic bacteria include the secretion of antimicrobial peptides, production of SCFAs and a reduction in the pH in the surrounding environment, stimulation of the host's immune system, and lactose metabolism and food digestion (Piatek et al., 2020; Nair et al., 2017; Mogna et al., 2016). These are known as indirect mechanisms because they improve the host's overall health and well-being (Nair et al., 2017). Direct effects include the production of antimicrobial compounds, such as bacteriocins, hydrogen peroxide, and organic acids. Probiotics directly inhibit the growth of pathogenic bacteria by disrupting their adhesion ability and affecting quorum sensing in pathogenic bacteria (Piatek et al., 2020; Nair et al., 2017; Mogna et al., 2016). Gram-negative bacteria are typically associated with causing disease in the GI tract (Kaur et al., 2018).

1.5. Problem statement

MOS production is on the rise world wide due to an increase in its demand for use as prebiotics (Mano et al., 2018). Prebiotics are gaining a lot of interest in the feed industry, as the use of antibiotics in feed is being banned in some countries. Moreover, natural substrates that can be used for the mass production of MOS are also being investigated. Waste substrates such as palm kernel cake and copra meal have been used to produce prebiotic MOS (Suryawanshi and

Kango, 2021; Jana and Kango, 2020). Lignocellulosic biomass waste offers an attractive alternative to food-based products to produce value-added products such as prebiotics. Mannanases can be used to degrade LBW into prebiotics such as MOS that have health benefits to humans and animals.

There is an abundance of waste produced in South Africa from agricultural and forestry activities. This waste has the potential to be used as neutraceuticals, and can be used to produce prebiotic oligosaccharides without interfering with food production and other economic activities.

1.6. Hypothesis

Prebiotic MOS enzymatically produced from pretreated PP and PSD will have a positive effect on the growth of probiotic bacteria.

1.7. Aims and objectives

1.7.1. Aims

The project aims to enzymatically produce MOS from LBW pineapple pulp (PP) and pine sawdust (PSD), and to determine their prebiotic and bioactive activities.

1.7.2. Objectives

The above aims were achieved by accomplishing the following objectives:

- To partially purify *A. niger* Man26A using dia-filtration;
- Tocharacterise the pH optimum, temperature optimum, and temperature stability of Man26A;
- To pre-treat and determine the carbohydrate composition, morphology, and characteristics of untreated and pretreated PP and PSD;
- To produce MOS from PP and PSD;
- To determine the stability of MOS produced from PP and PSD; and
- To determine the prebiotic effect of MOS produced from PP and PSD on beneficial bacteria.

Chapter 2: Partial purification and characterisation of Man26A

2.1. Introduction

Endo-β-(1,4)-mannanases (E.C. 3.2.1.78), also called mannanases, are glycoside hydrolase (GH) enzymes that randomly hydrolyse the backbone of mannan polysaccharides (Malgas et al., 2015a; Malgas et al., 2015b). The degradation of the mannan backbone by mannanases leads to the production of mannooligosaccharides (Mano et al., 2018; Malgas et al., 2015a; Moreira and Filho, 2008). Mannanases are classified into different GH families, namely, GH5, GH26, GH113 and GH134, based on their amino acid sequence similarities (Bågenholm et al., 2019; Von Freiesleben et al., 2018; Malgas et al., 2015a). Mannanases are expressed in numerous organisms, including bacteria and fungi, and some have been reported to be expressed in insects, such as in the hindguts of some termites (Hsu et al., 2018).

There are conflicting claims in the literature regarding the substrate specificity of GH26 mannanases. Some suggest that the activity of GH26 mannanases is hindered by the presence of galactose substituents on the mannan backbone, while others suggest that GH26 mannanases are more active on heterogenous mannan substrates such as galactomannans and glucomannans (Mandelli et al., 2020; Bågenholm et al., 2019). These discrepancies may be caused by differences in the origin of the mannanases used in previous studies. It has been suggested that fungal mannanases may contain carbohydrate-binding modules (CBMs), such as CBM35, which can attach to β-mannans, uronic acids and galactose residues (Von Freiesleben et al., 2018). Von Freiesleben et al. (2016) further demonstrated the ability of GH26 mannanases to hydrolyse heterologous substrates, demonstrating that they are more capable of hydrolysing these substrates than their GH5 counterparts.

GH26 mannanase activity has been evaluated on different mannan substrates, and data support the suggestion of GH26 mannanases having a higher preference for galactomannans, especially locust bean gum (LBG) (Bågenholm et al., 2019; Von Freiesleben et al., 2016; Malgas et al., 2015a). Mannan hydrolysis is also influenced by the solubility of the substrate, with soluble substrates being more hydrolysable than insoluble substrates (Bååth et al., 2018). This is true for both GH5 and GH26 mannanases, as demonstrated by Bååth et al. (2018), where the effect of acetylation on mannan hydrolysis was studied. The acetylated mannans were relatively insoluble, which hindered the ability of mannanases to hydrolyse them.

In this study, an *A. niger* derived mannanase, Man26A, was partially purified and biochemically characterised. Furthermore, Man26A was used to hydrolyse different model mannan substrates; LBG, guar gum (GG), and ivory nut mannan (INM), to pilot the potential use of the enzyme in the production of prebiotic mannooligosaccharides from mannan-containing agricultural residues.

2.2. Aims and objectives

2.2.1. Aim

To partially purify and biochemically characterise Man26A, and to determine its specific activity on model mannan substrates.

2.2.2. Objectives

- To partially purify Man26A using dia-filtration;
- To determine the molecular weight of Man26A using SDS-PAGE;
- To determine the pH optimum of Man26A;
- To determine the temperature optimum and stability of Man26A;
- To determine the specific activity of Man26A on model mannan substrates;
- To determine the action pattern and hydrolysis product pattern of Man26A on thin layer chromatography (TLC) using model mannan substrates; and
- To quantify the MOS produced from model mannan substrates using high-performance liquid chromatography (HPLC).

2.3. Methods

2.3.1. Purification of Man26A using dia-filtration

The *Aspergillus niger* mannanase, Man26A, was prepared as described by Magengelele et al. (2021). The recombinant enzyme was partially purified using 30 kDa MW Amicon® Ultra Centrifugal Filters (Darmstadt, Germany) spun at 4000 × *g* for 20 minutes using Heraeus Megafuge Benchtop Centrifuge (Waltham, MA, USA) at 4°C, and the fraction remaining in the membrane (retentate) was retained for experimental use. The concentration of partially purified enzyme was determined using the Bradford method (Bradford, 1976), using bovine serum albumin (BSA) as a suitable standard. Briefly, 25 µl of the sample was added into a microtiter plate to 230 µl Bradford reagent and incubated at room temperature for 20 minutes

before reading wavelength at 595 nm using a BioTek Epoch Microplate Spectrophotometer (Winooski, USA).

2.3.2. SDS-PAGE

To determine the efficiency of the purification procedure, a 12% SDS-PAGE gel using the method described by Laemmli (1970) was prepared. Man26A was mixed in a 4:1 ratio with 5× sodium dodecyl sulphate (SDS) sample buffer (50 mM Tris HCl (pH 6.8); 40% (w/v) glycerol; 3% (w/v) SDS; 0.14% (w/v) bromophenol blue; 5% (w/v) β-mercaptoethanol), and boiled for 5 minutes at 95°C. The samples were then centrifuged at 16 060 × *g* for 2 minutes. A volume of 15 µl of sample was loaded onto the gel, and the gel was run at 120 V for 2 hours. The gel was then stained with Coomassie blue (0.1% (w/v) Coomassie Brilliant Blue G250; 20% (w/v) methanol and 15% (w/v) glacial acetic acid) for 15 minutes, destained twice with destaining solution (45% (w/v) methanol 10% glacial acetic acid) and used to determine the molecular weight of Man26A.

2.3.3. Enzyme activity assay

A reaction mixture containing 2% (w/v) of guar gum or locust bean gum and/or ivory nut mannan, and 50 mM citrate buffer (pH 5) was incubated with 0.0025 mg/ml of Man26A. The reaction was carried out at 50°C for 30 minutes and subsequently terminated by heat inactivation for 5 minutes at 100°C using a Labnet AccuBlock dry bath (Edison, USA). The samples were then centrifuged at 16 060 × *g* for five minutes and the reducing sugar content was determined using the 3,5-dinitrosalicylic acid (DNS) method described by Miller (1959), using mannose as a suitable standard. A volume of 150 µl of the sample was mixed with 300 µl of DNS reagent (1% (w/v) NaOH; 1 % (w/v) dinitrosalicylic acid; 20 % (w/v) sodium potassium tartrate; 0.2% (w/v) phenol and 0.05% (w/v) sodium metabisulphite). The mixture was heated at 100°C (Labnet AccuBlock dry bath) for 7 minutes and cooled on ice for 5 minutes. From this mixture, 250 µl of the sample was added to a 96 well microtiter plate, and the absorbance was read at 540 nm using a BioTek Epoch Microplate reader.

2.3.4. Determining the pH optimum of Man26A

The pH optimum of Man26A was determined using a pH range of 2 – 10, prepared using 50 mM Britton-Robinson universal buffer (Britton and Robinson, 1931). Assays were performed with a 2% (w/v) LBG as described in Section 2.3.3 above.

2.3.5. Determining the temperature optimum and temperature stability of Man26A

The temperature optimum of Man26A was determined in a temperature range of 30 – 90°C. Hydrolysis was conducted as described in Section 2.3.3 above with 2% (w/v) LBG as substrate. To determine the temperature stability of Man26A, the enzyme was incubated for a period of 0, 1, 3, 6, 12, 24, 48 and 72 hours at 50°C (Labnet AccuBlock dry bath, Edison, USA). Hydrolysis was performed using 2% (w/v) LBG and the reducing sugar release was determined as described in 2.3.3.

2.3.6. Determining the action pattern and hydrolysis product pattern of Man26A

2.3.6.1. Thin layer chromatography

TLC silica gel plates (Merck) were used to visualise the different model mannan substrates, using purified mannooligosaccharides as standards (mannose (M1), mannobiose (M2), mannotriose (M3), mannotetraose (M4), mannopentaose (M5), mannohexaose (M6)) (Megazyme™). The mobile phase used was a solvent composed of 2:1:1 (v/v) butanol: water: acetic acid. The plates were developed twice for two hours each. For visualisation, the plates were sprayed with 95:5% (v/v) methanol: sulphuric acid and 0.3% (w/v) 1-naphthol to stain the saccharides and heated at 110°C in an oven to develop spots.

2.3.6.2. High-performance liquid chromatography

MOS were quantified using a Shimadzu RID-20A HPLC system (Shimadzu Corporation, Kyoto, Japan) that is equipped with a refractive index detector (RID) using a CarboSep CHO 411 column (Concise Separations, San Jose, CA, USA). Distilled water in isocratic mode was used as the mobile phase. The column oven was set at 80°C and separation was performed for 35 minutes at a flow rate of 0.3 ml per minute. The samples were injected at an injection volume of 20 µl.

2.4. Results

2.4.1. Purification of Man26A

A purification table for Man26A was constructed to determine the purity of Man26A obtained from purification using 30 kDa MW Amicon® Ultra Centrifugal filters. The fold purification and yield of Man26A are represented in Table 2.1 below.

Table 2.1: Purification table of Man26A purified by dia-filtration

Man26A fractions	Volume (ml)	Total protein (mg)	Activity (U/ml)	Total activity (U)	Specific activity (U/mg)	Fold purification	Yield (%)
Crude	15	0.088	0.26	3.84	43.6	1	100
Ultra-filtration	0.2	0.029	7.88	1.58	54.3	1.25	41.1

The yield obtained from partially purifying Man26A using dia-filtration was 41.1%, with a fold purification of 1.25.

2.4.2. SDS-PAGE

To determine the purity and molecular weight of Man26A after dia-filtration, a 12% SDS-PAGE gel was prepared (Figure 2.1).

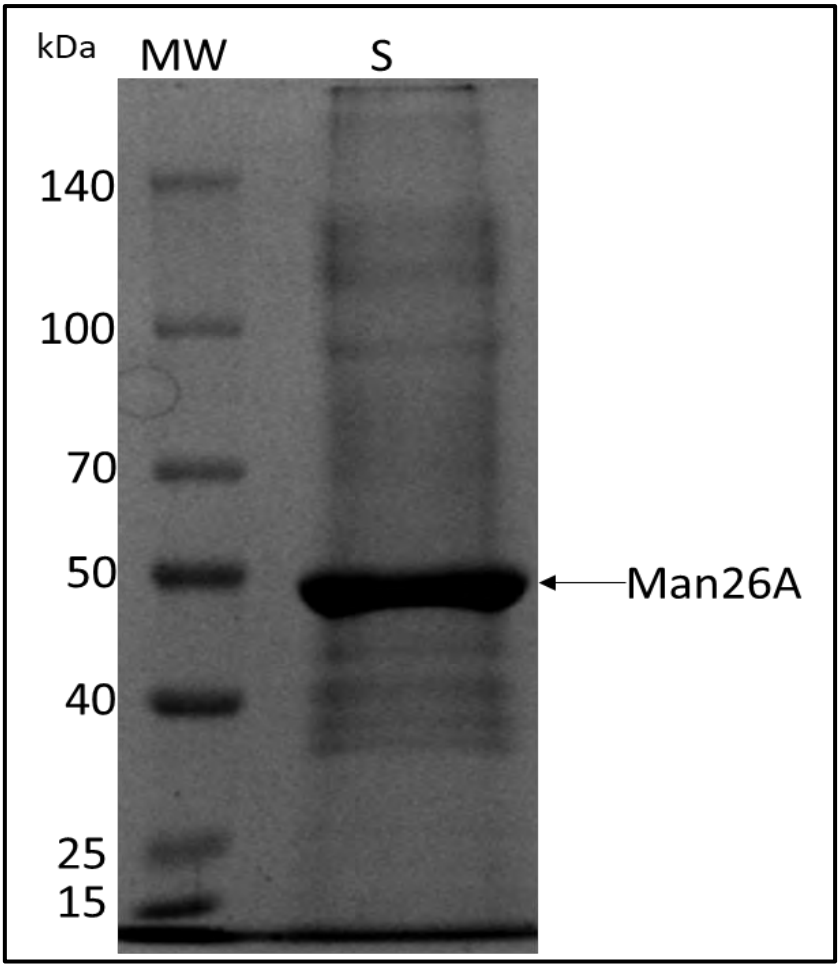

Figure 2.1: SDS-PAGE gel of partially purified Man26A. MW: Thermo Scientific® Protein Molecular Marker 26612 ladder; S: sample of diafiltrated Man26A.

The molecular weight of Man26A was deduced to be approximately 46 kDa using the migration values of the Thermo Scientific® Protein Molecular Marker 26612 ladder in the SDS-PAGE gel. There were other bands observed on the gel, which suggests that Man26A was not pure, but the major band observed was that of Man26A.

2.4.3. pH optimum of Man26A

The pH optimum of Man26A was determined by incubating the enzyme with 2% (w/v) of the model mannan substrate LBG at 50°C at different pH values ranging from 2 – 10. The universal buffer was used to make up the different pH values. The results obtained for the temperature optimum assay of Man26A are presented in Figure 2.2.

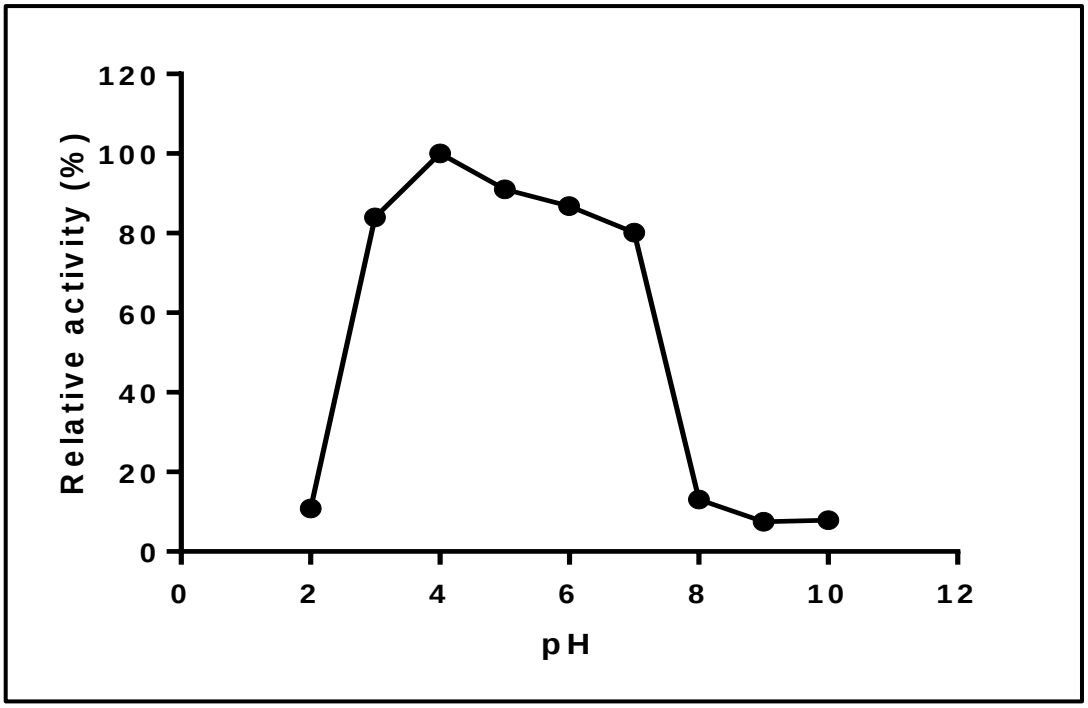

Figure 2.2: The pH optimum profile of Man26A. Values represent means ±SD (n = 3).

The pH profile of Man26A was evaluated using LBG as a model substrate. Man26A showed the highest activity at pH 4.0 but displayed high activity over a broad pH range, with up to 90% of the activity retained between pH 3.0 and 7.0.

2.4.4. Temperature optimum and temperature stability of Man26A

The temperature optimum (Figure 2.3.A) and temperature stability (Figure 2.3.B) of Man26A were determined using 2% (w/v) of the model mannan substrate LBG.

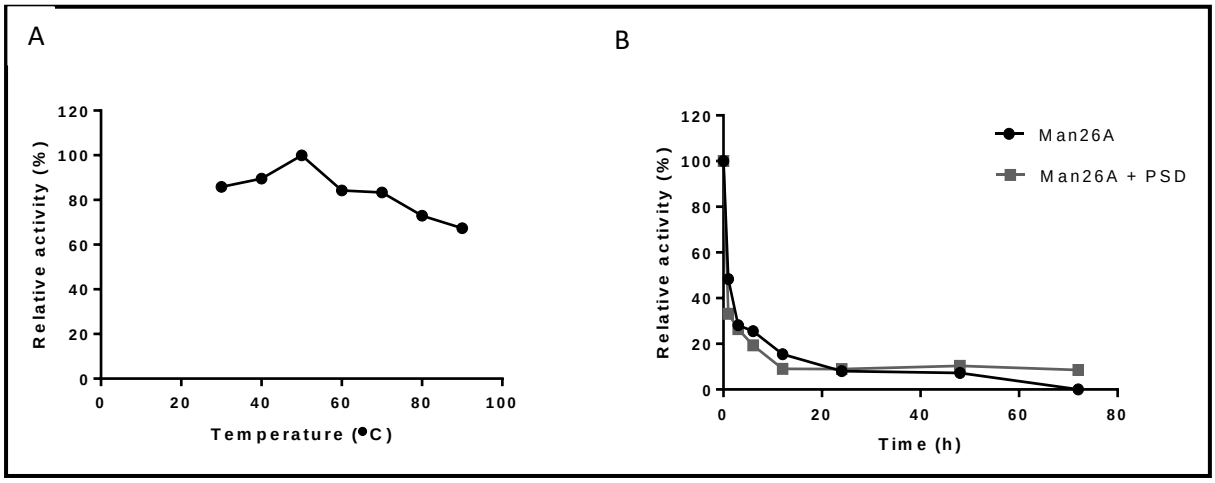

Figure 2.3: Temperature studies with Man26A: (A) temperature optimum profile of Man26A and (B) temperature stability profile for Man26A. Values represent means ±SD (n = 3).

The optimum reaction temperature of Man26A was determined to be 50°C, using LBG as a substrate. The optimum temperature of Man26A was subsequently used to determine the stability of Man26A. The results indicate that Man26A lost approximately 52% of its activity after 1 hour of incubation at 50°C and all its activity was abolished after 72 hours of incubation at this temperature. Man26A was not stable even when incubated in the presence of substrate, where it followed the same trend of losing activity after 1 hour of incubation. The loss of activity reached a plateau after 12 hours in the presence of pine sawdust (PSD), where it remained constant up to 72 hours of incubation.

2.4.5. Man26A substrate specificity

Man26A specific activity was determined by incubating the enzyme with 2% (w/v) of each model mannan substrate at 50°C for 30 minutes. The specific activity of Man26A on model mannan substrates is presented in Table 2.2**.**

Table 2.2: Specific activity (U/mg) of Man26A on model mannan substrates. Values represent means ±SD (n = 3).

Substrate	Specific activity (U/mg)
Guar gum (GG)	29.07±1.87
Locust bean gum (LBG)	52.27±1.53
Ivory nut mannan (INM)	57.25±1.02

Man26A exhibited higher specific activity on the unsubstituted mannan substrate INM and on the less substituted LBG (57.25 U/mg and 52.27 U/mg, respectively). The lowest specific activity was observed for the more highly substituted GG, which displayed a specific activity of 29.07 U/mg.

2.4.6. Analysis of the action pattern of Man26A and hydrolysis products on model mannan substrates

TLC was used to identify the products obtained from the hydrolysis of model mannan substrates (Figure 2.4.). Hydrolysis products were obtained by incubating the samples at 50°C for 30 minutes.

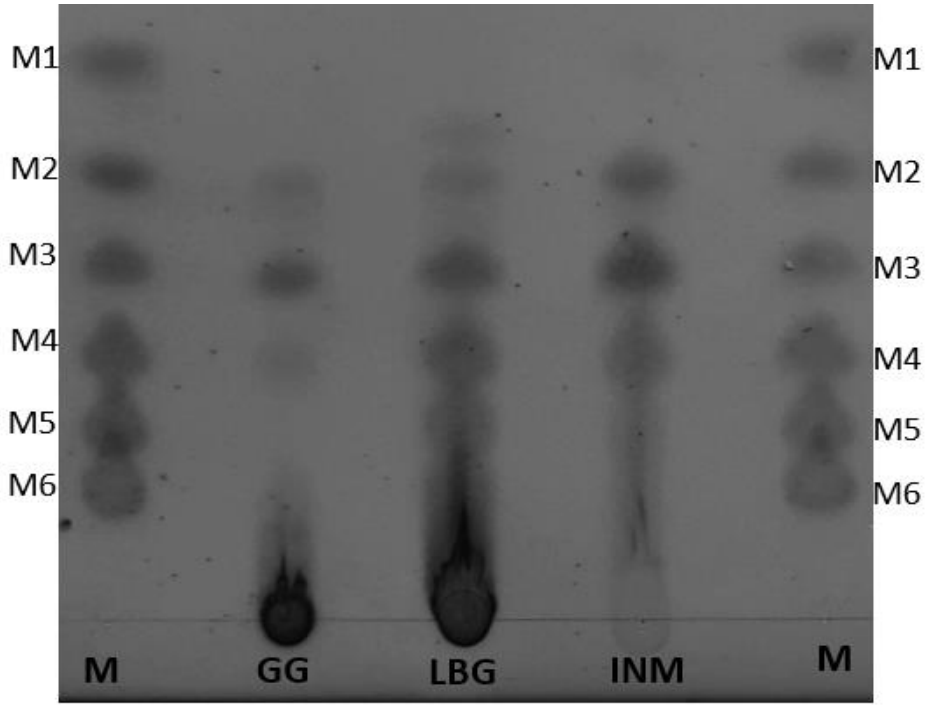

Figure 2.4: Action pattern and hydrolysis products of Man26A on model mannan substrates. M1 – M6: mannosyl standards mannose, mannobiose, mannotriose, mannotetraose, mannopentaose, and mannohexaose, respectively; M: MOS standards.

Man26A produced MOS of different lengths from the different model mannan substrates. On GG, MOS ranging from M2 to M3 and low levels of M4 were observed. LBG hydrolysis displayed MOS running between M1 and M2, and M2 to M5, with MOS with a DP higher than 5 being unresolved. INM hydrolysis, on the other hand, displayed the least MOS diversity with only M2, M3 and M4 being observed on the plate, and no unresolved MOS of higher DP observed. The results obtained from HPLC analysis of these samples are presented in Table 2.3 below.

Table 2.3: HPLC analysis of MOS produced from model mannan substrates.

	MOS produced (mg/ml)						
Substrate	M1	M2	M3	M4	M5	M6	TRS*
GG	-	0.501	0.470	0.245	0.956	2.44	2.31
LBG	-	0.780	0.627	1.41	2.01	2.00	3.71
INM	-	-	0.313	0.742	-	-	3.11

**TRS – total reducing sugars as determined by the DNS method.*

The reducing sugar profile on HPLC indicates that M6 was the major product for GG, with a calculated reducing sugar concentration of 2.44 mg/ml. M5 was the second highest, followed by M2, M3, and M4 which had concentrations of 0.956, 0.501, 0.470, and 0.245 mg/ml, respectively. LBG had M5 and M6 as the major products, with concentrations of 2.01 and 2.00 mg/ml, respectively. These were followed by M4, M2, and M3 with concentrations of 1.41, 0.780, and 0.627 mg/ml, respectively. Finally, INM had M4 as the major product with a concentration of 0.742 mg/ml, and M3 at 0.313 mg/ml. The concentration of M2 was not detected for INM on HPLC, although it was observed on TLC. A low concentration of M2 for INM may be the cause of the peak not being detected on HPLC.

2.5. Discussion

In this study, an *Aspergillus niger* derived GH family 26 mannanase, Man26A, was partially purified and biochemically characterised. The specific activities of the enzyme were determined on various model mannan substrates. Finally, the action pattern of Man26A was investigated from the hydrolysis products obtained from its hydrolysis of model mannan substrates. The studies conducted on Man26A using model mannan substrates were conducted to optimise the enzymatic production of prebiotic mannooligosaccharides (MOS).

A fold purification of 1.25 was obtained for Man26A, following purification using Amicon filters, which is lower than a fold purification of 2.6 obtained for another Man26A, purified using size exclusion chromatography (Zhao et al., 2011). Faint bands were observed on an SDS-PAGE gel following purification of the enzyme, but the most prominent band was observed at a MW of 46 kDa, corresponding to Man26A. Zhao et al. (2011) obtained a single band with a MW of 45 kDa on SDS-PAGE for purified *An*Man26A, and Wang et al. (2021) obtained a MW of 39kDa for deglycosylated *An*Man26, which were expressed in *Pichia*

pastoris. This finding is in the molecular weight range of other GH26 mannanases, which have been found to have molecular weights ranging from 34.4 to 59.4 kDa (von Freiesleben et al., 2018).

The partially purified Man26A showed higher specific activity towards the linear mannan, INM, and the less substituted galactomannan, LGB - compared to the more highly substituted GG galactomannan. This finding is in agreement with that of another fungal GH26 mannanase from *Podospora anserina* (*Pa*Man26A), which showed higher specific activity towards LBG (86 U/mg) (Couturier et al., 2011). Another study on a *Myceliophthora thermophila* derived mannanase showed a similar trend to that of *Pa*Man26A, with the enzyme having a higher specific activity towards carob galactomannan (220 U/mg) (Katsimpouras et al., 2016). Contrary to these studies, the specific activities of Man26A on INM and LBG used in our study were comparable, as no significant differences were observed. Couturier et al. (2011) and Katsimpouras et al. (2016) reported specific activity values of 46 U/mg and 182 U/mg for linear mannan, respectively. According to Von Freiesleben et al. (2018), GH26 mannanases are known to prefer soluble substrates, and because of this, the expected result would be for Man26A to be more active towards the soluble galactomannan substrates LBG and GG. Although INM is an insoluble substrate, the lack of galactose substituents on this mannan substrate could be the reason why Man26A displayed a higher specific activity - as Couturier et al. (2011) and Katsimpouras et al. (2016) have speculated that the presence of galactose substituents may negatively impact enzyme's activity. Therefore, the higher galactose substitution on GG compared to LBG accounts for the enzyme's lower activity towards GG. The galactose substituents on GG hinder enzyme activity, compared to the less substituted LBG (vVon Freiesleben et al., 2016).

The pH and temperature optima of Man26A showed a broad range of 4 – 8 and 30 - 80℃, respectively, which was comparable to other fungal GH26 mannanases (Von Freiesleben et al., 2018; Malgas et al., 2015a; Couturier et al., 2011). Man26A showed poor thermal stability at the optimum temperature of 50℃, with more than 50% of the enzyme's activity lost within the first hour of incubation. This finding agrees with the results obtained by Malgas et al. (2015a), where Man26A showed higher stability at 37℃ compared to 50℃. It has been proposed that the thermostability of an enzyme can be improved by having the enzyme attach to the surface of a polysaccharide (Longo and Combes, 1999). Other strategies that have been proposed for the improvement of thermal stability of an enzyme include the addition of soluble additives, engineering of enzymes, immobilisation, and chemical modification of the enzyme (Longo and

Combes, 1999). A study by Blibech et al. (2018) revealed improved thermal stability for a *Penicillium occitanis* mannanase immobilised on chitin with glutaraldehyde.

The model mannan substrates in our study produced a diverse range of MOS. GG produced M2–M4, and higher DP MOS that were not resolved on TLC. LBG produced MOS which migrated between M1 and M2, as well as M2–M5, as well as MOS with a higher DP. INM produced the least diverse MOS, as it only produced M2–M4, with M4 being the most prominent MOS. LBG and GG hydrolysis products from GH26 fungal mannanases are in agreement with results obtained by Bågenholm et al. (2019) and Jana et al. (2018), where the major hydrolysis products obtained using LBG as substrate were M1–M5 and M1–M4 with higher DP MOS, respectively. GG produced M2–M5 and M1–M4 with higher DP MOS. The hydrolysis products obtained from INM hydrolysis were also observed during hydrolysis with a GH5 mannanase, and produced M2–M4 as the major hydrolysis products (Rahmani et al., 2017). LBG hydrolysis has also been shown to produce galactosyl substituted MOS, which migrate between the MOS standards (Magengelele et al., 2021). The galactosyl substituted MOS are observed between M1 and M2 for LGB. Because GG is more highly substituted compared to LBG, the hydrolysis products obtained from GG may be higher than galactosyl-mannose, which is why there is no product observed between M1 and M2 for GG derived MOS.

The product profile of MOS on HPLC was similar to that observed on TLC, as observed in Figure 2.4 and Table 2.4. Magengelele et al. (2021) used Man26A to produce MOS over a 24 hour period, and identified MOS with more diversity (variety) compared to those produced in this study. After 24 hours, LBG and GG produced M1–M6 as well as MOS with higher DP which were unresolved. The diversity of MOS produced by INM was also higher, as M1–M5 were produced from this substrate. The degree of hydrolysis and hydrolysis product pattern of MOS is affected by the degree of substitution of the mannan polymer (Magengelele et al., 2021; Srivastava and Kapoor, 2017). The highly substituted GG produces MOS of high diversity that are different from the less substituted LBG, which may contain galactose-substituted MOS as observed by Srivastava and Kapoor (2007). They observed α- and β-glycosidic linkages using FTIR spectroscopy, which relates to galactose and mannose linkages in LBG, respectively.

2.6. Conclusions

Man26A was partially purified via dia-filtration to a yield of 41.1% and a purification fold of 1.25. The molecular mass obtained for Man26A of 46 kDa corresponded to that of other

mannanases. Man26A works well in acidic conditions, and displayed the highest activity at pH 5 and displayed a broad temperature optimum, retaining up to 70% of its activity at 80℃. Man26A displayed poor stability at the optimum temperature of 50℃, with over 50% activity reduction after 1 h of incubation. The enzyme displayed high specific activity on INM and LBG, indicating that its catalysis is sterically hindered by the substitution on the mannan backbone. The action patterns of Man26A on TLC and HPLC revealed that MOS of different diversity from different model mannan substrates were produced due to the enzyme's action. Man26A was shown to have the ability to produce galactosyl substituted MOS from GG and LBG, due to hydrolysis products migrating between unbranched/linear MOS standards.

Chapter 3: Lignocellulosic biomass waste characterisation and optimisation of Man26A hydrolysis conditions

3.1. Introduction

The processing of lignocellulosic biomass (LB) generates an enormous amount of waste which has a negative effect on the environment because of the pollution it causes (Cho et al., 2020). Lignocellulosic biomass waste (LBW) has the potential to be converted into value-added products through enzymatic and acid hydrolysis (Cho et al., 2020). The value-added products can be in the form of mono- or oligo-saccharides, which have bioactive properties, such as antioxidant activity, prebiotic potential and anti-cancer activity (Cano et al., 2020; Jana and Kango, 2020; Zhang et al., 2018). LBW is a cheap, environmentally friendly and sustainable source for producing value-added products. This makes value-added products more accessible, as chemically synthesised value-added products are expensive and largely inaccessible for those living in developing countries (Jagtap et al., 2017). LBW can be classified into food waste, agricultural waste, forestry residues and municipal waste (Cho et al., 2020; Zoghlami and Paës, 2019).

The enzymatic degradation of LBW is an environmentally friendly method for its valorisation, as enzymes can result in lower energy costs of production, higher yields, generate fewer inhibitory products, and offer higher substrate selectivity than chemical catalysis (Cho et al., 2020). The main drawback in the utilisation of LB for production of value-added products, specifically during enzymatic hydrolysis, is its recalcitrance, which results in the need for a pretreatment step to make the substrate more accessible to the enzymes (Wi et al., 2015). The recalcitrance of LB is the rate-limiting step in its enzymatic conversion into value-added products (Houfani et al., 2020). The presence of lignin poses a problem for the enzymatic conversion of the hemicellulosic fraction of lignocellulosic biomass (Mafa et al., 2020; Kruyeniski et al., 2019; Park et al., 2015), as lignin increases the non-specific adsorption of the enzyme to the substrate, thereby inhibiting the efficiency of enzyme hydrolysis (Nan et al., 2018).

The removal of lignin through LB pretreatment improves the hydrolysis of polysaccharides (Kruyeniski et al., 2019; Yamabhai et al., 2014). Pretreatment methods are divided into physical, chemical, physicochemical, and biological pretreatments (Cho et al., 2020; Østby et al., 2020). Some pretreatment methods have drawbacks, such as not being environmentally friendly, being costly, and causing degradation of some of the polysaccharides making up the

hemicellulosic fraction (Kruyeniski et al., 2019). Some examples of pretreatment methods include hot water extraction (autohydrolysis), alkaline pretreatment, dilute acid pretreatment, steam explosion, and ionic liquid pretreatment (Kruyeniski et al., 2019; Wi et al., 2015; Van Dyk et al., 2013). A good pretreatment should be inexpensive, effective over a wide range of lignocellulosic feedstocks, ensure maximal lignin removal, generate less inhibitors for enzymatic degradation and fermentation, and exhibit minimal loss of polysaccharides (Østby et al., 2020; Kucharska et al., 2018; Wi et al., 2015). Sodium chlorite pretreatment is an oxidative pretreatment method that meets the requirements of a good pretreatment method, as it effectively removes lignin with minimal inhibitory product formation and minimal loss of polysaccharides under controlled conditions (Park et al., 2015; Siqueira et al., 2013). Concentrated phosphoric is known to be a cellulose solvent that produces swollen cellulose (Weidner et al., 2020). The advantage of phosphoric acid pretreatment is that the substrate is more hydrolysable due to the formation of armophous cellulose (Zhang et al., 2007). The residual phosphoric acid does not have any inhibitory effects on subsequent hydrolysis (Zhang et al., 2007).

In this chapter, the biomass wastes pineapple pulp (PP) and pine sawdust (PSD) were pretreated and characterised to determine the polysaccharides present in the wastes. The wastes were pretreated, and their chemical and thermal properties were evaluated. The wastes were then enzymatically hydrolysed using Man26A and the reaction conditions (time, enzyme concentration, and substrate concentration) were optimised for the production of prebiotic MOS.

3.2. Aims and objectives

3.2.1. Aim

To pretreat and characterise the biomass waste substrates pineapple pulp (PP) and pine sawdust (PSD) and to the optimise reaction conditions for prebiotic production.

3.2.2. Objectives

- To delignify PP and PSD using sodium chlorite/acetic acid;
- To swell PP and PSD using phosphoric acid;
- To determine the chemical composition of PP and PSD;
- To determine the chemical changes that occur during pretreatment of PP and PSD using Fourier-transform infrared spectroscopy (FTIR);

- To determine the thermal stability of PP and PSD using thermogravimetric analysis (TGA);
- To examine the morphology of PP and PSD using scanning electron microscopy (SEM); and
- To hydrolyse PSD and PP for MOS production using Man26A

3.3. Methods

3.3.1. Sodium chlorite delignification of PP and PSD

Sodium chlorite and acetic acid were used to delignify PP and PSD according to the protocol by Siqueira et al. (2013). For each gram of substrate used, 0.3 g sodium chlorite, 0.1 ml anhydrous acetic acid and 32 ml water were incubated at 70℃ in a water bath. The mixture was shaken every 20 minutes during incubation. The samples were removed from the water bath after two hours and the same amount of sodium chlorite and acetic acid were added, and the samples were incubated further for another two hours. The samples were removed from the water bath and cooled down at room temperature. The mixture was filtered using a cheesecloth and washed with one litre of deionised water. The samples were then dried at room temperature for 48 hours until a constant weight was obtained.

3.3.2. Phosphoric acid swelling of PP and PSD

In a 50 ml Schott bottle, one gram of delignified substrate was mixed with 8 ml of 84% ortho-phosphoric acid using a glass rod. The slurry was incubated in a water bath at 50℃ for 30 minutes and the reaction was terminated in a water bath with ice. The hemicellulose in the mixture was precipitated with 40 ml of anhydrous acetone. The slurry was centrifuged 4000 × *g* at room temperature for 20 minutes using a Benchtop Heraeus centrifuge. The pellet was washed twice with 40 ml of acetone. The pellet was then washed again twice with water.

3.3.3. Determining the carbohydrate composition of PP and PSD

The agricultural substrates were characterised using a modified sulphuric acid method by Sluiter et al. (2010) (National Renewable Energy Laboratory-NREL). About 300 mg of the untreated and pretreated samples were added in glass test tubes. They were then hydrolysed with 3 ml of 72% (v/v) sulphuric acid. During this process, the samples were incubated at 30℃ for an hour with frequent mixing. After this, the samples were transferred into Schott bottles and the concentration of the sulphuric acid was diluted down to 3% (v/v) by adding 74 ml of deionized water and autoclaved for an hour at 120℃ to remove the sugar from the samples. Following hydrolysis, the fractions were filtered to remove the insoluble lignin from the sugar

solutions. The insoluble fraction was dried in an oven at 50°C for 48 hours. A volume of 10 ml of sample was neutralised with 1 g of sodium carbonate prior to analysis. The presence of glucose, galactose, xylose, and mannose (K-GLUC, K-ARGA, K-XYLOSE, and K-MANGL) was estimated using Megazyme sugar kits according to the supplier's instructions. Soluble phenolics were estimated using a modified Folin-Ciocalteu method (Folin and Ciocalteu, 1927). A volume of 190 µl of soluble hydrolysate was mixed with 20 µl Folin reagent in eppendorf tubes. These were left to stand for one minute at room temperature before adding 50 µl of 2 M Na_2CO_3. The tubes were incubated at 40°C in a Labnet Accublock digital dry bath for 30 minutes, while covered in tinfoil. The absorbance was read at 765 nm in a 96-well microtitre plate using a BioTek Epoch Microplate Spectrophotometer (Winooski, USA). The concentration of soluble phenolics was determined from the gallic acid standard curve (Appendix B, Figure B.3).

3.3.4. Thermogravimetric analysis of untreated and pretreated biomass

A Perkin-Elmer analyser (Waltham, MA, USA) was used for analysis. Approximately 3 mg of untreated and pretreated samples were placed on a platinum pan, and the pan was placed in a chamber with a stream of 20 ml/min of nitrogen. The chamber was heated from 30°C to 750°C with an increase of 20°C/min.

3.3.5. FTIR analysis of untreated and pretreated biomass

A Spectrum 100 FTIR spectrometer system (Perkin Elmer, Waltham, MA, USA) was used to determine the chemical changes that occur with subsequent pretreatments. The FTIR spectra were recorded in quadruplicate in the range of 650-4000 cm^{-1} with a resolution of 4 cm^{-1}.

3.3.6. Microscopy

3.3.6.1. Scanning electron microscopy

A scanning electron microscope (SEM), JOEL JSM 840, was used for analysis, the untreated and pretreated agricultural substrates were mounted on a metal stub, dried using a critical point-drying process and coated with a thin layer of gold prior to SEM analysis (Cross, 2001). Images were captured at 1000× magnification.

3.3.6.2. Light microscopy

Two parts of a 5% (w/v) phloroglucinol prepared in 95% (v/v) ethanol were mixed with one part of concentrated HCl and applied to the untreated and the delignified substrates (Tao et al., 2009; Dashek,1997). The samples were then incubated at room temperature for 3 minutes. The

red colour produced by the presence of lignin in the staining procedure was visualized using an Olympus BX40 light microscope and photographed using an Olympus DP72 digital camera.

3.3.7. Hydrolysis of PP and PSD using Man26A

3.3.7.1. Hydrolysis of untreated and pretreated PP and PSD

Untreated, delignified, and phosphoric acid swollen (PAS) PP and PSD at 4% (w/v) were hydrolysed with 0.2 mg/ml Man26A over 24 hours in 50 mM citrate buffer (pH 5). The reaction was terminated by incubating the enzyme at 100°C in a dry bath for 5 minutes and the reducing sugars were estimated using the method in Section 2.3.3.

3.3.7.2. Enzyme dose dependent hydrolysis studies

Different concentrations of Man26A from 0.1 to 0.5 mg/ml were used to degrade 4% (w/v) of substrates at 50°C over 24 hours in 50 mM citrate buffer at pH 5. The reaction was terminated by incubating the enzyme at 100°C in a dry bath for 5 minutes and reducing sugars were estimated using the method in Section 2.3.3.

3.3.7.3. Time course hydrolysis studies

Reactions were conducted using 4% (w/v) of substrate and 0.1 mg/ml Man26A over 0, 1, 3, 6, 12, 24, 48, and 72 hours. Reducing sugars were estimated using the method in Section 2.3.3.

3.4. Results

3.4.1. Composition of untreated and treated PP and PSD

Following acid hydrolysis, the monosaccharide and lignin composition of untreated and treated PP and PSD were determined using Megazyme kits. The phenolic content of the substrates was estimated using a modified Folin-Ciocalteu method. The results are presented in Table 3.1 below.

Table 3.1: Substrate composition analysis for PP and PSD

	Pineapple pulp			Pine sawdust		
Content (%)	**Untreated**	**Delignified**	**Del + PAS**	**Untreated**	**Delignified**	**Del + PAS**
Glucan[b]	36.41	33.39	27.72	50.47	49.63	47.85
Xylan[b]	5.39	2.61	1.92	3.94	2.00	1.34
Mannan[b]	6.74	6.45	6.520	11.59	11.20	10.32
Galactan[b]	5.62	6.27	6.922	11.76	11.56	9.18
Insolubles (Lignin + ash)[c]	29.0	13.3	8.67	49.7	24.0	20.0
Soluble phenolics	0.28	0.092	nd	0.27	nd	nd

[a]- DNS method, [b]-Megazyme™ sugar kits, [c]- weighing balance. nd – not detected

Table 3.1 represents the major monosaccharides calculated from untreated and pretreated PP and PSD. Glucan was the major polysaccharide fraction in both substrates. Untreated PSD had the highest glucan content of 50.47% compared to 36.41% obtained for untreated PP. PSD had higher mannan and galactan content of 11.59% and 11.76%, respectively, compared to 6.740% and 5.618% in PP. The insoluble fraction of the substrates decreased with each pretreatment, but it was relatively high for PSD, where 49.7, 24.0, and 20.0% were obtained. The insoluble component decreased drastically between untreated and pretreated samples, which could be attributed to lignin loss. Soluble phenolics decreased with each pretreatment to a point where they were negligible for Del + PAS PP and delignified and Del + PAS PSD.

3.4.2. Thermogravimetric analysis

Thermogravimetric analysis of LBW was conducted to determine the temperature at which the substrates decomposed completely. The thermogravimetric (TGA) and derivative thermogravimetric (DTG) results are displayed in Figure 3.1 below.

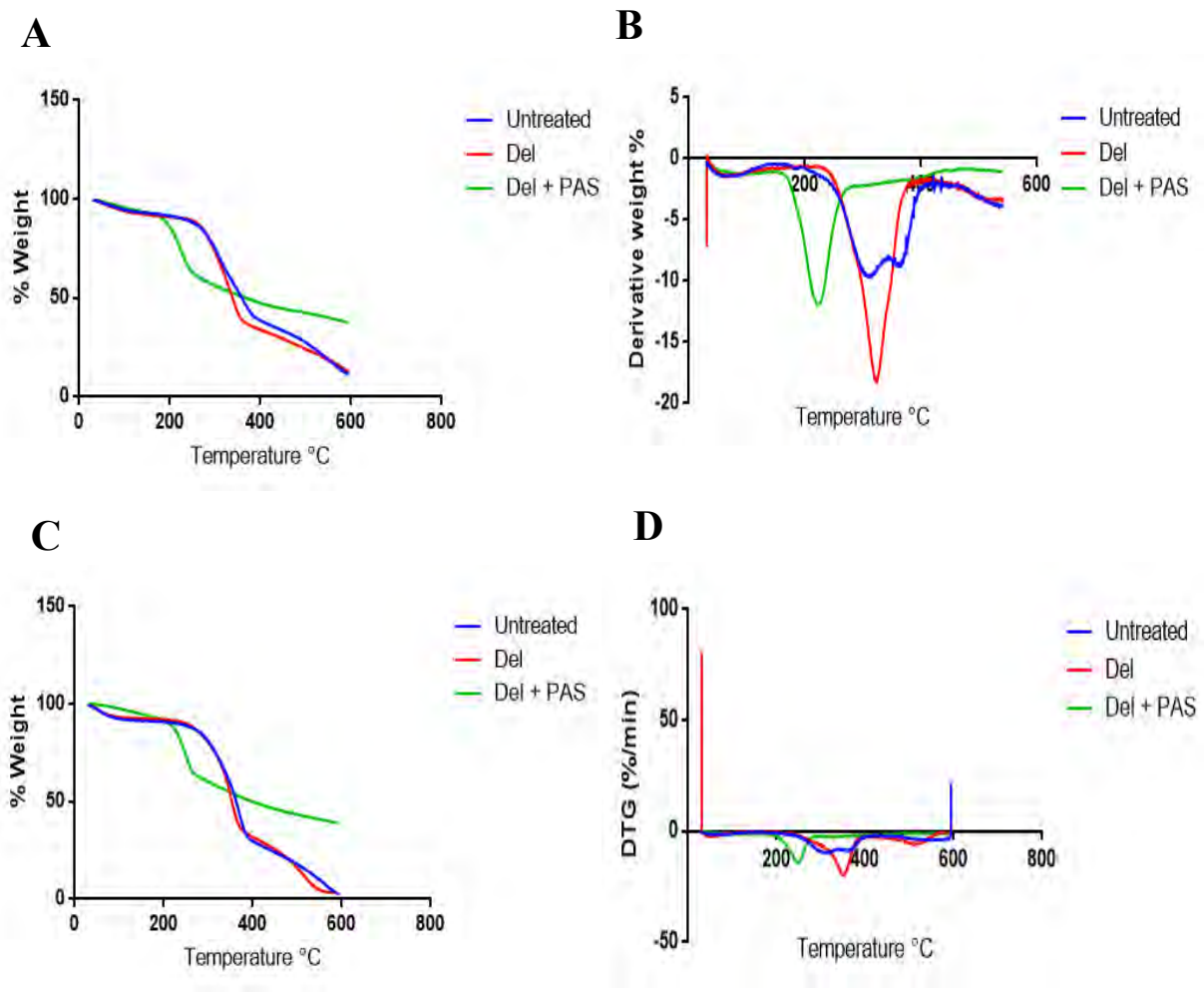

Figure 3.1: Thermograms for the decomposition of LBW. (A) PP thermogram ; (B) PP Derivative Thermogram (DTG); (C) PSD TGA; and (D) PSD DTG.

Figure 3.1A shows that the decomposition of untreated and delignified PP occurred at approximately the same temperature, although delignified PP decomposed slightly faster compared to untreated PP. Del + PAS PP decomposed faster compared to the untreated and delignified PP, as it started decomposing at 168°C compared to approximately 240°C for the untreated and delignified PP. All the samples had residual ash remaining at 600°C, although Del + PAS PP has a higher ash content compared to the untreated and delignified PP. The DTG

in Figure 3.2B supported these findings, as the rate of decomposition for Del + PAS PP was faster compared to untreated and delignified PP. Untreated and delignified PP decompose at around the same temperature, just over 200°C, but the rate of decomposition for delignified PP was shown to be higher, as it had a sharper peak compared to the peak observed for untreated PP. PSD was shown to exhibit the same trend as PP, where the untreated and delignified PSD decomposed at the same temperature (Figure 3.1C). They also took longer to decompose compared to Del + PAS PSD. Untreated and delignified PSD were completely decomposed at 600°C, while Del + PAS PSD had some residual ash at the same temperature. DTG data also supported the data shown by TGA (Figure 3.1D). Del + PAS PSD decomposed faster compared to untreated and delignified PSD, which started to decompose at approximately the same time.

3.4.3. Fourier-transform infrared spectroscopy

FTIR spectroscopy was used to investigate the chemical changes that occur in the LBW PP and PSD following delignification and PAS of the substrates. The FTIR spetra are shown in Figure 3.2 below.

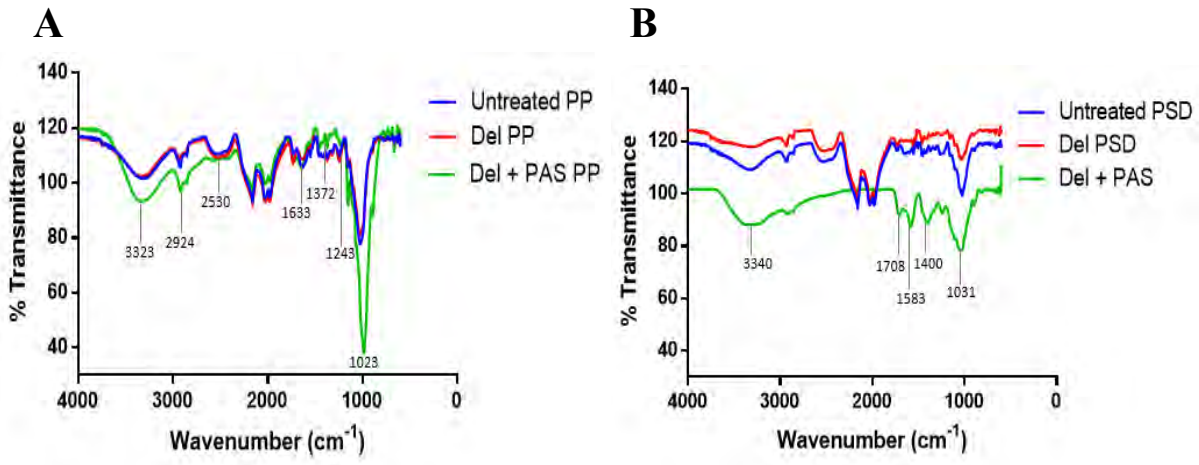

Figure 3.2: FTIR spectra of untreated, delignified, and delignified + PAS LBW substrates in a range of 400 – 4000 cm^{-1}. (A) PP and (B) PSD.

The FTIR spectra show changes in the chemical composition of untreated and pretreated LBW. Figure 3.2A shows a stronger absorption band for Del + PAS PP at approximately 1000 cm^{-1}. Significant changes were also observed between 3450 and 2614 cm^{-1} for PP. Figure 3.2B shows that the chemical composition of PSD remained constant throughout the different treatments. The peaks between 2185 and 2013 cm^{-1} observed both in Figures 3.2A and B may be attributed to background transmittance.

3.4.4. Scanning electron microscopy (SEM)

Untreated and pretreated PP and PSD samples were gold coated on a metal stub prior to obtaining images. SEM was performed to illustrate the differences in morphology of the untreated and pretreated PP and PSD samples, as shown in Figure 3.3.

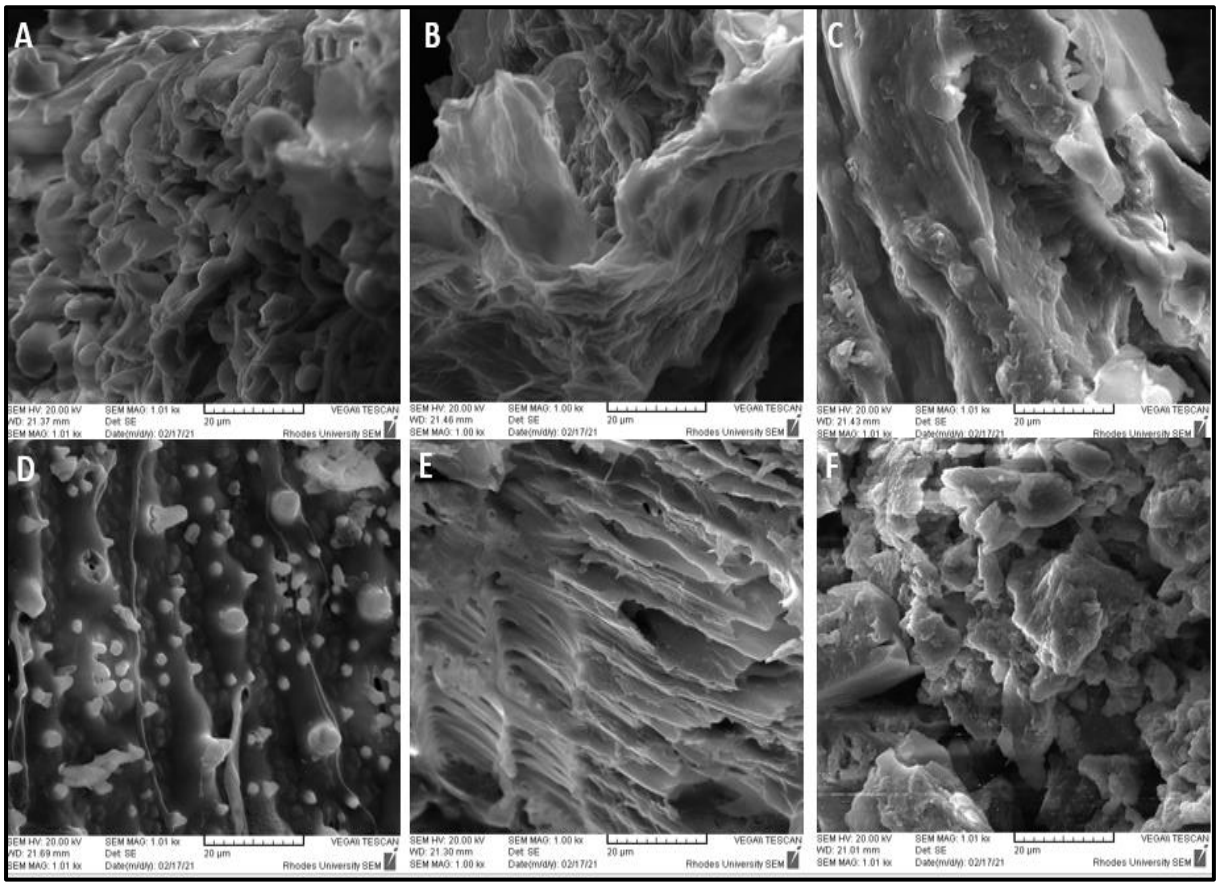

Figure 3.3: SEM images of untreated, delignified, and delignified + PAS PSD and PP at 1000× magnification. A: untreated PP; B: delignified PP; C: Del + PAS PP; D: untreated PSD; E: delignified PSD; and F: Del + PAS PP.

The surfaces of the untreated versus the pretreated substrates showed different morphologies for both PP and PSD. Untreated substrates; PP and PSD, displayed bud-like structures which are likely to be lignin (Figure 3.3A and D). The delignification of the substrates resulted in the removal of these buds on the surfaces of these substrates (Figure 3.3B and E). Figure 3.3E had a rougher surface compared to untreated PSD in Figure 3.1D which has a relatively smooth surface underneath the buds. PAS substrates had a relatively more puffed-up surface compared to the untreated and delignified substrates Figure 3.3C and F. The fibres on the PAS substrates were more compact compared to untreated and delignified substrates for PP and they showed disordered morphology in PSD.

3.4.5. Histochemical analysis for lignin

Histochemical analysis for the presence of lignin in PP and PSD was conducted using the Wiesner method. Two parts of 5% (w/v) phloroglucinol were mixed with one part concentrated HCl prior to staining, and the samples were viewed using an Olympus BX40 light microscope and images were captured using an Olympus DP72 digital camera. The images are presented in Figure 3.4.

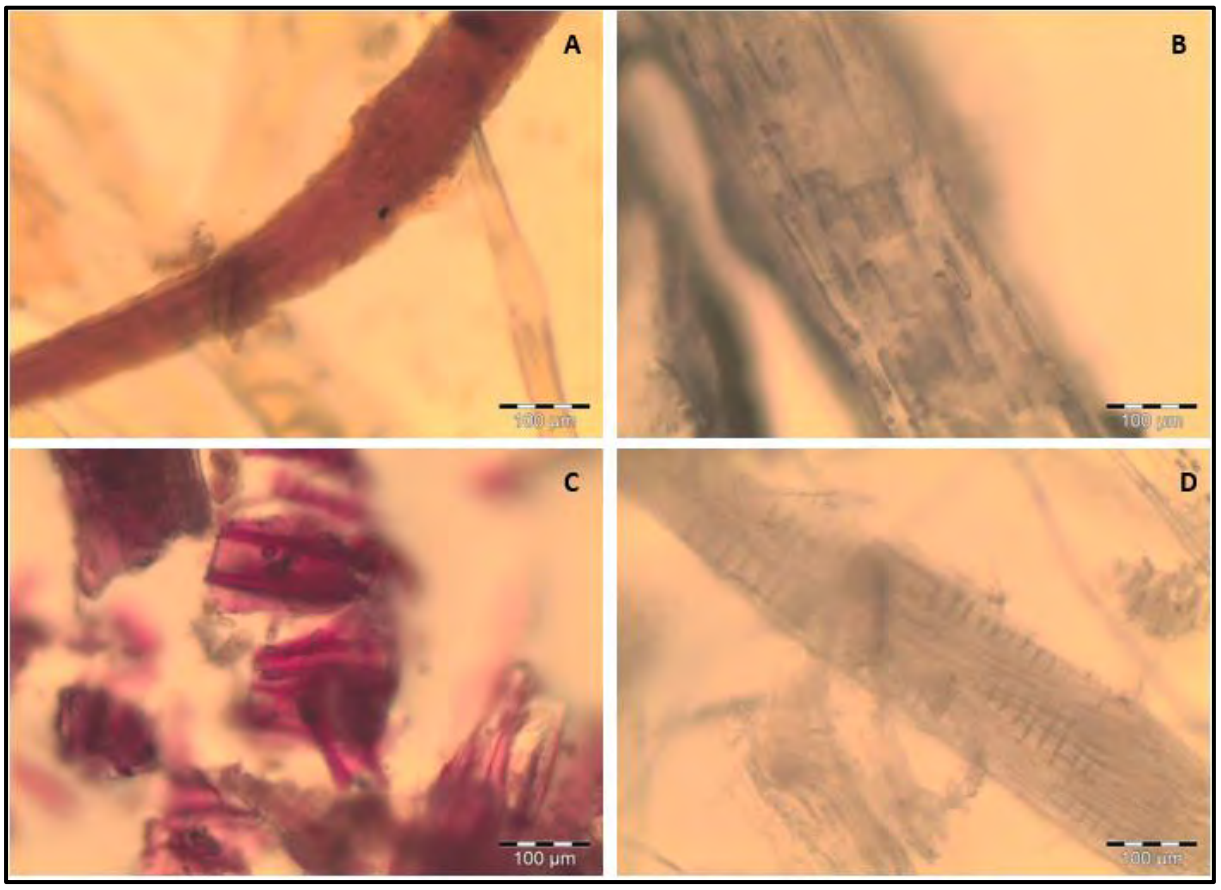

Figure 3.4: Histochemical analysis for lignin using the Wiesner method (phloroglucinol-HCl). (A) Untreated PP; (B) Delignified PP; (C) Untreated PSD; (D) Delignified PSD. Scale bar: 100 µm; 10× magnification.

Untreated PP was lightly stained by the phloroglucinol solution, indicating the presence of lignin in small amounts while delignified PP was not stained by the phloroglucinol solution (Figures 3.4A and B). Untreated PSD was heavily stained by the solution, indicating high levels of lignin in this biomass (Figure 3.4C), while delignified PSD was unstained, indicating that lignin was removed upon pretreatment (Figure 3.4D).

3.4.6. Optimisation of Man26A reaction conditions on PP and PSD

3.4.6.1. Hydrolysis of untreated and pretreated biomass

To determine which pretreatment released the highest amount of reducing sugars when hydrolysed with Man26A, untreated, delignified (Del) and phosphoric acid swollen (PAS) PP and PSD samples were hydrolysed with 0.2 mg/ml of Man26A at 50°C over a 72-hour period. The results obtained are presented in Figure 3.5 below.

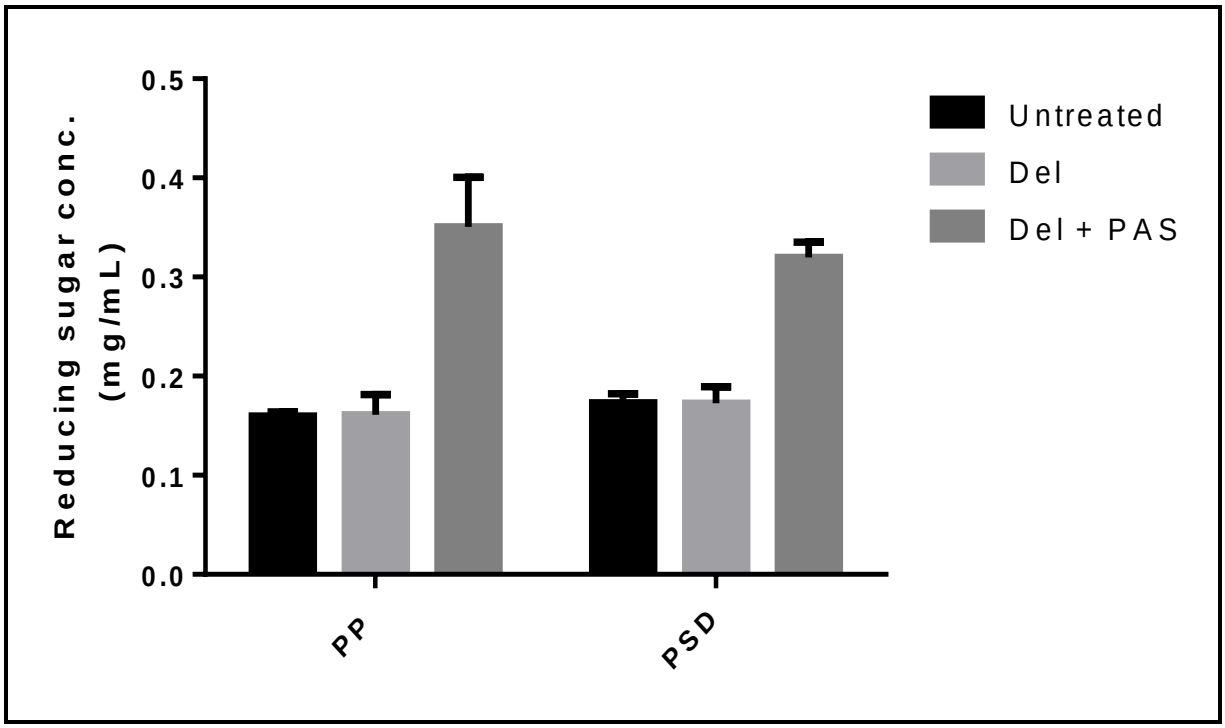

Figure 3.5: Hydrolysis of untreated, delignified, and delignified and phosphoric acid swollen biomass wastes using Man26A. Values represent means ± SD (n = 3).

Hydrolysis of untreated, delignified and PAS PP and PSD using Man26A showed a difference in the concentrations of reducing sugars released, as seen in Figure 3.5. Untreated and Del substrates released reducing sugars to a concentration of approximately 0.16 to 0.17 mg/ml. These concentrations were lower compared to those released from the Del + PAS substrates, which released reducing sugar concentrations above 0.3 mg/ml from each substrate. Del + PAS substrates were therefore employed in further studies.

3.4.6.2. Optimising enzyme concentration and reaction time

To establish the optimum conditions for hydrolysis of Del + PAS PP and Del + PAS PSD by Man26A, enzyme loading and time studies were conducted for the substrates. For enzyme loading studies, different concentrations of Man26A were used with 4% (w/v) substrate. The time study was conducted at intervals of 0, 1, 3, 6, 12, 24, 48, and 72 hours, using 4% (w/v) substrate and 0.1 mg/ml of enzyme. The results are shown in Figures 3.6A and B below.

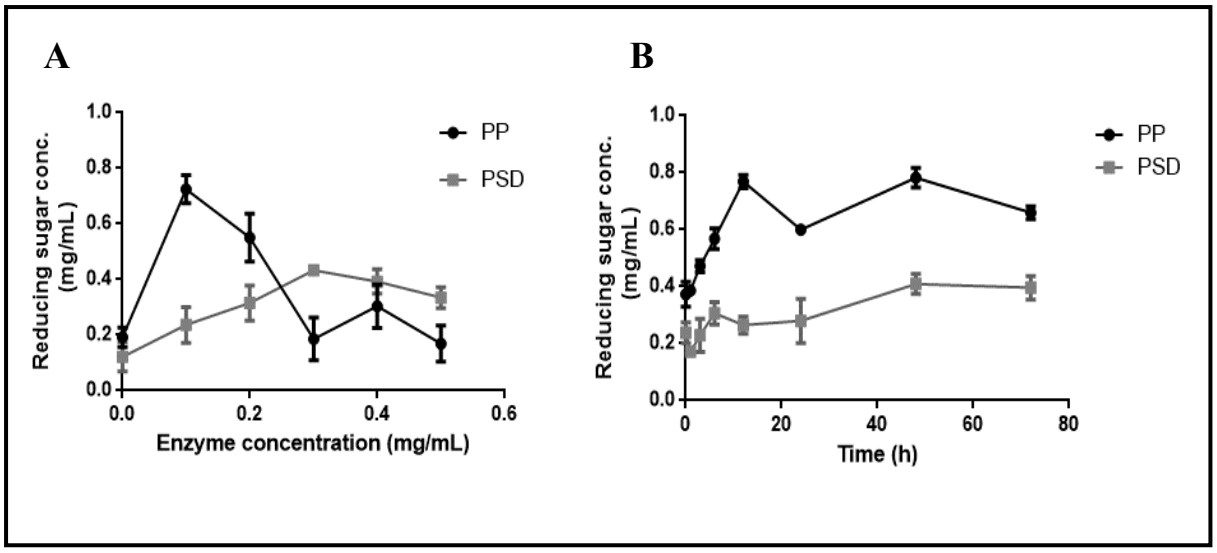

Figure 3.6: Optimising Man26A reaction conditions on LBW substrates. A) optimising Man26A enzyme loading and B) Man26A reaction over time. The values represent means ± SD (n = 3).

Figure 3.6A shows that the highest reducing sugar concentration of approximately 0.7 mg/ml was obtained at 0.1 mg/ml for PP. A decrease in the reducing sugar concentration was observed at 0.3 mg/ml of enzyme loading. The highest reducing sugar concentration of approximately 0.4 mg/ml was obtained at 0.3 mg/ml of enzyme for PSD. There was a slight decrease in the reducing sugar produced by PSD at enzyme concentrations above 0.3 mg/ml. From Figure 3.6B, it can be seen that the highest concentration of reducing sugar was released from PP at 12 hours of hydrolysis, while the highest concentration of reducing sugar released from PSD was obtained after 48 hours of hydrolysis.

3.5. Discussion

In this study, LBW was pretreated using two different pretreatment methods, namely delignification using sodium chlorite/acetic acid, and swelling with phosphoric acid. The carbohydrate composition of the untreated and pretreated substrates was determined. The

change in the chemical structure of untreated and pretreated substrates was assessed using FTIR, while the effects of pretreatment on the morphology of the substrates were visualised using SEM and light microscopy. Finally, the optimal hydrolysis conditions for both substrates were established for the optimal production of MOS.

Carbohydrate composition analysis for both substrates revealed a high glucan content compared to other sugars. The glucose detected in these samples accounts for glucose in both the cellulose and hemicellulose fractions of the biomass (Gao et al., 2013). The decrease observed in the carbohydrate fraction, specifically for glucose, may be due to the solubilisation of some of the cellulose during pretreatment. It has been reported that some pretreatment methods solubilise the cellulose and hemicellulose fractions (Siqueira et al., 2013). The values for the monosaccharide composition of PP were inconsistent with those reported in literature, as reported by Malgas and Pletschke (2020) and Smith and Harris (1995). The differences in the composition of the monosaccharides may be attributed to the site where the pineapples were harvested. The glucan and mannan composition for PSD was consistent to that of Kangas et al. (2019) and Satari et al. (2019). The xylan and galactan values, however, were different to literature values. Higher galactan values were reported in this study compared to literature values, while lower xylan values were reported in this study compared to literature values. Literature values for the carbohydrate composition of PP and PSD sugars are presented in Table 3.3 below.

Table 3.3: Literature values for the monosaccharide composition of pineapple pulp and pine sawdust

	% composition				
	Glucan	Mannan	Xylan	Galactan	References
PSD	40.30; 38.2	11.69; 11.3	6.29; 8.5	2.18; 4.3	Kangas et al. 2019; Satari et al. 2019;
PP	32.5; 47	1.5; 2.25	22.8; 29	2.5; 7.25	Malgas and Pletschke, 2020; Smith and Harris, 1995.

The FTIR spectra for both PP and PSD displayed transmittance peaks corresponding to polysaccharides at 3338, 1977, 1635, 1371 and 1028 cm^{-1} (Hu et al., 2019). Stretching bands were observed in the –OH region between 3000 and 3600 cm^{-1} for both untreated PP and PSD. This stretching may also be attributed to the presence of lignin and phenolic groups (Charis et al., 2020; Hadidi et al., 2020; Cavali et al., 2020). The peak at 1028 cm^{-1} may be attributed to the presence of a pyranose ring, which is part of the polysaccharides present in these substrates (Hu et al., 2019). These results indicate that the substrates have characteristics of polysaccharides, which have been shown to be present in the samples.

TGA analysis revealed that untreated and delignified samples begin to break down at approximately 250°C for both PP and PSD. This is the temperature at which biomass substrates commonly start to break down with heating (Márquez-Montesino et al., 2021; Hadidi et al., 2020). The rate of decomposition of the untreated samples is slightly lower than delignified samples, as lignin decomposition occurs over a wide range of temperatures, which may even exceed 400°C (Márquez-Montesino et al., 2021). Del + PAS samples start to break down much earlier compared to the untreated and delignified samples. This is relatively unexplained in literature, but it could be caused by the disruption of crystalline cellulose caused by pretreatment, which would cause the samples to degrade faster. The Del + PAS samples also contain a higher ash content at the end of the reaction, which may be attributed to the presence of phosphoric acid.

SEM analysis revealed differences on the surfaces of untreated and pretreated substrates. Untreated substrates showed bud-like structures that are most likely to be lignin, whereas these were removed with subsequent pretreatment steps. The surface of delignified substrates had a rough structure that indicates that the lignin layer had been removed from the surface. Removal of lignin has been shown to result in a coarse and uneven surface due to the fibre structure being damaged (Nan et al., 2018). SEM images of PP and PSD by Selvam et al. (2014) and Cavali et al. (2020) showed a change in surface morphology, where external microfibres on the surface of PP were shown to be removed to reveal an altered structure with a rough surface. Similarly, the SEM images for PSD showed a rough surface containing pores post delignification. Zhang et al. (2006) showed that phosphoric acid swollen cellulose (PASC) and Avicel were more amorphous compared to untreated substrates, which supports the results in this study. Lignin removal upon pretreatment was also observed with light microscopy, where lignin containing samples were stained violet because of the reaction between phloroglucinol and the cinnamaldehyde end-groups of lignin (Mitra and Loqué, 2014). Delignified samples

for both PP and PSD remained unstained and exhibited an opaque colour under light microscopy, which indicates that lignin had been removed in these samples. Several papers have reported that lignin containing samples appear red under light microscopy, compared to samples that do not have lignin (Sim et al., 2020; Raina et al., 2020).

In this study, low concentrations of reducing sugars were produced by enzymatic hydrolysis using Man26A, even after the substrates had been delignified. Enzymatic hydrolysis of untreated PP and PSD produced approximately 0.16 to 0.17 mg/ml of reducing sugars from both substrates. This indicated the need for a second pretreatment step. Enzymatic hydrolysis of PAS substrates was more efficient, compared to the enzymatic degradation of substrate only pretreated with sodium chlorite/acetic acid. Delignification using sodium chlorite has been shown to increase the susceptibility of LB to enzymatic hydrolysis (Park et al., 2015). A disadvantage of delignification is the compacting of polysaccharides following the removal of lignin, known as hornification (Koo et al., 2020; Yang et al., 2018). Hornification is a result of cellulose being partially dried after lignin removal (Koo et al., 2020). This may make it difficult for the enzyme to hydrolyse the polysaccharides (Koo et al., 2020). Lignin has been shown to play a key role in preventing cellulose re-crystallinity (Sun et al., 2014). A two-step pre-treatment process is often required to overcome the recalcitrance of LB during its enzymatic degradation (Houfani et al., 2020). Phosphoric acid swelling of cellulose is a widely studied pretreatment method that results in crystalline cellulose being changed into amorphous cellulose, thereby increasing the susceptibility of LB to enzymatic degradation (Zhang et al., 2018). Sun et al. (2014) also showed that delignification followed by dilute acid pretreatment significantly increased sugar release, compared to untreated or delignified samples.

3.6. Conclusions

The monosaccharide composition of untreated and pretreated substrates was successfully determined using Megazyme kits. The thermal properties of the substrates were determined using thermogravimetry, and the chemical composition of untreated and pretreated substrates was analysed using FTIR. Delignification of PP and PSD was successful, as shown by SEM and histochemical analysis data. A second pretreatment step, phosphoric acid swelling of the substrates, was necessary to release more reducing sugars from the samples. The hydrolysis parameters for the hydrolysis of both substrates were optimised for the production of reducing sugars from PP and PSD. Del + PAS substrates at 8% (80 mg/ml) substrate loading and 0.1 mg/ml of enzyme over 24 hours were used for further experiments. In the next chapter, MOS

produced from Del + PAS PP and PSD will be characterised according to structural and bioactivity properties.

Chapter 4: Characterisation of mannooligosaccharides derived from lignocellulosic biomass waste

4.1. Introduction

Mannooligosaccharides (MOS) are short chain mannan-derived oligosaccharides with a degree of polymerisation (DP) of approximately one to ten (Jana et al., 2021a; Suryawanshi and Kango, 2021; Mano et al., 2018). MOS are divided into α- and β-MOS, depending on whether they are derived from yeast cell walls or plants, respectively (Jana et al., 2014; Kango et al., 2020; Yamabhai et al., 2014). α-MOS are derived from mannans that are linked by α-1,6-linkages in the mannan polymer, while β-MOS are derived from mannans with β-1,4-glycosidic bonds (Kango et al., 2020). Many studies have shown the production of MOS using model mannan substrates, such as locust bean gum (LBG), guar gum (GG), ivory nut mannan (INM), and konjac gum mannan (KGM). These substrates generate MOS with different substitution patterns and varying DP, depending on the substitution ratios in the mannans. The highly viscous and highly substituted GG has been shown to produce MOS with a DP>6 when hydrolysed enzymatically (Magengelele et al., 2021). INM is unsubstituted and a relatively short polysaccharide that is insoluble and less susceptible to enzymatic hydrolysis, in comparison to GG and LBG (Magengelele et al., 2021; Monteiro et al., 2019; Grimaud et al., 2019).

MOS can be synthesised by physical, chemical and enzymatic methods (Kango et al., 2020; Yamabhai et al., 2014). Physical methods for the production of MOS include radiation degradation, but these usually produce high molecular weight polysaccharides with low yields of mannan (Li et al., 2020). Chemical synthesis methods have the drawback of requiring pH neutralisation post hydrolysis, which can lead to changes in the nature of the MOS by changing their chemical composition (Jana et al., 2021a). No such drawback exists in the physical method of MOS synthesis, although equipment such as batch reactors are required for production (Jana et al., 2021a). The enzymatic production of MOS is the most preferred method, as enzyme hydrolysis can be kinetically controlled to produce the desired end products, and a higher recovery of food-grade MOS has been reported (Jana and Kango, 2020; Jian et al., 2015).

MOS can be used as dietary fibre as they have been shown to have prebiotic potential. In addition, MOS can exhibit antioxidant, antitumorigenic and antiglycation activities, and can be

used to prevent fat storage (Jana and Kango, 2020; Jian et al., 2015). The use of MOS as prebiotics has received increased attention in recent years and much research has been done to elucidate the prebiotic activity of MOS. Jana and Kango (2020) have also shown the antioxidant potential of MOS using the 2,2'-azino-bis(3-ethylbenzothiazoline-6-sulfonate) ($ABTS^{+\bullet}$) and (2,2-diphenyl-1-picryl-hydrazyl-hydrate) (DPPH) radical scavenging methods.

In this study, Man26A was used to produce MOS from biomass waste substrates delignified and phosphoric acid swollen pineapple pulp and pine sawdust (Del + PAS PP and PSD). The produced MOS were then characterised by determining their diversity, chemical composition and stability.

4.2. Aims and objectives

4.2.1. Aim

To characterise MOS produced from lignocellulosic biomass waste substrates by Man26A hydrolysis by determining their diversity, chemical composition and stability.

4.2.2. Objectives

- To analyse the action pattern and hydrolysis products of Man26A on LBW substrates using thin layer chromatography (TLC) and high performance liquid chromatography (HPLC);
- To determine the chemical composition of the produced MOS using FTIR;
- To determine the thermal properties of the MOS produced from LBW substrates;
- To determine the effect of pH on MOS produced from LBW substrates; and
- To determine the effect of bile salts and digestive enzymes on the MOS produced from (Del + PAS PP and PSD.

4.3. Methods

4.3.1. Characterisation of the produced MOS

The action pattern of Man26A and the hydrolysis products obtained from Del + PAS PP and PSD were characterised using the TLC and HPLC methods described in Sections 2.3.7.1 and 2.3.7.2, respectively.

4.3.2. FTIR analysis of produced MOS

FTIR analysis of produced MOS was conducted as described in Section 3.3.5.

4.3.3. Determination of the effect of temperature on the stability of MOS

The thermal stability of the produced MOS was determined using TGA as described in Section 3.3.4.

4.3.4. Determination of the effect of pH on the stability of MOS

The MOS was incubated in a Britton-Robinson Universal buffer with pH values ranging from 2 to 10 and incubated for 3 hours at room temperature. The reducing sugar content was determined using the DNS method as described in 2.3.3. TLC was conducted as described in Section 2.3.7.1.

4.3.5. Assessment of the gastrointestinal tolerance of the produced MOS

Bile salts (0.3% (w/v)), 1 mg/ml of pepsin, trypsin, mucin and α-amylase were prepared in 50 mM citrate buffer (pH 5.0). PP and PSD derived MOS were incubated with the different samples in a 1:1 ratio and incubated at 37°C for 4 hours. Reducing sugars were quantified using the DNS method as described in Section 2.3.3 and TLC was conducted as described in Section 2.3.7.1.

4.4. Results

4.4.1. Analysis of the action pattern and hydrolysis products of Man26A on lignocellulosic biomass waste substrates

TLC was used to identify the products obtained from the hydrolysis of Del + PAS PP and PSD (Figure 4.1).

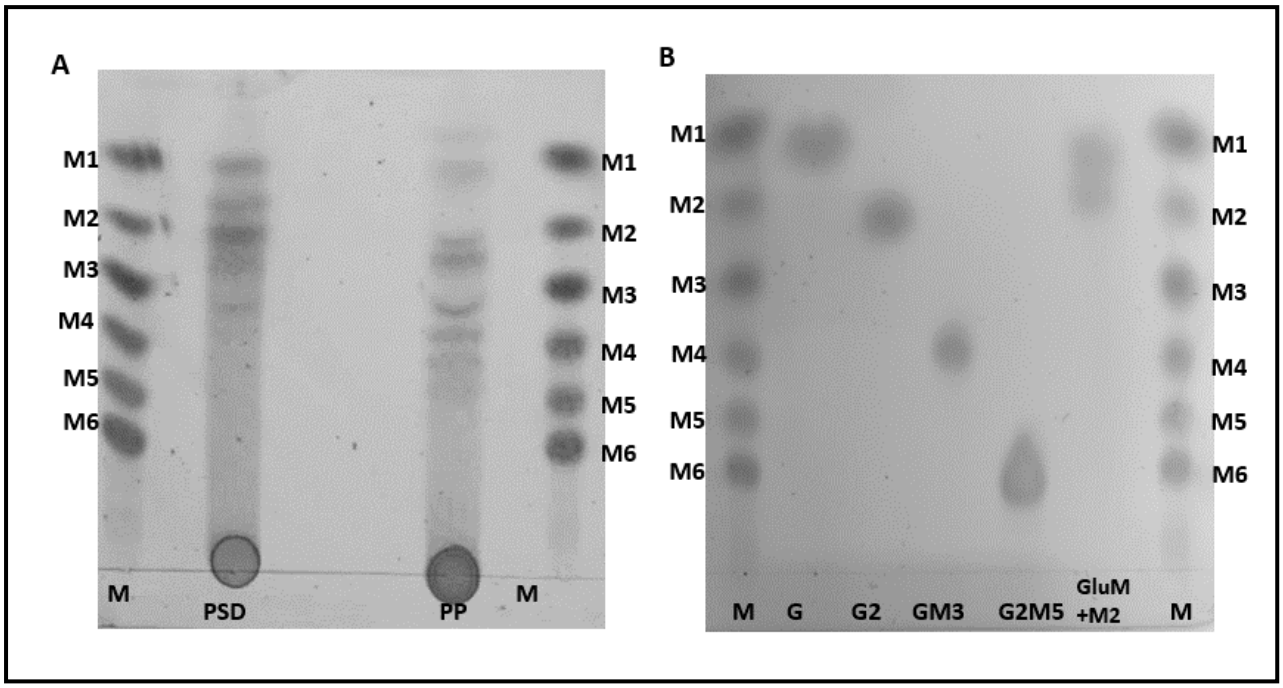

Figure 4.1: Action pattern and hydrolysis products of Man26A. A) MOS derived from Del + PAS PP and PSD. M1–M6: mannosyl standards mannose, mannobiose, mannotriose, mannotetraose, mannopentaose and mannohexaose, respectively; M: MOS standards. B) Galatosyl standards running alongside MOS standards. M1 – M6: MOS standards; G: galactose; G2: galactobiose; GM3: Galactosyl-mannotriose; G2M5: digalactosyl-mannopentaose; GluM + M2: Glucosyl mannobiose.

Figure 4.1A shows MOS derived from Del + PAS PP and PSD. Del + PAS PSD produced bands running between M1 and M2, a band at M2, and a smaller band between M3 and M4 on TLC. Del + PAS PP produced a band running just below M1, two bands running between M2 and M3, bands running between M3 and M4, and a poorly resolved band running between M4 and M5. Similar results were observed with HPLC, as seen in Table 4.1 below. Figure 4.2B depicts galactose standards running between mannose standards, which confirms the identity of MOS running between mannose standards in Figure 4.1A as galactose substituted MOS. Glucose substituted MOS also run in between the MOS standards, as can be seen with GluM + M2, which also suggests that substituted MOS generally run in between MOS standards.

Table 4.1: MOS profile for Del + PAS PP and PSD derived MOS obtained by hydrolysis with Man26A (as determined by HPLC)

	MOS produced (mg/ml)						
Substrate	M1	M2	M3	M4	M5	M6	TRS*
PP	0.0264	0.0865	0.206	0.139	0.186	0.0878	0.635
PSD	0.223	0.140	-	0.165	-	-.	0.761

**TRS – total reducing sugars as determined by the DNS method.*

The MOS profile obtained using HPLC shows that Del + PAS PP produced DP1 – 6 MOS. Mannotriose (M3) was the major MOS produced at a concentration of 0.206 mg/ml, followed by mannopentaose (M5) and mannotetraose (M4) at 0.186 and 0.139 mg/ml, respectively. Del + PAS PSD derived MOS were less diverse compared to those obtained from Del + PAS PP, having only M1, M2, and M4. Del + PAS PSD produced M1 as the major product at a concentration of 0.223 mg/ml. M2 and M4 had concentrations of 0.140 and 0.165 mg/ml, respectively.

4.4.2. FTIR analysis of MOS

FTIR analysis of the MOS produced from Del + PAS PP and PSD using Man26A was conducted to determine their chemical properties. The results are presented in Figure 4.2 below.

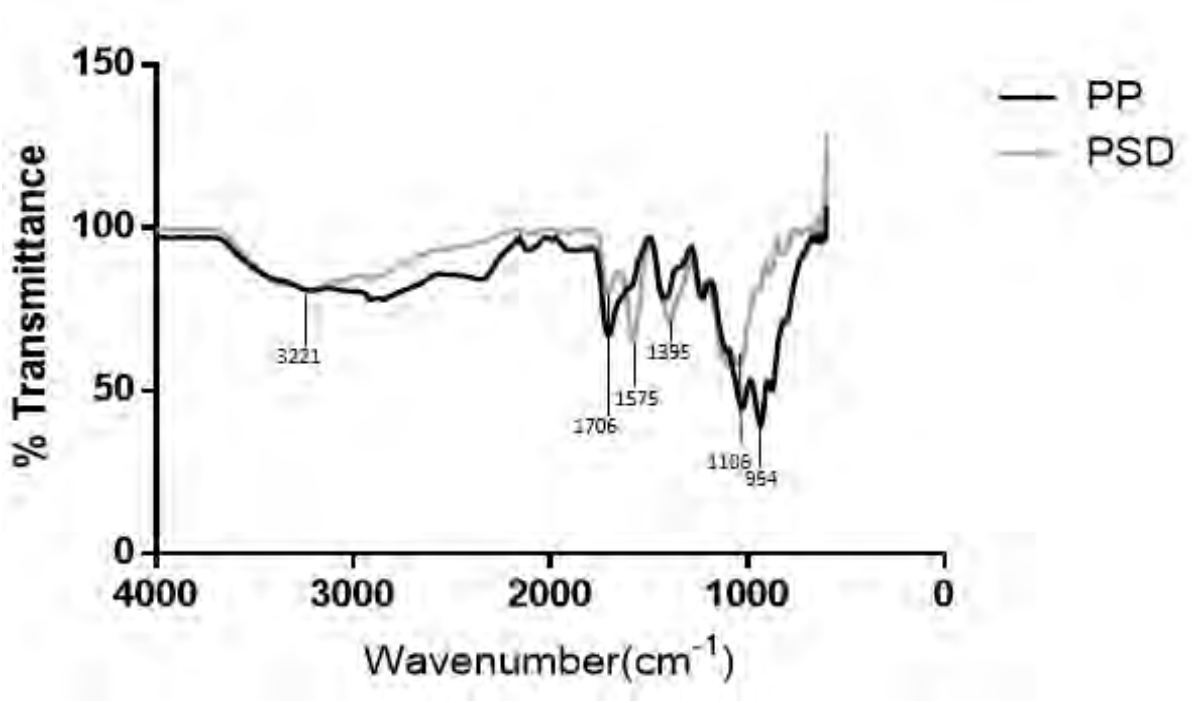

Figure 4.2: FTIR analysis of MOS produced from Del + PAS PP and PSD.

FTIR analysis of MOS revealed a peak associated with the presence of carbohydrates at approximately 3220 cm^{-1}. Peaks corresponding to acetyl groups were also observed at approximately 1706 cm^{-1} for both samples. A peak at 1575 cm-1 was observed for Del + PAS PSD derived MOS.

4.4.3. The effect of temperature on MOS stability

The effect of temperature on the stability of MOS produced from Del + PAS PP and PSD was determined using TGA, and the results are displayed in Figure 4.3 below.

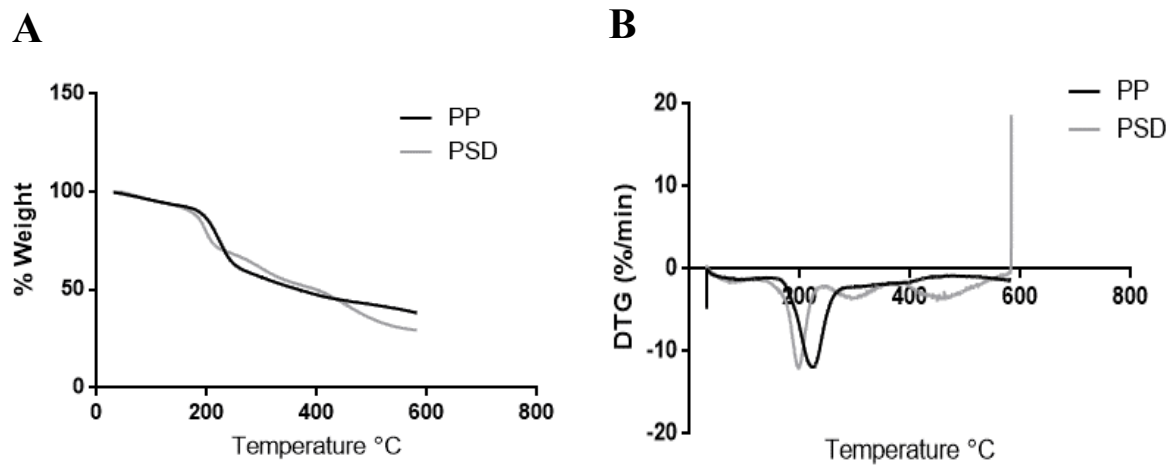

Figure 4.3: The effect of temperature on the stability of Del + PAS PP and PSD derived MOS. (A) TGA and (B) DTG thermograms of Del + PAS PP and PSD derived MOS.

Figures 4.3A and B show that the MOS derived from Del + PAS PP and PSD are stable at temperatures below 213 and 191°C, respectively. Thermal decomposition occurred faster in PSD derived MOS than it did for PP derived MOS. Residual mass was observed for MOS derived from both substrates.

4.4.4. The effect of pH on MOS stability

To determine the effect of pH on MOS derived from Del + PAS PP and PSD, these samples were incubated at different pH vlaues at 37°C for a period of 3 hours (Figure 4.4).

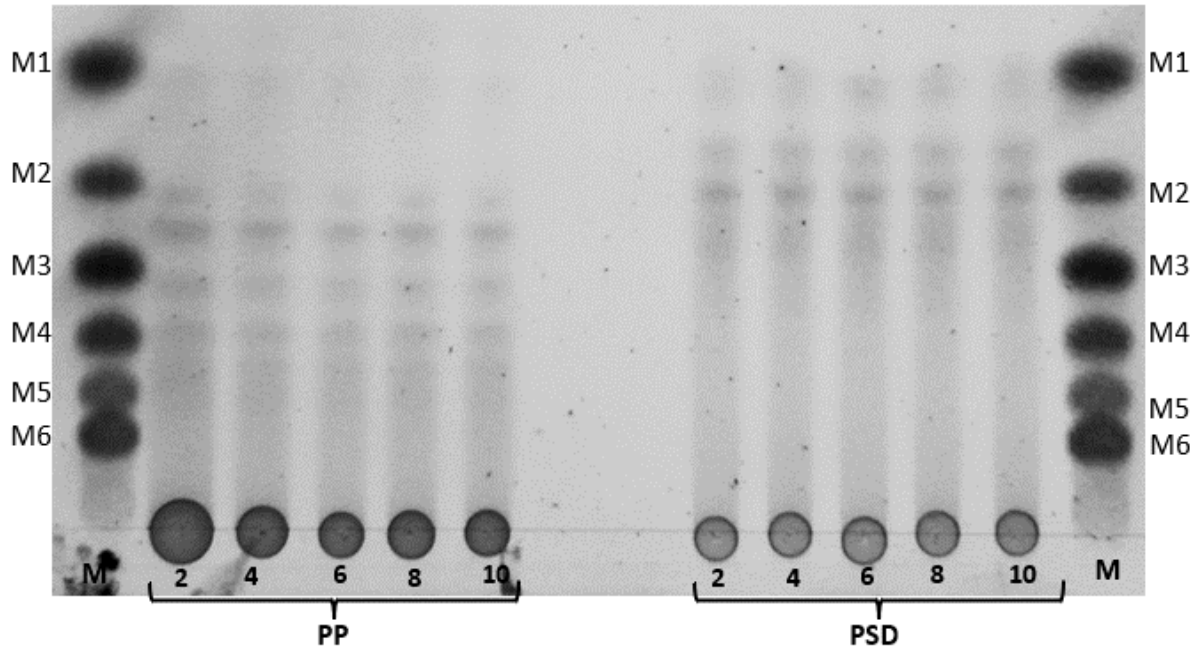

Figure 4.4: TLC representing the effect of pH on the stability of MOS produced from Del + PAS PP and PSD by Man26A. M: MOS standards; M1 – M6: mannose, mannobiose, mannotriose, mannotetraose, mannopentaose and mannohexaose. PP – pineapple pulp; PSD – pine sawdust.

Figure 4.4 shows the MOS profile observed on TLC for the stability of MOS at different pH conditions, ranging from pH 2 to 10. It shows that the MOS diversity remains unchanged from the MOS observed in Figure 4.1 and the MOS profile obtained using HPLC (Table 4.1).

4.4.5. Gastrointestinal tolerance test

To determine the effect of bile salts and GI tract enzyme, PP and PSD derived MOS were incubated at 37°C with 0.3% (w/v) bile salts and 1 mg/ml of either α-amylase, trypsin, mucin and pepsin. The results obtained are displayed in Figure 4.5 below.

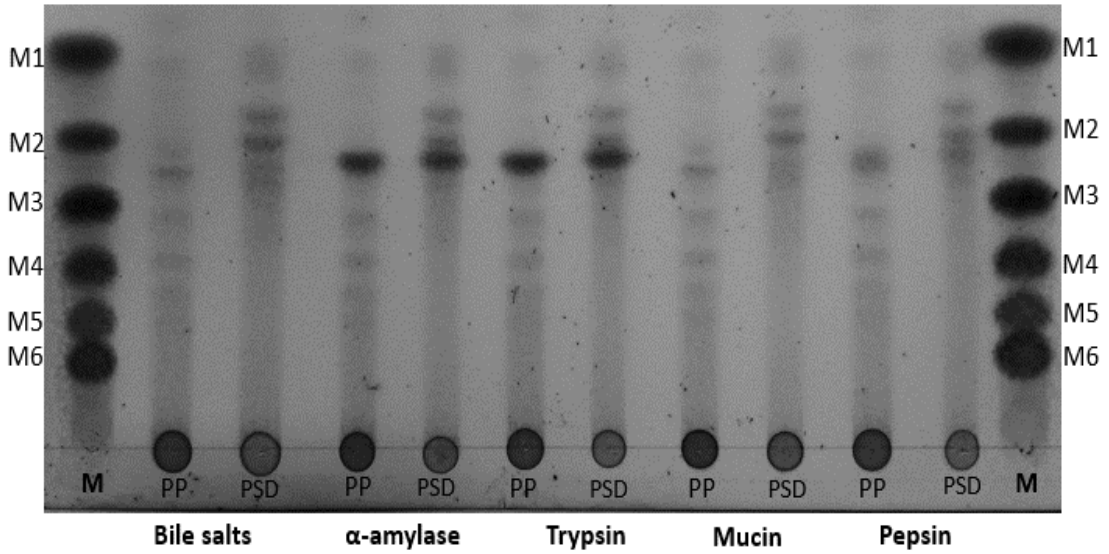

Figure 4.5: The effect of bile salts and digestive enzymes on the stability of Del + PAS PP and PSD derived MOS. M – MOS standards; PP – pineapple pulp; PSD – pine sawdust.

Figure 4.5 shows that Del + PAS PP and PSD derived MOS are resistant to digestion by bile salts and digestive enzymes, as seen on the TLC plate. The diversity of MOS observed in Figure 4.5 is the same as that seen in Figure 4.1A, indicating that these MOS may survive passing through the GI tract and remain unchanged.

4.5. Discussion

MOS were produced by the enzymatic hydrolysis of model mannan substrates LBG, GG and INM using Man26A. The produced MOS were characterised according to the diversity of the MOS obtained post hydrolysis, their stability under different temperatures and pH for model mannan substrates and their antioxidant activity. Characterisation of MOS produced from the hydrolysis of model mannan substrates was conducted to determine the action pattern of Man26A and to predict the behaviour of the hydrolysis products under different conditions.

Del + PAS PP and PSD produced MOS with varying DP. TLC shows that MOS produced from enzymatic hydrolysis of Del + PAS PSD produced MOS running between M1 and M2, M2, and a small band between M3 and M4. These results were similar to those observed using HPLC, where the highest reducing sugar quantified was M1 at a concentration of 0.223 mg/ml, followed by M4 at 0.165 mg/ml and M2 at 0.140 mg/ml. Del + PAS PP derived MOS had a

higher diversity compared to those of Del + PAS PSD. MOS produced ran between the MOS standards, which suggested that these MOS were substituted. Del + PAS PP derived MOS also revealed a greater diversity upon analysis with HPLC, where MOS from M1 to M6 were observed. Enzymatic hydrolysis of galactoglucomannan has been previously reported to produce mainly mannobiose (M2), with MOS with a DP of 3 – 8 also observed (Polari et al., 2012). The hydrolysis of spruce galactoglucomannan (SpGGM) with CjMan26A also yielded M2 as its primary MOS. M3 was also produced in substantial amounts, with minimal M1 and M4 observed (Bååth et al., 2018). These findings correlate with those obtained in this current study, as oligosaccharides running just above and below M2 were the main oligosaccharides observed on TLC. These may be MOS with glucose or galactose substitution, i.e. glucosyl-mannose, glucosyl-mannobiose, galactosyl-mannobiose, or galactosyl-glucosyl-mannobiose, as galactosyl substituted MOS have previously been reported to migrate in between MOS standards (Magengelele et al., 2021).

MOS produced from Del + PAS PP and PSD showed thermal stability at temperatures below 200°C for PP and PSD, as shown through the thermogravimetric analysis of these products in Figure 4.3. Thermal decomposition of oligosaccharides occurs over different stages. Water from the samples evaporates first, between 50 and 150°C, followed by degradation of low molecular weight oligosaccharides, degradation of the hemicellulose backbone, and then finally, degradation of the residue to gaseous products (Dávila et al., 2019; Srivastava et al., 2017). MOS produced from Del + PAS PP and PSD were stable at different pHs. This is shown by the sugar profiles on TLC which remained unchanged at all the pH ranges tested (Figure 4.4). MOS may be added to foods that undergo frying, baking, and roasting during their use as functional foods. It is, therefore, important to consider their stability under different thermal conditions for their effective utilisation (Srivastava et al., 2017). The processing of food products for preservation may expose them to significant heat-flow density (Zhang et al., 2021; Matusek et al., 2009). The reducing sugars are not degraded under these conditions, which indicates that the MOS produced from LBW substrates can survive the manufacturing process, with the biological activity of the MOS remaining unchanged. Zhang et al. (2021) evaluated the stability of MOS produced from LBG and palm kernel cake (PKC) by autoclaving them at 121°C and 15 lbs pressure and found that the MOS remained relatively unaffected by high temperature and pressure.

The stability of MOS in the presence of bile salts and the digestive enzymes α-amylase, trypsin, mucin and pepsin was also investigated (Figure 4.5). It was shown that they are resistant to hydrolysis by bile salts and different digestive enzymes. This suggests that PP and PSD derived MOS are not digested by human gastric enzymes and may pass through the GI tract unchanged. This makes MOS suitable for application as they will only be hydrolysed by the probiotic bacteria that exist in the human gut. No studies on the stability of MOS in the presence of digestive enzymes and bile salts are available in literature to support our findings.

4.6. Conclusions

Man26A produced different MOS with different DPs from PP and PSD. A more diverse array of MOS was produced from PP, with MOS ranging from M1 – M6, as observed by HPLC. The MOS produced were stable at various pH values, and were stable at temperatures below 250°C. These MOS were also resistant to bile salts and digestive enzymes. This part of the study showed that PP and PSD derived MOS are suitable for use as prebiotics. In the next chapter, the prebiotic activity of MOS derived from PP and PSD will be assessed, in order to ascertain whether these MOS have a positive influence on the growth of probiotic bacteria, as well as other beneficial biological effects.

Chapter 5: *In vitro* prebiotic effect of MOS; influence on bacterial growth and surface properties, and antioxidant effect

5.1. Introduction

Prebiotics promote the growth of beneficial organisms while inhibiting the growth of pathogenic bacteria (Gibson et al., 2017). Prebiotics have gained much interest because of their beneficial effect on human and animal health, where they have potential to replace antibiotics, which have been banned for use in livestock farming in Europe, due to increased microbial resistance (Utami et al., 2013). There has been increasing interest in using agricultural waste substrates for the production of prebiotics, because these feedstocks are inexpensive and abundant, as they are produced in large amounts from various agro-processing industries (Faryar et al., 2015). Mannan-rich agricultural waste substrates such as spent coffee grounds (SCG), palm kernel cake (PKC) and copra meal (CM) have been used as a source of prebiotic MOS (Jana and Kango, 2020; Pérez-Burillo et al., 2019). Prebiotic MOS obtained from LBW show the same potential for their use as MOS prebiotics which are made from model mannan substrates (Jana et al., 2021a). Prebiotics obtained from LBW can therefore be manufactured in large amounts because of the abundance of LBW, which will benefit both the environment and human health (Hlalukana et al., 2021).

Prebiotic oligosaccharides have been shown to increase the adhesion properties of probiotics to the intestinal mucosa (Monteagudo-Mera et al., 2019). Probiotic bacteria have been documented to possess auto-aggregation properties and biofilm formation capability (Monteagudo-Mera et al., 2019; Trunk et al., 2018). Bacterial auto-aggregation and biofilm formation enable probiotics to survive unfavourable environmental conditions, such as increased resistance to gastric pH, temperature and mechanical forces (Trunk et al., 2018; Salas-Jara et al., 2016). Biofilms are beneficial as they allow bacteria to reside in the gut for long periods of time, exerting a more sustained probiotic effect on the host, as they do not get washed out of the host easily like their planktonic counterparts (Monteagudo-Mera et al., 2018; Salas-Jara et al., 2015). A class of molecules known as agglutinins influence bacterial auto-aggregation, and these can be proteins or carbohydrates known as exopolysaccharides (Trunk et al., 2018).

Many known probiotic bacteria belong to the Gram-positive lactic acid bacteria (LAB) and are mainly from the *Lactobacillus* and *Bifidobacterium* genera (Kimelman and Shemesh, 2019).

LAB is usually found in milk and dairy products, and are industrially important microorganisms (Yerlikaya et al., 2020; Akpinar et al., 2011), where *Lactobacillus bulgaricus* and *Streptococcus thermophilus* are used as yoghurt starter cultures. *L. bulgaricus* and *S. thermophilus* have a symbiotic relationship in yoghurt cultures (Yerlikaya et al., 2020). *Bacillus subtilis* is a spore forming bacterium commonly found in soils or the GI tracts of humans (Kimelman and Shemesh, 2019). *B. subtilis* promotes the growth and cell viability of LAB, as well as helping to maintain a balance in the beneficial gut microbiota (Kimelman and Shemesh, 2019).

In this section, the effect of MOS produced from PP and PSD on probiotic bacteria (*L. bulgaricus*, *S. thermophilus* and *B. subtilis*) were determined based on their influence on the growth, auto-aggregation and biofilm formation of these probiotic strains.

5.2. Aims and objectives

5.2.1. Aim

To determine the biological effect of MOS produced from PP and PSD by assessing their prebiotic effect, biofilm formation ability and antioxidant potential.

5.2.2. Objectives

- To determine the prebiotic effect of MOS on probiotic bacteria (*L. bulgaricus*, *S. thermophilus* and *B. subtilis*);
- To determine the influence of MOS on the auto-aggregation ability of the probiotics;
- To determine the influence of MOS on the biofilm formation ability of the probiotics;
- To determine the antioxidant ability of the produced MOS; and
- To determine the effect of bile salts on the activity of MOS.

5.3. Methods

5.3.1. Scaling up MOS production from PP and PSD

Using the optimised conditions determined in Section 4.4.3. MOS production was scaled up to 12 ml reactions using 0.1 mg/ml Man26A and 80 mg/ml (8% (w/v)) substrate concentration for both PP and PSD. The reactions were carried out for 24 hours, rotating at 50 rpm at 50°C in 50 mM citrate buffer at pH 5.

5.3.2. Determining the prebiotic effect of MOS produced from PP and PSD on probiotic bacteria

Probiotic bacteria (1% (v/v)) (*L. bulgaricus*, *S. thermophilus* and *B. subtilis*) were grown overnight at 37°C in Luria Broth (1% (w/v) tryptone; 1% (w/v) NaCl; 0.5% (w/v) yeast extract powder), with shaking at 150 rpm (BJPX-200B Shaking Incubator, Jinan, China). Following incubation, the OD600 reading of the bacterial cells was taken, and the bacterial cultures were diluted down to an OD reading of 0.1 using 1× M9 minimal media (3.39% (w/v) Na_2HPO_4; (1.5% (w/v) KH_2PO_4; 0.5% (w/v) NH_4Cl; 0.25% (w/v) NaCl). A 5 ml reaction consisting of 4 ml of bacterial culture and 1 ml of 1 mg/ml carbon source (MOS as the test and glucose as the positive control) was incubated for 7 hours with shaking at 150 rpm (BJPX-200B Shaking Incubator, Jinan, China) at 37°C. Following incubation, 250 µl of the cell culture was aliquoted for OD600 measurement, and 50 µl of 0.2 mg/ml of *p*-iodonitrotetrazolium chloride was added to the cells, which were incubated for 1 hour at 37°C, without shaking. The absorbance was then read at 490 nm to determine the viability of the cells.

5.3.3. Determination of the influence of MOS on auto-aggregation

Cells were harvested by centrifugation at 16 060 ×*g* for 5 minutes and resuspended in buffer containing 0.2% (w/v) of either glucose as a positive control or MOS produced from PP and PSD and adjusted to an OD600 reading of 0.5±0.05. The bacterial suspensions were incubated at room temperature and monitored at different time intervals (0 – 5 hrs). The auto-aggregation percentage was expressed as $[1 – (A_t/A_0)] \times 100$, where A_t represents absorbance at t = 5 h and A_0 represents absorbance at t = 0 h.

5.3.4. Determining the influence of produced MOS on the biofilm forming ability of prebiotic bacteria

Cells were harvested according to Section 5.3.3. Sterile, untreated 96-well plates were used to grow bacteria supplemented with 0.2% (w/v) of either MOS or glucose as a positive control. Plates were incubated at 37°C for 24 h. After incubation, the absorbance was measured at 600 nm. Following this, the plates were washed with distilled water three times and stained for 20 minutes using 0.1% (w/v) crystal violet. The plates were washed a further three times with distilled water to remove unbound crystal violet. Bound cells were quantified by adding 300 µl of acetone/ethanol (20:80, v/v) and the absorbance was measured at 540 nm. Biofilm growth at 540 nm was normalised with cell growth at 600 nm.

5.3.5. Detection of short chain fatty acids (SCFA) production using TLC

The presence of SCFA in the culture broths with various carbon sources was analysed according to a modified method described by Lee et al. (2001). Briefly, 1 mg/ml standard solutions containing acetic acid (AA), butyric acid (BA), citric acid (CA), lactic acid (LA) and propanoic acid (PA) were prepared. The samples were spotted on a silica gel plate which was developed twice using a mobile phase containing acetone-water-chloroform-methanol-ammonium hydroxide (60:2:6:10:22). The plate was then dried and dipped in a staining solution containing 0.25 g bromophenol blue and 0.25 g bromocresol green in 100 ml of 80% (v/v) methanol. The plate was left to dry, and the spots were visualised as the plate dried in the fume hood. The same process was followed for the SCFA samples obtained from the prebiotic studies.

5.3.6. Determining the antioxidant activity of MOS

A modified radical scavenging assay according to Amna et al. (2018) was employed. Briefly, ABTS (7 mM) and potassium persulfate (35 mM) were dissolved in distilled water and the mixture was incubated in the dark at room temperature overnight to generate free radicals. The radicals were mixed with either gallic acid, water, or Del + PAS PP and PSD in a 10:1 ratio in a 96-well plate. A concentration of 0.02 mg/ml of gallic acid was used as a positive control and water was used as a negative control. The plate was incubated in the dark at room temperature for 20 minutes before reading the absorbance at 740 nm.

5.4. Results

5.4.1. Prebiotic effect of MOS produced from PP and PSD

The prebiotic activity of MOS on probiotic bacteria; *L. bulgaricus*, *S. thermophilus* and *B. subtilis* is presented in Figure 5.1 below.

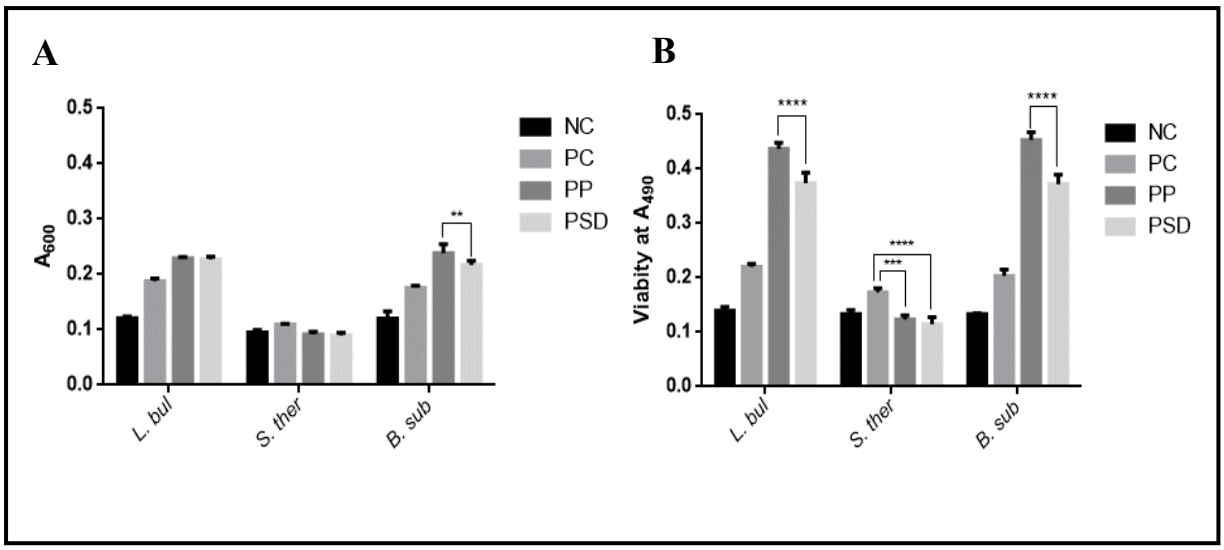

Figure 5.1: Prebiotic effect of MOS produced from Del + PAS PP and PSD on probiotic bacteria. A: OD600 reading of probiotic bacterial growth; B: Viability of probiotic bacteria supplemented with Del + PAS PP and PSD derived MOS. NC: negative control; PC: positive control; PP: pineapple pulp; PSD: pine sawdust. Values are represented as mean values ± SD (n = 3). *(p-value < 0.05)

Bacterial growth measured at 600 nm showed that all the bacteria grew when supplemented with MOS produced from Del + PAS PP and PSD as a carbon source (Figure 5.1A). Probiotics supplemented with MOS had a higher growth rate compared to the negative and positive controls. Cell densities for *L. bulgaricus* supplemented with Del + PAS PP and PSD derived MOS increased to the same level, whereas Del + PAS PP derived MOS had a slightly higher positive effect on *B. subtilis* growth, compared to Del + PAS PSD derived MOS (p-value < 0.05). There was no increase in the cell densities for *S. thermophilus* at 600 nm - no significant difference in growth was observed between the negative control and the bacteria grown in Del + PAS PP and PSD derived MOS supplemented media for *S. thermophilus*. Cell viability studies on the probiotic bacteria corroborated cell density measurements (Figures 5.1A and B). MOS had a positive effect on the growth and proliferation of *L. bulgaricus* and *B. subtilis*. MOS did not have any effect on the growth of *S. thermophilus*. Cell viability assays for both *L. bulgaricus* and *B. subtilis* showed that Del + PAS PP derived MOS had a significantly higher effect on the growth of probiotic bacteria compared to Del + PAS PSD derived MOS (Figure 5.1B). Cell viability was the lowest for *S. thermophilus.*

5.4.2. Influence of MOS on auto-aggregation and biofilm-forming capability of bacteria

The biofilm-forming ability of probiotics was investigated by incubating the probiotic bacteria supplemented with MOS for 24 hours at 37°C in a 96-well microtiter plate and recording the

growth at OD600. The bound bacteria were subsequently stained with crystal violet and washed with acetone/ethanol before obtaining readings at OD540. The normalised results are shown in Figure 5.2.

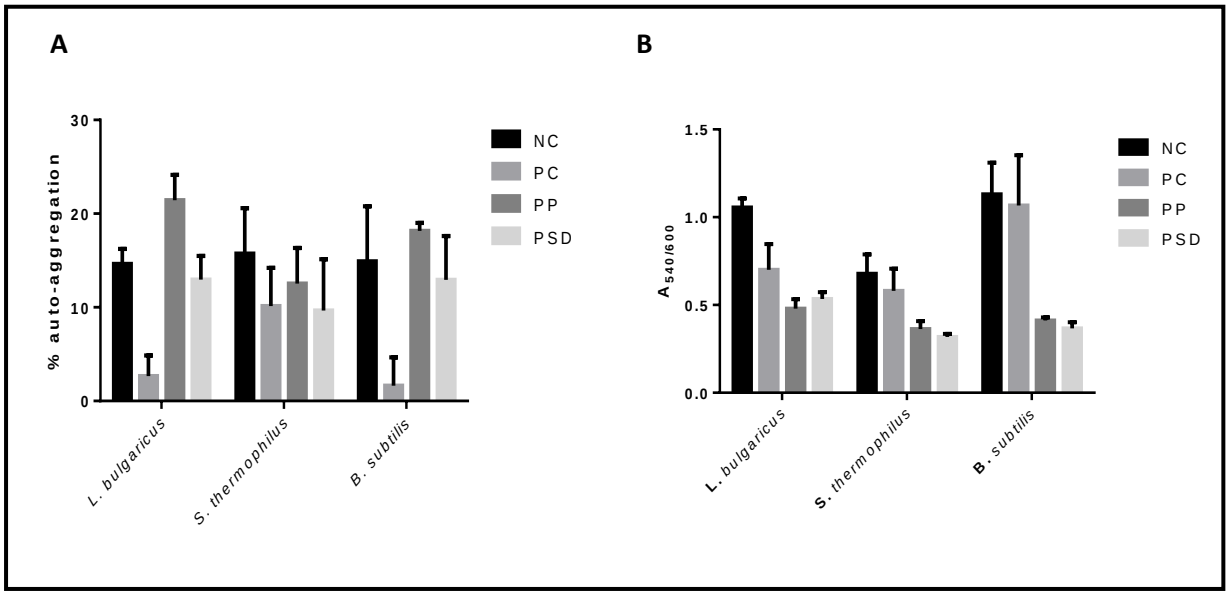

Figure 5.2. Auto-aggregation and biofilm formation enhancement ability of MOS produced from Del + PAS PP and PSD on probiotic bacteria. A) Auto-aggregation potential of probiotic bacteria; B) Biofilm formation ability of probiotic bacteria. NC: negative control; PC: positive control; PP: pineapple pulp; PSD: pine sawdust. Values are represented as mean values ± SD (n = 4).

Figure 5.2A shows that prebiotic MOS derived from Del + PAS PP and PSD did not have an effect on the auto-aggregation ability of the probiotic bacteria. The biofilm-formation ability of the probiotic bacteria was suppressed by supplementing the probiotics with MOS, as seen in Figure 5.2B.

5.4.3. Visualisation of SCFA

To analyse the fermentation products from probiotic bacteria following prebiotic studies, SCFAs were extracted and analysed on TLC. The results are displayed in Figure 5.3.

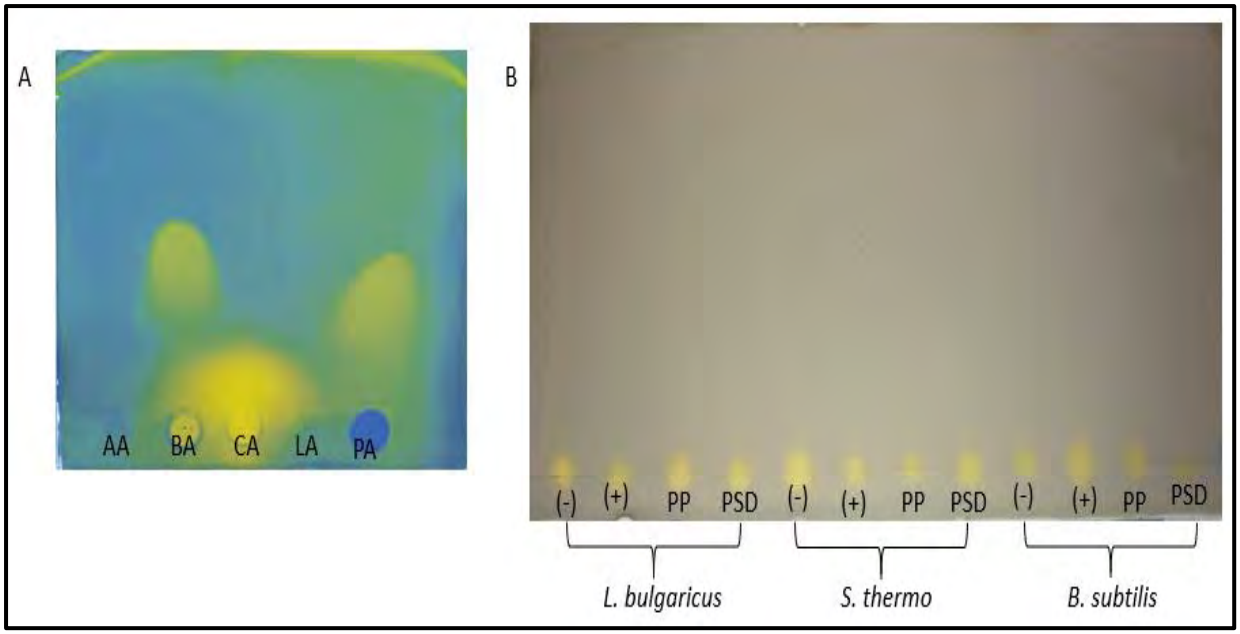

Figure 5.3: TLC for visualisation of SCFA produced by probiotic bacteria following fermentation of MOS derived from Del + PAS PP and PSD. A) Organic acid standards: AA – acetic acid; BA – Butyric acid; CA – citric acid; LA – lactic acid; PA – propanoic acid. B) Products from probiotic bacteria: (-) – negative control; (+) – positive control; PP – pineapple pulp; PSD – pine sawdust.

Figure 5.3A, which contains organic acid standards, shows products for BA, CA, and PA. No distinguishable spots were observed for AA and LA on the plate. No SCFAs were observed on the test TLC plate (Figure 5.3B), which suggests that SCFA produced by probiotic bacteria were not detectable.

5.4.4. Antioxidant activity of MOS

To determine the radical scavenging ability of the produced MOS, $ABTS^{+\bullet}$ and potassium sulphate were used. The results for the radical scavenging ability of 1 mg/ml PP and PSD derived MOS and 0.02 mg/ml gallic acid as a positive control are shown in Figure 5.4 below.

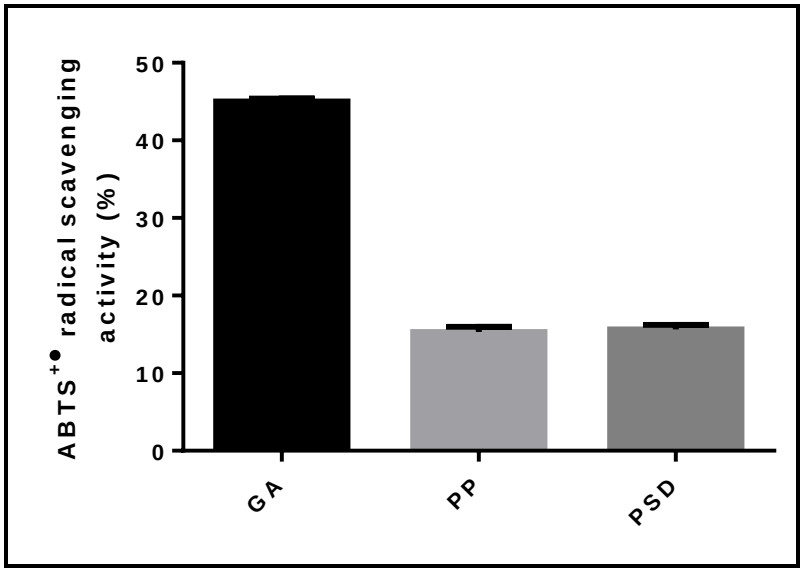

Figure 5.4: ABTS+● radical scavenging ability of MOS produced from hydrolysis using Man26A. Values are represented as mean values ± SD (n = 3).

The radical scavenging abilities of PP and PSD were shown to be approximately 15%. This was significantly lower compared to gallic acid, which was used as a positive control, which had a radical scavenging ability of 45%.

5.5. Discussion

MOS produced from pretreated PP and PSD were tested for their prebiotic potential and their ability to influence bacterial adherence properties. The prebiotic activity was determined using cell density and cell viability assays. Adherence properties were determined using auto-aggregation and biofilm formation studies. MOS produced from PP and PSD had a prebiotic effect on the probiotic strains, *L. bulgaricus* and *B. subtilis*. These strains had higher cell density and cell viability values in media supplemented with MOS, compared to the negative control with no carbon source and the positive control supplemented with glucose as a carbon source. MOS produced from the PP, which contains glucomannan, had a higher prebiotic effect compared to MOS produced from PSD, which is a softwood containing galactoglucomannan. However, supplementing the growth media with MOS did not have an effect on the growth of *S. thermophilus*. Several studies have shown prebiotic potential of MOS on *Lactobacillus* and *Bifidobacterium* species *in vitro* by observing the growth of these bacteria in the presence of MOS derived from different sources (Jana and Kango, 2020; Mary et al., 2019; Rungruangsaphakun and Keawsimpong, 2018). Model mannan substrates and mannan-rich

agricultural wastes have been reported to display prebiotic properties through enhancement of the growth of probiotic bacteria (Magengelele et al., 2021; Jana and Kango, 2020; Mary et al., 2019; Srivastava et al., 2017; Gosh et al., 2015). MOS derived from PP and PSD, therefore, can potentially be used as dietary prebiotics for the increased growth of beneficial bacteria in the gut.

Auto-aggregation and biofilm formation studies showed that probiotic bacteria had low auto-aggregation and biofilm-forming ability. Brink et al. (2006) observed a decreased adherence of probiotic strains in the presence of prebiotics. The production of enzymes that digest prebiotic substrates may result in the reduced production of adhesins, which leads to bacteria being unable to form biofilms (Kadlec and Jakubec, 2014). The fermentation of prebiotics by probiotic bacteria requires the production of enzymes that digest these substrates, and the fermentation of complex prebiotics, such as those derived from GGM, may result in the decreased production of adhesins (Kadlec and Jakubec, 2014). Magengelele et al. (2021) reported decreased auto-aggregation in probiotic bacteria supplemented with GG derived MOS. They suggested that high DP MOS may interfere with bacterial auto-aggregation. There have been no reports in the literature thus far, regarding the ability of MOS prebiotics to decrease biofilm formation in probiotic bacteria. Reports by Suryawanshi and Kango (2021) on MOS produced from CM, KG, and LBG, and by Magengelele et al. (2021) on MOS produced from INM, LBG, and GG, showed increased biofilm formation. Our study did not provide evidence of bacterial adherence in the presence of MOS produced from Del + PAS PP and PSD, which may be explained by the type of mannan present in these substrates. Magengelele et al. (2021) noted that the biofilm-forming capability of MOS may be influenced by both DP and substitution of both galactose and glucose units on the mannan backbone.

There were no detectable SCFAs produced from the fermentation of MOS when analysed on TLC in this study. The change in pH of the M9 media used to grow probiotic bacteria was determined, and it was shown that there was no significant difference in the pH of the negative control media compared to that of the MOS supplemented media (see Appendix C). This could suggest that more sophisticated methods of detecting the presence of SCFAs may be required, such as gas chromatography (GC), capillary electrophoresis and high performance ion exchange chromatography (HPIEC) (Zhang et al., 2020). It has been suggested that the type of media used to grow bacteria and the conditions under which they are grown, influence the production of SCFAs, as Brink et al. (2006) found that bacteria grown on normal MRS broth

containing dextrose produced more SCFAs compared to bacteria grown on MRS broth without dextrose.

The antioxidant ability of the produced MOS was determined using the ABTS radical scavenging method, where the C-2 and C-6 hydroxyl groups of the produced MOS were hypothesised to transfer an H-atom to react with the free ABTS radicals (Jana and Kango, 2020; Kang et al., 2014). In this study, the radical scavenging ability of MOS derived from both PP and PSD was approximately 15%. This was lower compared to MOS derived from palm kernel cake (PKC) and copra meal (CM), which displayed a radical scavenging ability of 68.03% and 61.77% at 1000 µg/ml, respectively (Jana and Kango, 2020). Antioxidant studies conducted on oligosaccharides suggest that oligosaccharides with a lower DP have higher radical scavenging potential than oligosaccharides with a higher DP, suggesting that a higher degree of enzymatic hydrolysis could increase the radical scavenging ability of MOS (Kang et al., 2014). In a study conducted by Timbaraj et al. (2018) on yellow lupin polysaccharides (YLPs), results showed that YLP-2 had a higher radical scavenging ability compared to YLP-1 and YLP-3. In addition to YLP-2 having a lower MW than YLP-1, a higher galactose content was observed in YLP-2 (Timbaraj et al., 2018). No studies have been found that demonstrate that galactose substitution enhances the antioxidant ability of MOS; however, Liu and Huang (2018) have shown that derivatisation of yeast cell wall mannan influenced its antioxidant ability, with derivatised mannan displaying higher antioxidant ability. The modification conducted on the mannans included phosphorylation, sulphonation, carboxymethylation and carboxymethylation-phosphorylation (Liu and Huang, 2018). Phosphorylation and carboxymethyl-phosphorylation were reported to enhance the radical scavenging ability by up to 15% compared to unmodified mannan (Liu and Huang, 2018).

5.6. Conclusions

MOS produced from Del and PAS PP and PSD showed enhanced growth of probiotic bacteria compared to the controls, confirming that MOS produced from these substrates can be used as prebiotics for the selective growth of beneficial bacteria. There was little bacterial adherence observed (in terms of auto-aggregation and biofilm formation) in probiotic bacteria when supplemented with MOS. The determination of the metabolic products from the fermentation of prebiotics was inconclusive, as there were no SCFAs observed using TLC. The MOS

produced from Del + PAS PP and PSD displayed similar antioxidant potential as quantified by $ABTS^{+\bullet}$ radical scavenging activity.

Chapter 6: General discussion, conclusions and future recommendations

6.1. General discussion and conclusions

The aim of this study was to investigate the ability of a recombinant fungal mannanase, Man26A (derived from *A. niger*), to hydrolyse lignocellulosic biomass waste substrates, pineapple pulp (PP) and pine sawdust (PSD), for the generation of prebiotic MOS. Man26A was partially purified and concentrated using dia-filtration and biochemically characterised to determine the optimal hydrolysis conditions for producing MOS. The action pattern and hydrolysis products of Man26A were determined using model mannan substrates. Following the characterisation of Man26A, the enzyme was used to hydrolyse lignocellulosic biomass waste (LBW) PP and PSD. Due to recalcitrance of LBW, the substrates were pretreated prior to enzymatic hydrolysis. The monosaccharide composition of the substrates was determined using Megazyme sugar kits. This was followed by analysis of the thermal properties of the untreated and pretreated wastes, and analyses of their chemical properties. The morphological changes on the surface of the LBW substrates were observed using SEM, and the changes that occurred due to lignin removal were observed using light microscopy. The optimal conditions for the degradation of the LBW, i.e., hydrolysis time, enzyme and substrate concentration, were investigated - and MOS from LBW were produced according to the optimised hydrolysis conditions. The biological effects of the produced MOS, such as the prebiotic activity of MOS, the effects of MOS on bacterial surface properties, and radical scavenging activity of produced MOS, were investigated. The effects of MOS on bacterial surface properties were by investigating the effect of MOS on the auto-aggregation and biofilm forming capability of bacteria supplemented with MOS. Finally, the ability of the probiotic bacteria to produce SCFAs was also studied.

Concentrated Man26A was partially purified with a fold purification of 1.25 and a 41.1% yield. The molecular mass of Man26A, as determined by SDS-PAGE, was approximately 46 kDa. The fold purification may be increased by using techniques such as ammonium sulphate precipitation, affinity chromatography and by size exclusion chromatography on Superdex, as performed by Zhao et al. (2011). Man26A efficiently hydrolysed less substituted mannan substrates, as seen by its high specific activity on INM and LBG, compared to the more highly substituted GG. These findings are in agreement with those reported by Magengelele et al.

(2021). GH26 mannanases, with a few exceptions, are hindered by galactose substitutions (Von Freiesleben et al., 2016). The pH and temperature optima of the enzyme are comparable to those of other fungal GH26 mannanases. Man26A had poor thermal stability at its optimal temperature of 50°C. The thermal stability of an enzyme is important for industrial application of enzymes and can be improved by using methods such as protein engineering and enzyme immobilisation (You et al., 2016; Masuda et al., 2014).

Mannanases have been used to produce prebiotic MOS with a varying DP (Zhang et al., 2021; Suryawanshi and Kango, 2021; Jana and Kango, 2020). Furthermore, mannanases from different families produce MOS that are diverse (Jana et al., 2021a; Bååth et al., 2018; Tailford et al., 2009). GH26 mannanases predominantly produce mannobiose and mannotriose from LBG (Couturier et al., 2013). MOS produced by the enzymatic hydrolysis of model mannan substrates have been used to elucidate the action pattern and the hydrolysis product pattern of different mannanases, providing insight into the mode of action of different mannanases and the effect of having structures such as CBMs on their activity (Rahmani et al., 2017). In this study, an *A. niger* derived Man26A produced mainly M2 to M6 from GG, M1 to M5 from LBG and, M2 to M4 from INM. The hydrolysis of these model mannan substrates proved to be more effective for INM, as there were no unresolved MOS of higher DP observed on TLC, suggesting that INM was completely hydrolysed into M2 to M4. The results obtained for the hydrolysis of model mannan substrates agree with those previously observed in literature (Bågenholm et al., 2019; Jana et al., 2018; Rahmani et al., 2017). Literature on the enzymatic hydrolysis of lignocellulosic substrates mainly focuses on the conversion of cellulose (glucose) into value-added products or fuels, such as that conducted by Von Freiesleben et al. (2018), which investigates the uses of mannanases to boost the hydrolysis of softwoods. Limited studies are available on the hydrolysis of mannans from galactoglucomannan into MOS.

The enzymatic hydrolysis of untreated lignocellulosic biomass has been shown to be difficult and may even be unfeasible due to its recalcitrance, which necessitates the use of pretreatment methods (Otieno and Ahring, 2012). Morrison (2013) investigated the effects of hemicellulases on the hydrolysis of LB and found that mannanase activity on untreated PP was not detectable, which further illustrates the need for pretreatment prior to enzymatic hydrolysis. The carbohydrate component of LB consists mainly of glucose (cellulose) and a lower content of hemicelluloses (mannan and xylan) (Von Freiesleban et al., 2018; Bombeck et al., 2017). The increased interest in MOS has resulted in a heightened interest in using the hemicellulosic fraction of biomass for beneficiation into value-added products. This can be seen in various

studies aimed at enzymatically degrading softwoods, for example, in studies by Bååth et al. (2018) and Von Freiesleben et al. (2018). Selecting the best substrate for enzymatic hydrolysis is also important, which means considering the composition of the LB to be used for the production of prebiotics (Otieno and Ahring, 2012). Softwoods are mainly composed of mannan, which would make them better substrates for the production of prebiotic MOS compared to hardwoods (Otieno and Ahring, 2012). In this study, PP, which is an agricultural waste which commonly contains *O*-acetyl-galactoglucomannan, and PSD, a softwood LBW, displayed similar potential for MOS production, as reflected in similar concentrations of reducing sugars being produced during enzymatic hydrolysis. This illustrates that the hemicellulosic content of the LB is not the only factor influencing hydrolysis, but that the type of pretreatments used, and their effectiveness, also play a significant role in the oligosaccharides produced by the different LBWs (Otieno and Ahring, 2012). Mannan-rich agro-wastes such as palm kernel cake (PKC), copra meal (CM), and spent coffee grounds (SCG) have previously been used to produce prebiotic MOS and are therefore good candidates for the commercial production of MOS using endomannanases (Suryawanshi and Kango, 2021; Jana and Kango, 2020; Nguyen et al., 2019). It is worth noting that the removal of lignin during pretreatment also influences the hemicellulosic fraction, which is solubilised to oligomers and monomers during the delignification process (Ayeni and Daramola, 2017). It is therefore important to ensure that a delignification procedure that results in the lowest amount of hemicellulosic solubilisation is selected for use in hemicellulose beneficiation studies, such as hydrogen peroxide pretreatment conducted by Ayeni and Daramola (2017) - which resulted in only 13% of hemicellulose solubilisation, compared to other pretreatments, such as hydrogen peroxide and sodium hydroxide, where up to 79% of hemicellulose was solubilised. Delignification of LB using acetic acid is another cost-effective and environmentally friendly pretreatment method because of its recyclability (Zhang et al., 2017).

The growth of probiotic bacteria was enhanced in the presence of MOS produced from both delignified + PAS PP and PSD. MOS produced from LBW substrates have previously been shown to enhance the growth of beneficial bacteria (Suryawanshi et al., 2021; Wongsiridetchai et al., 2021; Jana and Kango, 2020). Del + PAS PP derived MOS had a higher effect on the growth of probiotic bacteria compared to Del + PAS PSD derived MOS. MOS produced from these substrates displayed poor ability to influence bacterial surface properties such as auto-aggregation and biofilm forming capability of the bacteria. The poor influence of MOS on auto-aggregation and biofilm formation may be attributed to the type of MOS used, as it has

previously been shown that different prebiotic substrates have different effects on the auto-aggregation ability of probiotic bacteria (Pan et al., 2017). Magengelele et al. (2021) used model mannan substrates to demonstrate that differently substituted MOS display differences in the auto-aggregation potential of probiotic bacteria. This study showed that MOS with a high DP, and highly substituted MOS, reduced auto-aggregation. SCFAs were not detected on TLC following fermentation of MOS by probiotic bacteria. The detection of SCFAs can be difficult because they are volatile compounds (Zhang et al., 2020). The extraction process can lead to sample loss due to its volatility (Kim et al., 2019). The detection of SCFAs in samples may be improved by using more sophisticated methods, such as GC, HPLC and spectrophotometric techniques (Zhang et al., 2020; Kim et al., 2019). MOS produced from PP and PSD displayed antioxidant activity using the ABTS radical scavenging method. Antioxidant activity of PP and PSD was comparable to that of LBG.

Future recommendations

The glucomannan and galactoglucomannan components of the Del + PAS PP and PSD substrates could be extracted prior to enzymatic hydrolysis, to ensure that the enzyme activity is not hindered by other carbohydrates in the biomass.

Hydrolysis products obtained from LBW can be analysed using methods such as high-performance anion-exchange chromatography/pulsed amperometric detection (HPAEC-PAD), which is one of the more popular technologies for the detection of oligosaccharides in recent years (Mechelke et al., 2017). Nuclear magnetic resonance (NMR) may also be used to accurately determine the various oligosaccharides produced.

The prebiotic effect of purified MOS may be evaluated further, in order to better understand which types of MOS have a more beneficial effect on the proliferation of probiotic bacteria, and which do not.

The effect of prebiotics on gut pathogenic bacteria can be investigated. This can be performed using a plate method to assess the prebiotic effect of MOS, where the inhibitory action of the probiotic bacteria may be observed as zones of clearance on plates. Further studies on the bioactive properties of MOS can be conducted, such as studies performed by Suryawanshi and Kango (2021), where the effect of MOS on cancer cells was investigated. The study can be elevated to cell work for *in vivo* experiments. The effect of prebiotics on diabetes can also be tested to further understand the effect of prebiotic use on the human body, as the gut microbiota has been shown to play a significant role in managing Type- 2 diabetes (Jana et al., 2021b).

References

Ahorsu, R., Medina, F., and Constanti, M. (2018). Significance and challenges of biomass as a suitable feedstock for bioenergy and biochemical production: A review. *Energies*. 11 (3366), 1-19.

Akpinar, A., Yerlikaya, O., and Kiliç, S. (2011). Antimicrobial activity and antibiotic resistance of *Lactobacillus delbrueki* ssp. *Bulgaricus* and *Streptococcus thermophilus* strains isolated from Turkish homemeade yoghurts. *African Journal of Microbiology Research*. 5(6), 675-682.

Al-Khalaifa, H., Al-Nasser, A., Al-Surayee, T., Al-Kandari, S., Al-Enzi, N., Al-Sharrah, T., Ragheb, G., Al-Qalaf, S., and Mohammed, A. (2019). Effect of dietary probiotics and prebiotics on the performance of broiler chickens. *Poultry Science*. 98(10), 4465-4479.

Álvarez, C., Reyes-Sosa, M., and Díez, B. (2016). Enzymatic hydrolysis of biomass from wood. *Microbial Biotechnology*. 9, 149-156.

Amin, F.R., Khalid, H., Zhang, H., Rahman, S.U., Zhang, R., Liu, G, and Chen, C. (2017). Pretreatment methods of lignocellulosic biomass for anaerobic digestion. AMB Express. 7(72), 2853158.

Amna, K.S., Park, S.Y., Kim, S.Y., Yoo, A.Y., Park, J.K. (2018). Antioxidant activity of manno-oligosaccharides derived from the hydrolysis of polymannan by extracellular carbohydrase of *Bacillus* N3. *Marine Bioscience and Biotechnology*. 10(1), 9-17.

Amorim, C., Silvério, S.C., Prather, K.L.J., and Rodrigues, L.R. (2019). From lignocellulosic residues to market: Production and commercial potential of xylooligosaccharides. *Biotechnology Advances*. 37, 107397.

An, N.T., Thien, D.T., Dong, N.T., Dung, P.L., and Du, N.V. (2010). Characterization of glucomannan from some *Amorphophallus* species in Vietnam. *Carbohydrate Polymers*. 80, 308-311.

Arevalo-Gallegos, A., Ahmad, Z., Asgher, M., Parra-Saldivar, R., and Iqbal, H.M.N. (2017). Lignocellulose: a sustainable material to produce value-added products with a zero-waste approach – a review. *International Journal of Biological Macromolecules*. 99, 308-318.

Ariandi, Yopi, and Meryandini, A. (2015). Enzymatic hydrolysis of copra meal by mannanase from Streptomyces sp. BF3.1 for the production of mannooligosaccharides. *HAYATI Journal of Biosciences*. 22(2), 79-86

Ayeni, A.O. and Daramola, M.O. (2017). Lignocellulosic biomass waste beneficiation: evaluation of oxidative and non-oxidative pretreatment methodologies of South African corncob. *Journal of Environmental Chemical Engineering*. 5(2), 1771-1779.

Bååth, J.A., Martinez-Abad, A., Berglund, J., Larsbrink, J., Vilaplana, F., and Olsson, L. (2018). Mannanase hydrolysis of spruce galactoglucomannan focusing on the influence of acetylation on enzymatic mannan degradation. *Biotechnology for Biofuels*. 11(1), 114.

Bågenholm, V., Reddy, S.K., Bouraoui, H., Morrill, J., Kulcinskaja, E., Koropatkin, N.M., and Stålbrand, H. (2017). Galactomannan catabolism conferred by a polysaccharide utilization locus of *Bacteroides ovatus*. *The Journal of Biological Chemistry*. 292(1), 229-243.

Bågenholm, V., Wiemann, M., Reddy, S.K., Bhattacharya, A., Rosengren, A., Logan, D.T., and Stålbrand, H. (2019). A surface-exposed GH26 β-mannanase from *Bacteroides ovatus*: Structure, role, and phylogenetic analysis of *Bo*Man26B. *Journal of Biological Chemistry*. 294(23), 9100-9117.

Baidhe, E., Kigozi, J., Mukisa, I., Muyanja, C., Namubiru, L., and Kitarikawe, B. (2021). Unearthing the potential of solid waste generated along the pineapple drying process line in Uganda: A review. *Environmental Challenges*. 2,

Baig, K.S. (2020). Interaction of enzymes with lignocellulosic material: causes, mechanism and influencing factors. *Bioresources and Bioprocessing*. 7(21), 1-19.

Beig, B., Riaz, M., Naqvi, S.R., Hassan, M., Zheng, Z., Karimi, K., Pugazhendhi, A., Atabani, A.E., and Chi, N.T.L. (2021).Current challenges and innovative developments in pretreatment of lignocellulosic residues for biofuel production: A review. *Fuel*. 287, 119670.

Berglund, J., Azhar, S., Lawoko, M., Lindström, M., Vilaplana, F., Wohlert, J., and Henriksson, G. (2019). The structure of galactoglucomannan impacts the degradation under alkaline conditions. *Cellulose*. 26, 2155-2175.

Bernal-Lugo, I., Jacinto-Hernandez, C., Gimeno, M., Montiel, C.C., Rivero-Cruz, F., and Velasco, O. (2019). Highly efficient single-step pretreatment to remove lignin and hemicellulose from softwood. *BioResources*. 14(2), 3567-3577.

Blibech, M., Chaari, F., Bhiri, F., Dammak, I., Ghorbel, R.E., and Chaabouni, S.E. (2018). Production of manno-oligosaccharides from locust bean gum using immobilized *Penicillium occitanis* mannanase. *Journal of Molecular Catalysis B: Enzymatic*. 73(1-4), 111-115.

Bombeck, P.-L., Khatri, V., Meddeb-Mouelhi, F., Montplaisir, D., Richel, A., and Beauregard, M. (2017). Predicting the most appropriate wood biomass for selected industrial applications: comparison of wood, pulping, and enzymatic treatments using fluorescent-tagged carbohydrate-binding modules. *Biotechnology for Biofuels*. 10(293), 1-14.

Bradford, M.M. (1976). A rapid and sensitive method for the quantitation of microgram quantities of protein utilizing the principle of protein dye binding. *Analytical Biochemistry*. 72 (1-2), 248-254.

Brink, M., Todorov, S.D., Martin, J.H., Senekal, M., Dicks, L.M.T. (2006). The effect of prebiotics on production of antimicrobial compounds, resistance to growth at low pH and in the presence of bile, and adhesion of probiotic cells to intestinal mucus. *Journal of Applied Microbiology*. 100(4), 813-820.

Britton, H. T. S. and Robinson, R. A. (1931). Universal buffer solutions and the dissociation constant of veronal. Journal of the Chemical Society. 1, 1456-1462.

Brownawell, A.M., Caers, W., Gibson, G.R., Kendall, C.W.C., Lewis, K.D., Ringel, Y., and Slavin, J.L. (2012). Prebiotics and the health benefits of fiber: Current regulatory status, future research, and goals. *The Journal of Nutrition and Supplement*. 142, 962-974.

Campos, D.A., Coscueta, E.R., Valetti, N.W., Pastrana-Castro, L.M., Teixeira, J.A., Picó, G.A., and Pintado, M.M. (2019). Optimization of bromelain isolation from pineapple byproducts by polysaccharide complex formation. *Food Hydrocolloids*. 87, 792-804.

Campos, D.A., Ribeiro, T.B., Teixeira, J.A., Pastrana, L., and Pintando, M.M. (2020). Integral valorization of pineapple (*Ananas comosus* L.) by-products through a green chemistry approach towards added value ingredients. *Foods*. 9(60), 1-22.

Cano, M.E., García-Martin, A., Morales, P.C., Wojtusik, M., Santos, V.E., Kovensky, J., and Ladero, M. (2020). Production of oligosaccharides from agrofood wastes. *Fermentation*. 6(31), 1-27.

Cao, P., Wu, L., Pan, D., Zeng, X., Guo, Y., and Lian, L. (2019). Effects of oligosaccharides on the fermentation properties of *Lactobacillus plantarum*. *Journal of American Dairy Science*. 102, 2863-2872.

Cassellis, M.E.R., Pardo, M.E.S., López, M.R., and Escobedo, R.M. (2014). Structural, physicochemical, and functional properties of industrial residues of pineapple (*Ananas comosus*). *Cellulose Chemistry and Technology*. 48(7-8), 633-641.

Cavali, M., Soccol, C.R., Tavares, D., Torres, L.A.Z., Tanobe, V.O.A., Filho, A.Z., and Woiciechowski, A.L. (2020). Effect of sequential acid-alkaline treatment on physical and chemical characteristics of lignin and cellulose from pine (*Pinus* spp.) residual sawdust. *Bioresource Technology*. 316, 123884.

Chandra, J., George N., and Narayanankutty, S.K. (2016). Isolation and characterization of cellulose nanofibrils from arecanut husk fibre. *Carbohydrate Polymers*. 142, 158-166.

Chapla, D., Pandit, P., and Shah, A. (2012). Production of xylooligosaccharides from corncob xylan by fungal xylanase and their utilization by probiotics. *Bioresource Technology*. 115, 215-221.

Charis, G., Danha, G., and Muzenda, E. (2020). Characterizations of biomasses for subsequent thermochemical conversion: a comparative study of pine sawdust and acacia tortilis. *Processes*. 8(546), 8050456.

Chauhan, P.S., Puri, N., Sharma, P., and Gupta, N. (2012). Mannanases: microbial sources, production, properties and potential biotechnological applications. *Applied Microbiology and Biotechnology*. 93, 1817-1830.

Chen, C.-C., Lai, C.-C., Huang, H.-L., Huang, W.-Y., Toh, H.S., Weng, T.-C., Chuang, Y.-C., Lu, Y.-C., and Tang, H.-J. (2019). Antimicrobial activity of *Lactobacillus* species against carbapenem-resistant Enterobacteriaceae. *Frontiers in Microbiology*. 10(789), 1-10.

Cho, E.J., Trinh, L.T.P., Song, Y., Lee, Y.G., and Bae, H.-J. (2020). Bioconversion of biomass waste into high value chemicals. *Bioresource Technology*. 298, 122386.

Cho, E.J., Trinth, L.T.P., Song, Y., Lee, Y.G., and Bae, H.-J. (2020). Bioconversion of biomass waste into high value chemicals. *Bioresource Technology*. 298, 122386.

Couturier, M., Féliu, J., Bozonnet, S., Roussel, A., and Berrin, J.-G. (2013b). Molecular engineering of fungal GH5 and GH26 beta-(1,4)-mannanases toward improvement of enzyme activity. *PLOS One*. 8(11), e79800.

Couturier, M., Haon, M., Coutinho, P.M., Henrissat, B., Lesage-Meessen, L., and Berrin, J-G. (2011). *Podospora anserina* hemicellulases potentiate the *Trichoderma reesei* secretome for saccharification of lignocellulosic biomass. *Applied and Environmental Microbiology*. 77(1), 237-246.

Couturier, M., Roussel, A., Rosengren, A., Leone, P., Stålbrand, H., and Berrin, J.-G. (2013a). Structural and biochemical analyses of glycoside hydrolase families 5 and 26 β-(1,4)-mannanases from *Podospora anserina* reveal differences upon manno-oligosaccharide catalysis. *Journal of Biological Chemistry*. 288(20), 14624-14635.

Cross, R. (2001). The preparation of biological material for electron microscopy part3: The preparation of material for scanning electron microscopy (SEM). *Rhodes University Press*. Grahamstown.

Cuong, D.B., Dung, V.K., Hien, N.T.T, and Thu, D.T. (2013). Prebiotic evaluation of copra-derived mannooligosaccharides in White-leg shrimps. *Journal of Aquaculture Research and Development.* 4(5), 1-5.

Dahmen, N., Lewandowski, I., Zibek, S., and Weidtmann, A. (2018). Integrated lignocellulose value chains in a growing bioeconomy: status quo and perspectives. *GCB Bioenergy*. 11, 107-117.

Dashek, W. V. (1997). Methods in plant biochemistry and molecular biology. *Photosynthetica*. 53(4), 560.

Davani-Davari, D., Negahdaripour, M., Karimzadeh, I., Seifan, M., Mohkam, M., Masoumi, S.J., Berenjian, A., and Ghasemi, Y. (2019). Prebiotics: Definition, types, sources, mechanisms, and clinical applications. *Foods*. 8(92), 1-27.

Dávila, I., Gullón, B., Alonso, J.L., Labidi, J., Gullón, P. (2019). Vine shoots as new source for the manufacture of prebiotic oligosaccharides. *Carbohydrate Polymers*. 207, 34-43.
Dawood, A. and Ma, K. (2020). Applications of microbial β-mannanases. *Frontiers in Bioengineering and Biotechnology*. 8, 1-17.

Department of Agriculture, Forestry and Fisheries RSA, (2017). A profile of the South African pineapple market value chain. Publicly available government document. URL: https://www.nda.agric.za/doaDev/sideMenu/Marketing/Annual%20Publications/Commodity%20Profiles/field%20crops/Pineapple%20Market%20Value%20Chain%20Profile%202017.pdf [Accessed on 12/03/2021].

Department of Science and Technology RSA, (2013). The bio-economy strategy – South African government. Publicly available government document. URL: https://www.gov.za

Dhawan, S. and Kaur, J. (2007). Microbial mannanases: An overview of production and applications. *Critical Reviews in Biotechnology*. 27, 197-216.

Duque-Acevedo, M., Belmonte-Ureña, L.J., Yakovleva, N., and Camacho-Ferre, F. (2020). Analysis of the circular economic production models and their approach in agriculture and agricultural waste biomass management. *International Journal of Environmental Research and Public Health. 17, 9549*.

Faryar, R., Linares-Pastén, J.A., Immerzeel, P., Mamo, G., Andersson, M., Stålbrand, H., Mattiasson, B., and Karlsson, E.N. (2015). Production of prebiotic xylooligosaccharides from alkaline extracted wheat straw using the K80R-variant of a thermostable alkali-tolerant xylanase. *Food and Bioproducts Processing*. 93, 1-10.

Feng, W., Ao, H., and Peng, C. (2018). Gut microbiota, short-chain fatty acids, and herbal medicines. *Frontiers in Pharmacology*. 9, 1354.

Ferreira-Santos, P., Zanuso, E., Genisheva, Z., Rocha, C.M.R., and Teixeira, J.A. (2020). Green and sustainable valorization of bioactive phenolic compounds from *Pinus* by-products. *Molecules*. 25(12), 25122931.

Fillat, Ú., Ibarra, D., Eugenio, M.E., Moreno, A.D., Tomás-Pejó, E., and Martin-Sampero, R. (2017). Laccases as a potential tool for the efficient conversion of lignocellulosic biomass: a review. *Fermentation*. 3(2), 17.

Folin, O. & Ciocalteau, V. 1927. On tyrosine and tryptophane determinations in proteins. *Journal of Biological Chemistry*. 73, 627–648.

Fonteles, T.V. and Rodrigues, S. (2018). Prebiotic in fruit juice: processing challenges, advances, and perspectives. *Current Opinion in Food Science*. 22, 55-61.

Forsatkar, M.N., Nematollahi, M.A., Rafiee, G., Farahmand, H., and Martinez-Rodriguez, G. (2017). Effects of prebiotic mannan oligosaccharide on the growth, survival, and anxiety-like behaviours of zebrafish (*Danio rerio*). *Journal of Applied Aquaculture*. 29(2), 183-196.

Gao, J., Anderson, D., and Levie, B. (2013). Saccharification of recalcitrant biomass and integration options for lignocellulosic sugars from catchlight energy's sugar process (CLE Sugar). *Biotechnology for Biofuels*. 6(10),

Gibson, R.G., Hutkins, R., Sanders, M.E., Prescott, S.L., Reimer, R.A., Salminen, S.J., Scott, K., Stanton, C., Swanson, K.S., Cani, P.D., Verbeke, K., and Reid, G. (2017). The international scientific association for probiotics and prebiotics (ISAPP) consensus statement on the definition and scope of prebiotics. *Gastroenterology and Hepatology*. 14(8), 491-502.

Gosh, A., Verma, A.K., Tingirikari, J.R., Shukla, R., Goyal, A. (2015). Recovery and purification of oligosaccharides from copra meal by recombinant endo-β-mannanase and deciphering molecular mechanism involved and its role as potent therapeutic agent. *Molecular Biotechnology*. 57, 111-127.

Grimaud, F., Pizzut-Serin, S., Tarquis, L., Ladeveze, S., Morel, S., Putaux, J.-L., and Potocki-Veronese, G. (2019). *In vitro* synthesis and crystallization of β-1,4-mannan. *Biomacromolecules*. 20, 846-853.

Gutierrez-Macias, P., De Jesus, M.L.H., Barragan-Huerta, B.E. (2017). The production of biomaterials from agro-industrial waste. *Fresenius Environmental Bulletin.* 26(6), 4128-4152).

Hadidi, M., Amoli, P.I., Jeylani, A.Z., Hasiri, Z., Rouhafza, A., Ibarz, A., Khaksar, B., Tabrizi, S.T. (2020). Polysaccharides from pineapple core as a canning by-product: Extraction optimization, chemical structure, antioxidant and functional properties. International Journal of Biological Macromolecules. 163, 2357-264.

Han, S.-Y., Park, C.-W., Kwon, G.-J., Kim, N.-H., Kim, J.-C., and Lee, S.-H. (2020). Ionic liquid pretreatment of lignocellulosic biomass. *Journal of Forest and Environmental Science*. 36(2), 69-77.

Haq, I.U., Nawaz, A., Liaqat, B., Arshad, Y., Fan, X., Sun, M., Zhou, X., Xu, Y., Akram, F., and Jiang, K. (2021). Pilot scale elimination of phenolic cellulase inhibitors from alkali pretreated wheat straw for improved cellulolytic digestibility to fermentable saccharides. *Frontiers in Bioengineering and Biotechnology*. 9, 658159.

Hlalukana, N., Magengelele, M., Malgas, S., and Pletschke, B. (2021). Enzymatic conversion of mannan-rich plant waste biomass into prebiotic mannooligosaccharides. *Foods*. 10, 2010.

Hlerema, I.N. and Eiasu, B. (2017). Pineapple (*Ananas comosus*) plant material as supplement for maize residue-based oyster mushroom substrate and reduction of cadmium soil contamination. *HortScience*. 52(4), 667-671.

Houfani, A.A., Anders, N., Spiess, A.C., Baldrian, P., and Benallaoua, S. (2020). Insights from enzymatic degradation of cellulose and hemicellulose to fermentable sugars – a review. *Biomass and Bioenergy*. 134, 105481.

Hsu, Y., Koizumi, H., Otagiri, M., Moriya, S., and Arioka, M. (2018). Trp residue at subsite -5 plays a critical role in the substrate binding of two protisan GH26 β-mannanases from a termite hindgut. *Applied Microbiology and Biotechnology*. 102, 1737-1747.

Hu, H., Zhao, Q., Xie, Q., Xie, J., Sun, D. (2019). Polysaccharide from pineapple pomace: new insight into ultrasonic-cellulase synergistic extraction and hypoglycemic activities. *International Journal of Biological Macromolecules*. 121, 1213-1226.

Huang, J-W., Chen, C-C., Huang, C-H., Huang, T.-Y., Wu, T.-H., Cheng. Y.-S., Ko, T.-P., Lin, C.-Y., Liu, J.-R., Guo, R.-T. (2014). Improving the specific activity of b-mannanase from *Aspergillus niger* BKO1 by structure-based rational design. *Biochimica et Biophysica Acta (BBA) – Proteins and Proteomics*. 1844(3), 663-669.

Huang, Y., Liu, H., Yuan, H., Zhuang, X., Yuan, S., Yin, X., and Wu, C. (2018). Association of chemical structure and thermal degradation of lignins from crop straw and softwood. *Journal of Analytical and Applied Pyrolysis*. 134, 25-34.

Jagtap, S., Deshmukh, R.A., Menon, S., and Das, S. (2017). Xylooligosacharides production by crude microbial enzymes from agricultural waste without prior treatment and their potential application as nutraceuticals. *Bioresource Technology*. 245, 283-288.

Jana, U.K. and Kango, N. (2020). Characteristics and bioactive properties of mannooligosaccharides derived from agro-waste mannans. *International Journal of Biological Macromolecules*. 149, 931-940.

Jana, U.K., Kango, N., and Pletschke, B. (2021b). Hemicellulose-derived oligosaccharides: Emerging prebiotics in disease alleviation. *Frontiers in Nutrition*. 8, 670817.

Jana, U.K., Suryawanshi, R.K., Prajapati, B.P., and Kango, N. (2021a). Prebiotic mannooligosaccharides: Synthesis, characterization and bioactive properties. *Food Chemistry*. 342, 128328.

Jana, U.K., Suryawanshi, R.K., Prajapati, B.P., Soni, H., and Kango, N. (2018). Production optimization and characterization of mannooligosaccharide generating β-mannanase from *Aspergillus oryzae*. *Bioresource Technology*. 268, 308-314.

Jian, H.-L., Zhu, L.-W., Zhang, W.-M., Sun, D.-F., and Jiang, J.-X. (20132015). Enzymatic production of manno-oligosaccharides from *Gleditsia sinensis* galactomannan gum. *International Journal of Biological Macromolecules*. 55, 282-288.

Johnson, L.P., Walton, G.E., Psichas, A., Frost, G.S., Gibson, G.R., and Barraclugh, T.G. (2015). Prebiotics modulate the effects of antibiotics on gut microbial diversity and functioning *in vitro*. *Nutrients*. 7(6), 4480-497.

Kadlec, R. and Jakubec, M. (2014). The effect of prebiotics on adherence of probiotics. *Journal of Dairy Science*. 97(4), 1983-1990.

Kaira, G.S. and Kapoor, M. (2019). How substrate subsites in GH26 endo-mannanase contribute towards mannan binding. *Biochemical and Biophysical Research Communications*. 510, 358-363.

Kang, O.L., Ghani, M., Hassan, O., Rahmati, S., and Ramlmli, N. (2014). Novel agaro-oligosaccharide production through enzymatic hydrolysis: Physicochemical properties and antioxidant activities. *Food Hydrocolloids*. 42(2), 304-308.

Kangas, H., Felissia, F.E., Filgueira, D., Ehman, N.V., Vallejos, M.E., Imlmlauer, C.M., Lahtinen, P., Area, M.C., and Chinga-Carrasco, G. (2019). 3D printing high-consistency enzymatic nanocellulose obtained from a soda-ethanol-O_2 pine sawdust pulp. *Bioengineering*. 6(60), 1-12.

Katsimpouras, C., Dimarogona, M., Petropoulos, P., Christakopoulos, P., and Topakas, E. (2016). A thermostable GH26 endo-β-mannanase from *Myceliophthora thermophila* capable of enhancing lignocellulose degradation. *Biotechnologically relevant enzymes and proteinsApplied Microbiology and Biotechnology*. 100, 8385-8397.

Kaur, C.P., Vadivelu, J., and Chandramathi, S. (2018). Impact of *Klebsiella pneumoniae* in lower gastrointestinal tract diseases. *Journal of Digestive Diseases*. 19, 262-271.

Ketnawa, S., Chaiwut, P., and Rawdkuen, S. (2012). Pineapple wastes: A potential source for bromelain extraction. *Food and Bioproducts Processing*. 90(3), 385-391.

Khan, N., le Roes-Hill, M., Welz, P.J., Grandin, K.A., Kudanga, T., van Dyk, J.S., Ohlhoff, C., van Zyl, W.H., and Pletschke, B.I. (2015). Fruit waste streams in South Africa and their potential role in developing a bio-economy. *South African Journal of Science*. 111(5/6), 1—11.

Khare, A., Thorat, G., Bhimte, A., and Yadav, V. (2018). Mechanism of action of prebiotic and probiotic. *Journal of Entomology and Zoology Studies*. 6(4), 51-53.

Kimelman, H. and Shemesh, M. (2019). Probiotic bifunctionality of *Bacillus subtilis* – rescuing Lactic Acid Bacteria from desiccation and antagonizing pathogenic *Staphylococcus aureus*. *Microorganisms*. 7(407), 1-16.

Koo, B., Jo, J., and Cho, S.-M. (2020). Drying effect on enzymatic hydrolysis of cellulose associated with porosity and crystallinity. *Applied Sciences*. 10, 5545.

Kovacova, Z., Demcak, S., Balintova, M., Pla, C., and Zinicovscaia, I. (2020). Influence of wooden sawdust treatments on Cu(II) and Zn(II) removal from water. *Materials.* 13(16), 3575.

Kridtayopas, C., Rakangtong, C., Bunchasak, C., and Loongyai, W. (2019). Effect of prebiotic and symbiotic supplementation in diet on growth performance, small intestinal morphology, stress, and bacterial population under high stocking density condition of broiler chickens. *Poultry Science*. 98(10), 4595-4605.

Kruyeniski, J., Ferreira, P.J.T., Carvalho, M.G.V.S., Vallejos, M.E., Felissia, F.E., and Area, M.C. (2019). Physical and chemical characteristics of pretreated slash pine sawdust influence its enzymatic hydrolysis. *Industrial Crops & Products*. 130, 528-536.

Kucharska, K., Rybarczyk, P., Holowacz, I., Lukajtis, R., Glinka, M., and Kamiński, M. (2018). Pretreatment of lignocellulosic materials as substrates for fermentation processes. *Molecules*. 23(11), 2937.

Kurdi, P. and Hansawasdi, C. (2015). Assessment of the prebiotic potential of oligosaccharide mixtures from rice bran and cassava pulp. *LWT – Food Science and Technology*. 63(2), 1288-1293.

La Fata, G., Weber, P., Mohajeri, M.H. (2018). Probiotics and the gut immune system: indirect regulation. *Probiotics and Antimicrobial Proteins*.10, 11-21.

Laemmli, U.K. (1970). Cleavage of structural proteins during the assembly of the head of bacteriophage T4. *Nature*. 227 (5259), 680-685.

Laemmlmli, U.K. (1970). Cleavage of structural proteins during the assembly of the head of bacteriophage T4. *Nature*. 227 (5259), 680-685.

Lee, K.-Y., So, J.-S., and Heo, T.-R.(2001). Thin layer chromatographic determination of organic acids for rapid determination of bifidobacterial at genus level. *Journal of Microbiological Methods*. 45(1), 1-6.

Lefevre, M., Racedo, S.M., Denayrolles, M., Ripert, G., Desfougerés, T., Lobach, A.R., Simon, R., Pélerin, F., Jüsten, P., and Urdaci, M.C. (2017). Safety assessment of Bacillus subtilis CU1 for use as probiotic in humans. *Regulatory Toxicology and Pharmacology*. 83, 54-65.

Li, Y.-X, Liu, H.-J., Shi, Y.-Q., You, X., and Jiang, Z.-Q. (2020). Preparation, characterization, and prebiotic activity of manno-oligosaccharides produced from cassia gum by a glycoside hydrolase family 134 β-mannanase. *Food Chemistry*. 309, 125709.

Liu, F., Chang, W., Chen, M., Xu, F., Ma, J., and Zhong, F. (2020). Film-forming properties of guar gum, tara gum and locust bean gum. *Food Hydrocolloids*. 98, 105007.

Liu, Y. and Huang, G. (2018). The derivatization and antioxidant activities of yeast mannan. *International Journal of Biological Macromolecules*. 107(A), 755-761.

Longo, M.A. and Combes, D. (1999). Thermostability of modified enzymes: a detailed study. *Journal of Chemical Technology and Biotechnology*. 74, 25-32.

Mafa, M.S., Malgas, S., Battacharya, A., Rashamuse, K., and Pletschke, B.I. (2020). The effects of alkaline pretreatment on agricultural biomasses (corn cob and sweet sorghum bagasse) and their hydrolysis by a termite-derived enzyme cocktail. *Agronomy*. 10, 1211.

Magengelele, M., Hlalukana, N., Malgas, S., Rose, S., Van Zyl, W.E., and Pletschke, B. (2021). Production and in vitro evaluation of prebiotic mannooligosaccharides prepared with a recombinant *Aspergillus niger* endo-mannanase, Man26A. *Enzyme and Microbial Technology*. 150, 109893.

Majeed, M., Majeed, S., Nagabhushanam, K., Arumugam, S., Natarajan, S., Beede, K., and Ali, F. (2018). Galactomannan from *Trigonella foenum-graecum* L. seed: Prebiotic application and its fermentation by the probiotic *Bacillus coagulans* strain MTCC 5856. *Food Science and Nutrition*. 1-8.

Malgas, S. and Pletschke, B.I. (2020). Combination of CTec2 and GH5 or GH26 endo-mannanases for effective lignocellulosic biomass degradation. *Catalysis*. 10(1193)

Malgas, S., van Dyk, J.S., and Pletschke, B.I. (2015a). β -mannanase (Man26A) and α-galactosidase (Aga27A) synergism – A key factor for the hydrolysis of galactomannan substrates. *Enzyme and Microbial Technology*. 70, 1-8.

Malgas, S., van Dyk, J.S., and Pletschke, B.I. (2015b). A review of the enzymatic hydrolysis and synergistic interactions between β-mannanase, β-mannosidase and α-galactosidase. *World Journal of Microbiology and Biotechnology*. 31, 1167-1175.

Mandelli, F., de Morais, M.A.B., de Lima, E.A., Olivera, L., Persinoti, G.F., and Murakami, M.T. (2020). Spatially remote motifs cooperatively affect substrate preference of a ruminal GH26-type endo-β-1,4-mannanase. *Journal of Biological Chemistry*. 295(15), 5012-5021.

Mankar, A.R., Pandey, A., Modak, A., and Pant, K.K. (2021). Pretreatment of lignocellulosic biomass: A review on recent advances. *Bioresource Technology*. 334, 125235.

Manning, T.S. and Gibson, G.R. (2004). Prebiotics. *Best Practice & Research Clinical Gastroenterology*. 18(2), 287-298.

Mano, M.C.R., Neri-Numa, I.A., da Silva, J.B., Paulino, B.N., Pessoa, M.G., and Pastore, G.M. (2018). Oligosaccharide biotechnology: an approach of prebiotic revolution on the industry. *Applied Microbiology and Biotechnology*. 102(1), 17-37.

Márquez-Montesino, F., Trejo, F., Rutiaga-Quiñones, J.G., and Correa-Méndez, F. (2021). Kinetic study of heating pinewood sawdust with different methods using thermogravimetric analysis. Reaction Kinetics, *Mechanisms and Catalysis*. 132, 1057-1074.

Mary, P.R., Prashanth, K.V.H., Vasu, P., and Kapoor, M. (2019). Structural diversity and prebiotic potential of chain β-manno-oligosaccharides generated from guar gum by endo-β-mannanase (ManB-1601). *Carbohydrate Research*. 486,

Masuda, Y., Kugimiya, S.-I., and Kato, K. (2014). Improvement of thermal-stability of enzyme immobilized onto mesoporous zirconia. *Journal of Asian Ceramic Societies*. 2(1), 11-19.

Matusek, A., Merész, P., Le, T.K.D., and Örsi, F. (2009). Effect of temperature and pH on the degradation of fructo-oligosaccharides. *European Food Research and Technology*. 288, 355-365.

Mechelke, M., Herlet, J., Benz, J.P., Schwarz, W.H., Zverlov, V.V., Liebl, W., and Kornberger, P. (2017). HPAEC-PAD for oligosaccharide analysis—novel insights into analyte sensitivity and response stability. *Analytical and Bioanalytical Chemistry.* 409, 7169–7181.

Miller, G.L. (1959). Use of dinitrosalicylic acid reagent for determination of reducing sugar. *Analytical Chemistry*. 31(3), 426-428.

Minjares-Fuentes, R., Femenia, A., Comas-Serra, F., Rodríguez-González, V.M. (20172018). Compositional and structural features of the main bioactive polysaccharides present in the *Aloe vera* plant. *Journal of AOAC International*. 101(6), 1711-1719.

Mitra, P. P. and Loqué, D. (2014). Histochemical staining of *Arabidopsis thaliana* secondary cell wall elements. *Journal of Visualized Experiments*. 87(51381), online.

Mogna, L., Deidda, F., Nicola, S., Amoruso, A., Del Piano, M., and Mogna, G. (2016). In vitro inhibition of *Klebsiella pneumoniae* by *Lactobacillus delbrueckii* Subsp. *delbrueckii* LDD01 (DSM 22106): An innovative strategy to possibly counteract such infections in humans? *Journal of Clinical Gastroenterology*. 50, S136-S139.

Monteagudo-Mera, A., Rastall, R.A., Gibson, R.A., Charalampopoulos, D., D., and Chatzifragkou, A. (2019). Adhesion mechanisms mediated by probiotics and prebiotics and their potential on human health. *Applied Microbiology and Biotechnology*. 103, 6463-6472.

Monteiro, A., Miguez, I.S., Silva, J.P.R.B., and da Silva A.S.-A. (2019). High concentration and yield of mannose from acai (*Euterpe oleracea* Mart.) seeds via mannanase catalyzed hydrolysis. *Scientific Reports*. 9, 10939.

Moodley, P., Sewsynker-Sukai, Y., and Kana E.B.G. (2020). Progress in the development of alkali and metal salt catalysed lignocellulosic pretreatment regimes: Potential for bioethanol production. *Bioresource Technology*. 310, 123372.

Moran, V.C., Hoffmann, J.H., Donnelly, D., van Wilgen, B.W., and Zimmermann, H.G. (2000). Biological control of alien, invasive pine trees (Pinus species) in South Africa. Proceedings of the X International Symposium on Biological Control of Weeds. Pp, 941-953.

Moreira, L.R.S. and Filho, E.X.F. (2008). An overview of mannan structure and mannan-degrading enzyme systems. *Applied Microbiology and Biochemistry*. 79, 165-178.

Moreno, F.J., Corzo, N., Montilla, A., Villamiel, M., and Molano, A. (2017). Current state and latest advances in the concept, production and functionality of prebiotic oligosaccharides. *Current Opinion in Food Science*. 13, 50-55.

Morrison, D. (2013). Lignocellulosic waste degradation using enzyme synergy with commercially available enzymes and *Clostridium cellulovorans* XylanaseA and MannanaseA. MSc Thesis. Rhodes University, South Africa.

Mukosha, L., Onyango, M.S., Ochieng, A., and Kasaini, H. (2013). Development of better quality low-cost activated carbon from South African pine tree (*Pinus patula*) sawdust: characterization and comparative phenol adsorption. *International Journal of Chemical and Molecular Engineering*. 7(7), 546-556.

Mukosha, L., Onyango, M.S., Ochieng, A., and Kasaini, H. (2013). Development of better quality low-cost activated carbon from South African pine tree (*Pinus patula*) sawdust: characterisation and comparative phenol adsorption. *International Journal of chemical and Molecular Engineering*. 7(7), 546-556.

Mutaguchi, Y., Ohmori, T., Wakamatsu, T., Doi, K., and Ohshima, T. (2013). Identification, purification, and characterization of a novel amino acid racemase, isoleucine 2-epimerase, from *Lactobacillus* species. *Journal of Bacteriology*.195(22):5207-2515.

Nair, M.S., Amalaradjou, M.A., and Venkitanarayanan, K. (2017). Chapter one - antivirulence properties of probiotics in combating microbial pathogenesis. *Advances in Applied Microbiology*. 98, 1-29.

Nan, Y., Jia, L., Yang, M., Xin, D., Qin, Y., and Zhang, J. (2018). Simplified sodium chlorite pretreatment for carbohydrates retention and efficient enzymatic saccharification of silvergrass. *Bioresource Technology*. 261, 223-231.

Nguyen, Q.A., Cho, E.J., Lee, D.-S., and Bae, H.-J. (2019). Development of an advanced integrative process to create valuable biosugars including manno-oligosaccharides and mannose from spent coffee grounds. *Bioresource Technology*. 272. 209-216.

Olver, B., Van Dyk, J.S., Beukes, N., and Pletschke, B.I. (2011). Synergy between EngE, XynA, and ManA from *Clostridium cellulovorans* on corn stalk, grass and pineapple pulp substrates. *3 Biotech*.

Omwago, E.O., Njagi, E.N.M., Orinda, G.O., and Wanjau, R.N. (2013). Nutrient enrichment of pineapple waste using *Aspergillus niger* and *Trichoderma viride* by solid state fermentation. *African Journal of Biotechnology*. 12(43), 6193-6196.

Omwango, E.O., Njagi, E.N.M., Orindam G.O., and Wanjau, R.N. (2013). Nutrient enrichment of pineapple waste uing *Aspergillus niger* and *Trichoderma viride* by solid state fermentation. *African Journal of Biotechnology*. 12(43), 6193-6196.

Østby, H., Hansen, L.D., Horn, S.J., Eijsink, V.G.H., and Várnal, A. (2020). Enzymatic processing of lignocellulosic biomass: principles, recent advances and perspectives. *Journal of Industrial Microbiology and Biotechnology*. 47, 623-657.

Otieno, D.O. and Ahring, B.K. (2012). The potential for oligosaccharide production from the hemicellulose fraction of biomass through pretreatment processes: xylooligosaccharides

(XOS), arabinooligosaccahrides (AOS), and mannooligosaccharides (MOS). *Carbohydrate Research*. 360, 84-92.

Pan, M., Kumaree, K.K., and Shah, N.P. (2017). Physiological changes of surface membrane in *Lactobacillus* with prebiotics. *Journal of Food Science*. 82(3), 744-750.

Pangsri, P., Piwpankaew, Y., Ingkakul, A., Nitisinsprasert, S., and Keawsompong, S. (2015). Characterization of mannanase from Bacillus circulans NT 6.7 and its application in mannooligosaccharide preparation as prebiotic. *Springer Plus*. 4(771), 1-11. DOI: 10.1186/s40064-015-1565-7

Park, J., Shin, H., Yoo, S., Zoppe, J.O., and Park, S. (2015). Delignification of lignocellulosic biomass and its effect on subsequent enzymatic hydrolysis. *BioResources*. 10(2), 2732-2743.

Patel, S. and Goyal, A. (2012). The current trends and future perspectives of prebiotics research: a review. *3 Biotech*. 2, 115-125.

Pérez-Burillo, S., Pastoriza, S., Fernández-Arteaga, A., Luzón, G., Jiménez-Hernández, N., D'Auria, G., Francino, P., and Rufián,-Henares, J.Á. (2019). Spent coffee grounds extract, rich in mannooligosaccharides, promotes a healthier gut microbial community in a dose-dependent manner. *American Chemical Society*. 67(9), 2500-2509.

Pérezo-Burillo, S., Pastoriza, S., Fernández-Arteaga, A., Luzón, G., Jiménez-Hernández, N., D'Auria, G., Francino, M.P., and Rufián-Henares, J.Á. (2019). Spent coffee grounds extract, rich in mannooligosaccharides, promotes a healthier gut microbial community in a dose-dependent manner. *Journal of Agricultural and Food Chemistry*. 67(9), 2500–2509.

Piatek, J., Krauss, H., Ciechelska-Rybarczyk, A., Bernatek, M., Wojtyla-Buciora, P., and Sommermeyer, H. (2020). In-vitro growth inhibition of bacterial pathogens by probiotics and a synbiotic: product composition matters. *International Journal of Environmental Research and Public Health*. 17, 3332.

Polari, L., Ojansivu, P., Makela, S., Eckerman, C., Holmbom, B., and Salminen, S. (2012). Galactoglucomannan extracted from Spruce (*Picea abies*)as a carbohydrate source for probiotic bacteria. *Journal of Agricultural and Food Chemistry*. 60(44), 11037-11043.

Pongsapipatana, N., Damrongteerapap, P., Chantorn, S., Sintuprapa, W., Keawsompong, S., and Nitisinprasert, S. (2016). Molecular cloning of *kman* coding for mannanase from *Klebsiella oxytoca* KUB-CW2-3 and its hybrid mannanase characters. *Enzyme and Microbial Technology*. 89, 39–51.

Prajapati, V.D., Jani, G.K., Moradiya, N.G., Randeira, N.P., Nagar, B.J., Naikwadi, N.N., Variya, B.C. (2013). Galactomannan: a versatile biodegradable seed polysaccharide. *International Journal of Biological Macromolecules*. 60, 83–92.

Qiang, X., YonLie, C., and QianBing, W. (2009). Health benefit application of functional oligosaccharides. *Carbohydrate Polymers*. 77(3), 435–441.

Rahmani, N., Kashiwagi, N., Lee, J., Niimi-Nakamura, S., Matsumotom H., Kahar, P., Lisdiyanti, P., Yopi, Prasetya, B., Ogino, C., and Kondo, A. (2017). Mannan endo-1,4-β-mannosidase from Kitasatospora sp. Isolated in Indonesia and its potential production of mannooligosaccharides from mannan polymers. *AMB Express*. 7(100).

Raina, N., Slathia, P.S., Sharma, P. (2020). Experimental optimization of thermochemical pretreatment of sal (*Shorea robusta*) sawdust for bioethanol production by co-fermentation

using *Saccharomyces cerevisiae* (MTCC-36) and *Pichia stipites stipitis* (NCIM-3498). *Biomass and Bioenergy*. 143, 105819.

Rajani, J., Dastar, B., Samadi, F., Karimi, M.A., Abdulkhani, A., and Esfandyarpour, S. (2016). Effect of extracted galactoglucomannan oligosaccharides from pine wood (*Pinus brutia*) on *Salmonella typhimurium* colonisation, growth performance and intestinal morphology in broiler chicks. *British Poultry Science*. 57(5), 682–692.

Rezania, S., Oryani, B., Cho, J., Talaiekhozani, A., Sabbagh, F., Hashemi, B., Rupani, P.F., and Mohammadi, A.A. (2020). Different pretreatment technologies of lignocellulosic biomass for bioethanol production: An overview. *Energy*. 199, 117457.

Rungruangsaphakun, J., and Keawsompong, S. (2018). Optomization Optimization of hydrolysis conditions for the mannooligosaccharides copra meal hydrolysate production. 3 Biotech. 8(3), 169.

Rurangwa, E., Laranja, J.L., Van Houdt, R., Delaedt, Y., Geraylou, Z., Van de Wiele, T., Van Loo., J., Van Craeyveld, V., Courtin, C.M., Delcour, J.A., and Ollevier, F. (2009). Selected nondigestible carbohydrates and prebiotics support the growth of probiotic fish bacteria mono-cultures *in vitro*. *Journal of Applied Microbiology*. 106, 932–940.

Rusanen, A., Lappalainen, K., Kärkkäinen, J., Tuuttila, T., Mikola, M., and Lassi, U. (2019). Selective hemicellulose hydrolysis of Scots pine sawdust. *Biomass Conversion and Biorefinery*. 9, 283–291.

Salas-Jara, M.J., Ilabaca, A., Vega, M., Garcia, A. (2016). Biofilm forming *Lactobacillus*: New challenges for the development of probiotics. *Microorganisms*.4(3), 1-14.

Salavati, S.S. and Allenspach, K. (2017). Effects of different oligosaccharides on the growth of selected probiotic bacterial strains. *Journal of Microbial & Biochemical Technology*. 9(2), 572–576.

Salze, G., McLean, E., Schwarz, M.H., and Craig, S.R. (2008). Dietary mannan oligosaccharide enhances salinity tolerance and gut development of larval cobia. *Aquaculture*. 274, 148–152.

Samanta, A.K., Jayapal, N., Jayaram, C., Roy, S., Kolte, A.P., Senani, S., Sridhar, M. (2015). Xylooligosaccharides as prebiotics form agricultural by-products: Production and applications. *Bioactive Carbohydrates and Dietary Fibre*. 5, 62–71.

Satari, B., Karimi, K., and Kumar, R. (2019). Cellulose solvent-based pretreatment for enhanced second-generation biofuel production: a review. *Sustainable Energy and Fuels*. 3(11), 11–62.

Sathitsuksanoh, N., Zhu, Z., and Zhang, Y.-H. (2012). Cellulose solvent-based pretreatment for corn stover and avicel: concentrated phosphoric acid versus ionic liquid [BMIM]Cl. *Cellulose*.

Seddik, H.A., Bendali, F., Gancel, F., Spano, G., and Drider, D. (2017). *Lactobacillus plantarum* and its probiotic and food potentials. *Probiotics and Antimicrobial Proteins*. 9, 111-122.

Selaledi, L.A., Hassan, Z.M., Manyelo, T.G., and Mabelebele., M. (2020). The current status of the alternative use to antibiotics in poultry production: an African perspective. *Antibiotics*. 9(594),

Selvam, K., Govarthanan, M., Kamala-Kannan, S., Govindharaju, M., Senthilkumar, B., Selvankumar, T., and Sengottaiyan, A. (2014). Process optimization of cellulase production from alkali-treated coffee pulp and pineapple waste using *Acinetobacter* sp. TSK-MASC. *RSC Advances*. 4, 13045.

Sewsynker-Sukai, Y., David, A.N., and Kana, E.B.G. (2020). Recent developments in the application of kraft pulping alkaline chemicals for lignocellulosic pretreatment: Potential beneficiation of green liquor dregs waste. *Bioresource Technology*. 306, 123225.

Sharma, K., Dhillon, A., and Goyal, A. (2018). Insights into Structure and Reaction Mechanism of β-Mannanases. *Current Protein & Peptide Science*. 19(1), 34–47.

Silveira, J.L.M. and Bresolin, T.M.B. (2011). Pharmaceutical use of galactomannans. *Química Nova*. 34(2), 292-299.

Sim, S.J., Yong, S.H., Park, D., Choi, E., Seol, Y., Song, H.J., Jeong, M.J., Kim, H.G., and Choi, M.S. (2020). Influence of inorganic salts on biomass production biochemical composition, and bioethanol production of *Populus alba*. *Biogeosciences and Forestry*. 13(6), 566–574.

Singh, S., Singh, G., Arya, S.K. (2018). Mannans: An overview of properties and application in food products. *International Journal of Biological Macromolecules*. 119, 79–85.

Siqueira, G., Várnai, A., Ferraz, A. Milagres, A. M. F. (2013). Enhancement of cellulose hydrolysis in sugarcane bagasse by selective removal of lignin with sodium chlorite. *Applied Energy*. 10, 399–402.

Siveira, J.L.M. and Bresolin, T.M.B. (2011). Pharmaceutical use of galactomannans. *Quim. Nova*. 34(2), 292–299.

Sluiter, J. B., Ruiz, R. O., Scarlata, C. J., Sluiter, A. D. and Templon, D. W. (2010). Compositional analysis of lignocellulosic feedstocks 1: review and description of methods. *Journal of Agricultural and Food Chemistry*. 58(16), 9043–9053.

Smith, B.G. and Harris, P.J. (1995). Polysaccharide composition of unlignified cell walls of pineapple [Ananas comosus (L.) Merr.] fruit. *Plant Physiology*. 107(4), 1399–1409.

Soltanian, S., Aghbashio, M., Almasi, F., Homa, Hosseinzadeh-Bandbafha, H., Nizami, A.-S., Ok, Y.S., Lam, S.S., and Tabatabaei, M. (2020). A critical review of the effects of pretreatment methods on the exergetic aspects of lignocellulosic biofuels. *Energy Conversion and Management*. 212, 112792.

Soltanian, S., Aghbashlo, M., Almasi, F., Hosseinzadeh-Bandbafha, H., Nizami, A.-S., Ok, Y.S., Lam, S.S., and Tabatabaei, M. (2020). A critical review of the effects of pretreatment methods on the exergetic aspects of lignocellulosic biofuels. *Energy Conversion and Management*. 212, 112792.

Soni, H., Rawat, H.K., Pletschke, B.I., Kango, N. (2016). Purification and characterization of β-mannanase from *Aspergillus terreus* and its applicability in depolymerization of mannans and saccharification of lignocellulosic biomass. *3 Biotech*. 6(136), 1–11.

Srivastava, P.K. and Kapoor, M. (2017). Production, properties, and applications of endo-β-mannanases. *Biotechnology Advances*. 35, 1–19.

Srivastava, P.K., Panwar, D., Prashanth, K.V.H., and Kapoor, M. (2017). Structural characterisation and *in vitro* fermentation of β-mannooligosaccharides produced from locust

bean gum by GH-26 endo-β-1,4-mannanase (ManB-1601). *Journal of Agricultural and Food Chemistry*. 65, 2827–2838.

Sun, Q., Foston, M., Meng, X., Sawada, D., Pingali, S.V., O'Neill, H.M., Li, H., Wyman, C.E., Langan, P., Ragauskas, A.J., and Kumar, R. (2014). Effect of lignin content on changes occurring in poplar cellulose ultrastructure during dilute acid pretreatment. *Biotechnology for Biofuels*. 7(150), 1–14.

Suryawanshi, R.K. and Kango, N. (2021). Production of mannooligosaccharides from various mannans and evaluation of their prebiotic potential. *Food Chemistry*. 334, 127428.

Tailford, D.L., Ducros, V.M.-A., Flint, J.E., Roberts, S.M., Morland, C., Zechel, D.L., Smith, N., Bjørnvad, M.E., Borchert, T.V., Wilson, K.S., Davies, G.J., and Gilbert, H.J. (2009). Understanding how diverse β-mannanases recognize heterogeneous substrates. *Biochemistry*. 48, 7009–7018.

Tao, S.,Khanizadeh, S., Zhang, H. and Zhang, S. (2009). Anatomy, ultrastructure and lignin distribution of stone cells in two *Pyrus* species. *Plant Science*. 176, 413-419.

Tian, T., Freeman, S., Corey, M., German, B., and Barile, D. (2017). Chemical characterization of potentially prebiotic oligosaccharides in brewed coffee and spent coffee grounds. *Journal of Agricultural and Food Chemistry*. 65, 2784–2792.

Timbaraj, S.R., Phillips, M., Koyyalamudi, S.R., and Reddy, N. (2018). Yellow lupin (*Lupinus luteus* L.) polysaccharides: Antioxidant, immunomodulatory and prebiotic activities and their structural characterisation. *Food Chemistry*. 267, 319–328.

Trunk, T., Khalil, H.S., and Leo, J.C. (2018). Bacterial autoaggregation. *AIMS Microbiology*. 4(1), 140–164.

Ugwu, S.N. and Enweremadu, C.C. (2020). Ranking of energy potentials of agro-industrial wastes: bioconversion and thermo-conversion approach. *Energy Reports*. 6, 2794–2802.

Utami, W., Meryandini, A., and Wiryawan, K.G. (2013). Characterization of bacterial mannanase for hydrolyzing palm kernel cake to produce manno-oligosaccharides prebiotics. *Journal of Animal Science and Technology*. 36(3), 192–196.

Van Dyk, J.S., Gama, R., Morrison, D., Swart, S., and Pletschke, B.I. (2013). Food processing waste: Problems, current management and prospects for utilisation of the lignocellulose component through enzyme synergistic degradation. *Renewable and Sustainable Energy Reviews*. 26, 521–531.

Van Meer, H., Boehm, G., Stellaard, F., Vriesema, A., Knol, J., Havinga, R., Sauer, P.J., and Verkade, H.J. (2007). Prebiotic oligosaccharides and the enterohepatic circulation of bile salts in rats. *Journal of Physiological and Gastrointestinal Liver Physiology*. 294, G540–G547.

Van Wilgen, B.W. (2015). Plantation forestry and invasive pines in the Cape Floristic Region: Towards conflict resolution. *South African Journal of Science*. 111(7/8), 1–2.

Van Zyl., W.H., Rose, S.H., Trollope, K., Görgensm J.F. (2010). Fungal β-mannanases: Mannan hydrolysis, heterologous production and biotechnological applications. *Process Biochemistry*. 45, 1203-1213.

Von Freiesleben, P., Moroz, O.V., Blagova, E., Wiemann, M., Spodsberg, N., Agger, J.W., Davies, G.J., Wilson, K.S., Stålbrand, H., Meyer, A.N., and Krogh, K.B.R.M. (2019). Crystal

structure and substrate interactions of an unusual fungal non-CBM carrying GH26 endo-β-mannanase from *Yunnania penicillata*. *Scientific Reports*. 9(2266), 1–14.

Von Freiesleben, P., Spodsberg, N., Blicher, T.H., Anderson, L., Jørgensen, H., Stålbrand, H., Meyer, A.S., and Krogh, K.B.R.M. (2016). An *Aspergillus nidulans* GH26 endo-β-mannanase with a novel degradation pattern on highly substituted galactomannans. *Enzyme and Microbial Technology*. 83, 68–77.

Von Freiesleben, P., Spodsberg, N., Stenbæk, A., Stålbrand, H., Krogh, K.B.R., and Meyer, A.S. (2018). Boosting of enzymatic softwood saccharification by fungal GH5 and GH26 endomannanases. *Biotechnology for Biofuels*. 11(194), 1–14.

Wang, C., Zhang, J., Wang, Y., Niu, C., Ma, R., Wang, Y., Bai, Y., Luo, H., and Yao, B. (2016). Biochemical characterization of an acidophilic β-mannanase from Gloeophyllum trabeum CB900.73 with significant transglycosylation activity and feed digesting ability. *Food Chemistry*. 197, 474–481.

Wang, L., Tang, D.-Q., Kuang Y., Lin, F.-J., Su, Y. (2015). Structural characteristics of pineapple pulp polysaccharides and their antitumor cell proliferation activities. *Journal of the Science of Food and agriculture*. 95(12), 2554–2561.

Wang, N.N., Liu, J., Li, Y.X., Ma, J.W., Yan, Q.J., and Jiang Z.Q. (2021). High-level expression of a glycoside hydrolase family 26 β-mannanase from *Aspergillus niger* in *Pichia pastoris* for production of partially hydrolysed fenugreek gum. *Process Biochemistry*. 100, 90–97.

Wi, S.G., Cho, E.J., Lee, D.-S., Lee, Y.J., and Bae, H.-J. (2015). Lignocellulose conversion for biofuel: a new pretreatment greatly improves downstream biocatalytic hydrolysis of various lignocellulosic materials. *Biotechnology for Biofuels*. 8(228), 1–11.

Wongsiridetchai, C., Jonjaroen, V., Sawangwan, T., Charoenrat, T., and Chantorna, S. (2021). Evaluation of prebiotic mannooligosaccharides obtained from spent coffee grounds for nutraceutical application. *LWT – Food Science and Technology*. 148, 111717.

Yamabhai, M., Sak-Ubol, S., Srila, W., and Haltrich, D. (2014). Mannan biotechnology: from biofuels to health. *Critical Reviews in Biotechnology*. 36, 30–42.

Yang, X., Berthold, F., Berglund, L.A. (2018). Preserving cellulose structure: delignified wood fibers for paper structures of high strength and transparency. *Biomacromolecules*. 19, 3020–3029.

Yerlikaya, O., Akpinar, A., Saygili, D. (2020). Analysis of some physicochemical, rheological, sensorial, properties, and probiotic viability of fermented milks containing Enterococcus faecium and Enterococcus durans strains. *Journal of Food Processing and Preservation.* 44(8), 14553.

You, S., Tu, T., Zhang, L., Wang, Y., Huang, H., Ma, R., Shi, P., Bai, Y., Su, X., Lin, Z., Luo, H., and Yao, B. (2016). Improvement of the thermostability and catalytic efficiency of a highly active b-glucanase from Talaromyces leycettanus JCM12802 by optimizing residual

Zhang, R., Li, X-Y., Cen, X-L., Gao, Q-H., Zhang, M., Li, K-Y., Wu, Q., Mu, Y-L., Tang, X-H., Zhou, J-P., and Huang, Z-X. (2021). Enzymatic preparation of manno-oligasaccharides oligosaccharides from locust bean gum and palm kernel cake, and investigations into its prebiotic activity. *Electronic Journal of Biotechnology*. 49, 64–71.

Zhang, W., Alvarez-Gaitan, J.P., Dastyar, W., Saint, C.P., Zhao, M., and Short, M.D. (2018). Value-added products produced from waste activated sludge: A biorefinery perspective. *Water*. 10(5), 545.

Zhang, Y.H., Cui, J., Lymd, L.R., and Kuang, L.R., (2006). A transition from cellulose swelling to cellulose dissolution by o-phosphoric acid: evidence from enzymatic hydrolysis and supramolecular structure. *Biomacromolecules*. 7(2), 644–648.

Zhang, Y.H., Ding, S.-Y., Mielenz, J.R., Cui, J.-B., Elander, R.T., Laser, M., Himmel, M.E., McMillan, J.R., and Lynd, L.R. (2007). Fractionating recalcitrant lignocellulose at modest reaction conditions. *Biotechnology and Bioengineering*. 97(2), 214–223.

Zhao, W., Zheng, J., Zhou, and H.B. (2011). A thermotolerant and cold-active mannan endo-1,4-β-mannosidase from Aspergillus niger CBS 513.88: constitutive overexpression and high-density fermentation in *Pichia pastoris*. *Bioresource Technology*. 102, 7538–7548.

Zheng, J., Li, H., Zhang, X., Jiang, M., Luo, C., Lu, Z., Xu, Z., and Shi, J. (2018). Prebiotic mannan-oligosaccharides augment the hypoglycemic effects of metformin in correlation with modulating gut microbiota. *Journal of Agricultural and Food Chemistry*. 66(23), 5821-5831.

Zhou, M., Yang, L., Yang, S., Zhao, F., Xu, L., and Yong, Q. (2018). Isolation, characterization and in vitro anticancer activity of an aqueous galactomannan from the seed of *Sesbania cannabina*. *International Journal of Biological Macromolecules*. 113, 1241–1247.

Zhu, G., Xing, X., Wang, J., and Zhang, X. (2017). Effect of acid and hydrothermal treatments on the dye adsorption properties of biomass-derived activated carbon. *Journal of Materials Science*. 52, 7664-7676.

Zhu, Z., Sathitsuksanoh, N., Vinzant, T., Schell, D.J., McMillan, J.D., and Zhang, Y.-H.P. (2009). Comparative study and corn stover pretreated by dilute acid and cellulose solvent-based lignocellulose fractionation: enzymatic hydrolysis, supramolecular structure, and substrate accessibility. *Biotechnology and Bioengineering*. 103(4), 715–724.

Zoghlami, A. and Paës, G. (2019). Lignocellulosic biomass: understanding recalcitrance and predicting hydrolysis. *Frontiers in Chemistry*. 7(874), 1–11.

Appendices

Appendix A: List of chemicals

1-Naphthol	Sigma-Aldrich (Cat. No. N1000)
2-mercaptoethanol	Fluka (Cat. No. 63700)
3,5-Dinitrosalicylic acid	Sigma (Cat No. D0550)
ABTS	Sigma (Cat. No. A1888-1G)
Acetic acid	Sigma (Cat. No. A6283)
Acetone	Merck (Cat. No. 100014)
Acrylamide	Sigma (Cat. No. A8887)
Ammonium persulfate	Sigma Aldrich (Cat. No. A3678)
Bovine serum albumin (BSA)	Sigma (Cat. No. A7906)
Bradford reagent	Sigma (Cat. No. B6916)
Bromophenol blue	Sigma (Cat. No. B8026)
Butanol	Merk (Cat. No. 1.01990)
Citric acid	Merck (Cat. No. 1.00244)
Coomassie Brilliant Blue R250	Merck (Cat. No. 1.12553)
D-Glucose	Saarchem (Cat. No. 2676020)
Di-galactosyl-mannopentaose	Megazyme (Cat. No. O-GGM5)
D-Mannose	Sigma (Cat. No. M2069)
D-Mannose, D-Fructose & D-Glucose kit	Megazyme (Cat. No. K-MANGL)
D-Mannose, D-Fructose & D-Glucose kit	Megazyme (Cat. No. K-MANGL)
D-Xylose kit	Megazyme (Cat. No. K-XYLOSE)
Ethanol	Merck (Cat. No. 8.18700)
Galactosyl-mannotriose	Megazyme (Cat. No. O-GM3)

Glacial acetic acid	Merck (Cat. No. 1.00063)
Glycerol	Merck (Cat. No. 104057)
GOPOD kit	Megazyme (Cat. No. K-GLUC)
Guar galactomannan, medium viscosity	Megazyme (Cat. No. P-GGMMV)
Hydrochloric acid	Merck (Cat. No. 1.00319)
Imidazole	Merck (Cat. No. 1.04716)
Ivory nut mannan	Megazyme (Cat. No. P-MANIV)
L-Arabinose/D-Galactose Kit	Megazyme (Cat. No. K-ARGA)
Locust bean gum	Fluka (Cat. No. 62631)
Methanol	Merck (Cat. No. 8.22283)
N, N-methylenebisacrylamide	Sigma (Cat. No.M7279)
Nutrient Broth	Biolab, Merck (C24)
Phenol	Sigma (Cat. No. P3653)
Phosphoric acid	Merck (Cat. No. 100573)
Sodium azide	Merck (Cat. No. 8.22335)
Sodium carbonate	Merck (Cat. No. 1.06392.0500)
Sodium chloride	Saarchem (Cat. No. 5822320)
Sodium chlorite	Sigma (Cat. No. 244155)
Sodium dodecyl sulphate (SDS)	BDH biochemicals (Cat. No. 301754)
Sodium hydroxide	Saarchem (Cat. No. 5823200)
Sodium metabisulfite	Sigma-Aldrich (Cat. No.255556)
Sodium Potassium tartrate	Merck (Cat. No. 1.08087)
Sulfuric acid	Merck-Millipore (Cat. No. 1.01833)
Tris (hydroxymethyl) aminomethane	Merck (Cat. No. 1.08382)

Tryptone	Fluka (Cat. No. 70169)
Yeast extract	Biolab (Cat. No. BX6)

Appendix B: Standard curves for activity and protein determination

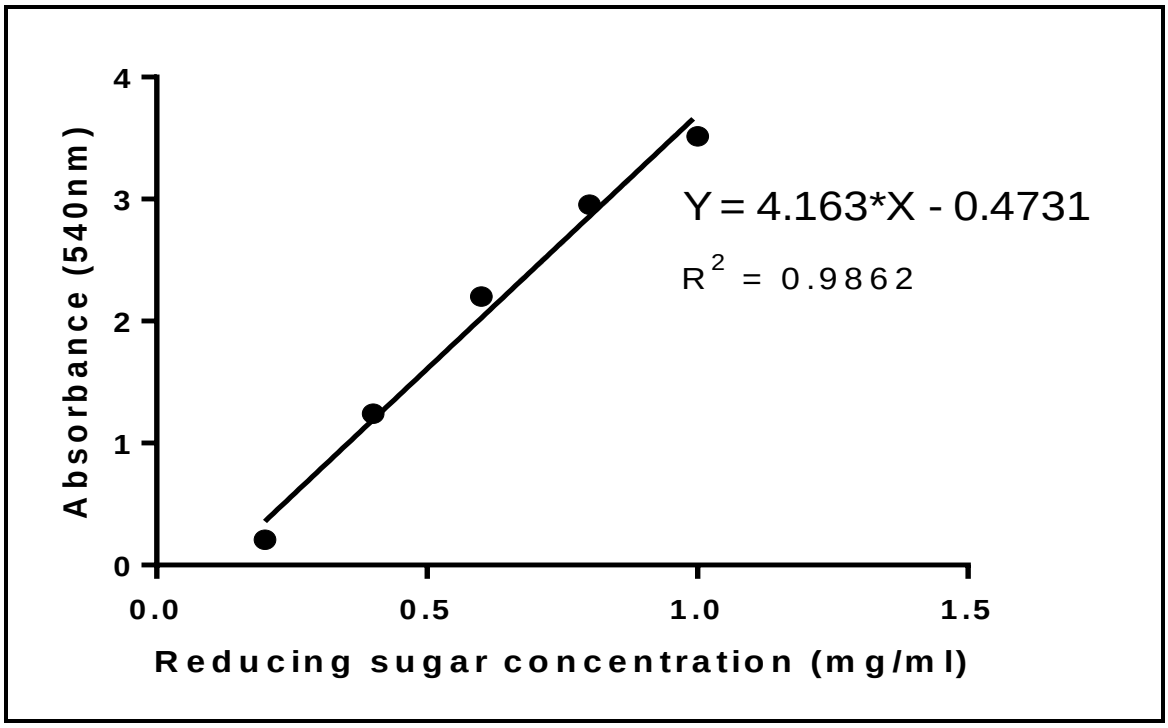

Figure B.1: DNS standard curve for determining reducing sugar concentration.

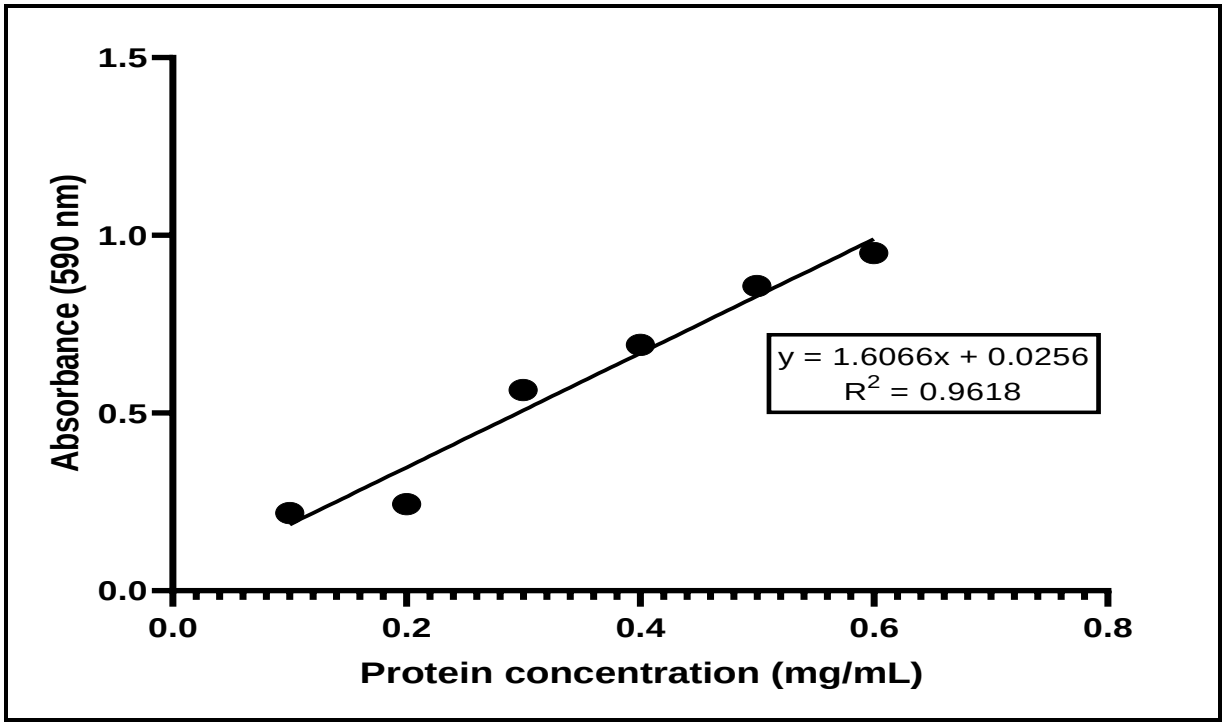

Figure B.2: Bradford's standard curve for the determination of protein concentration.

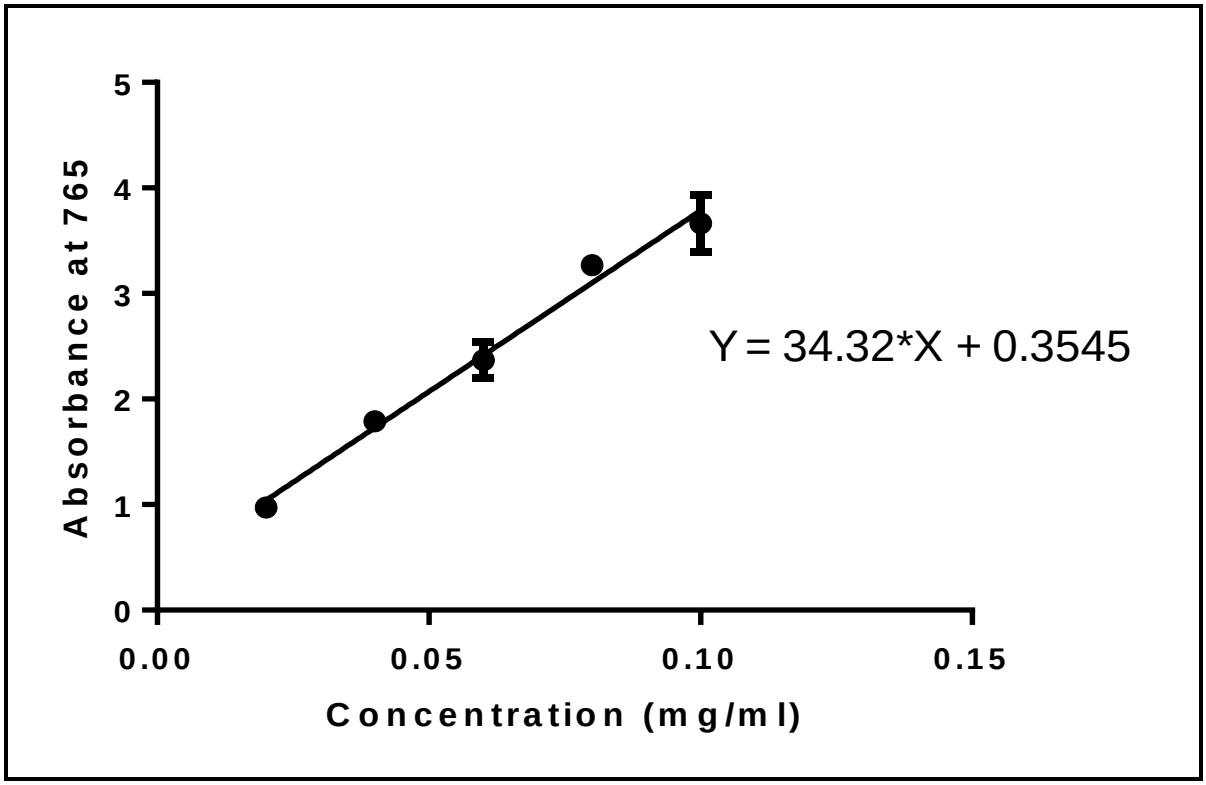

Figure B.3: Gallic acid standard curve using the Folin-Ciocalteu method. Values are represented as means ± SD, n=4.

Appendix C: Detection of SCFAs in growth media

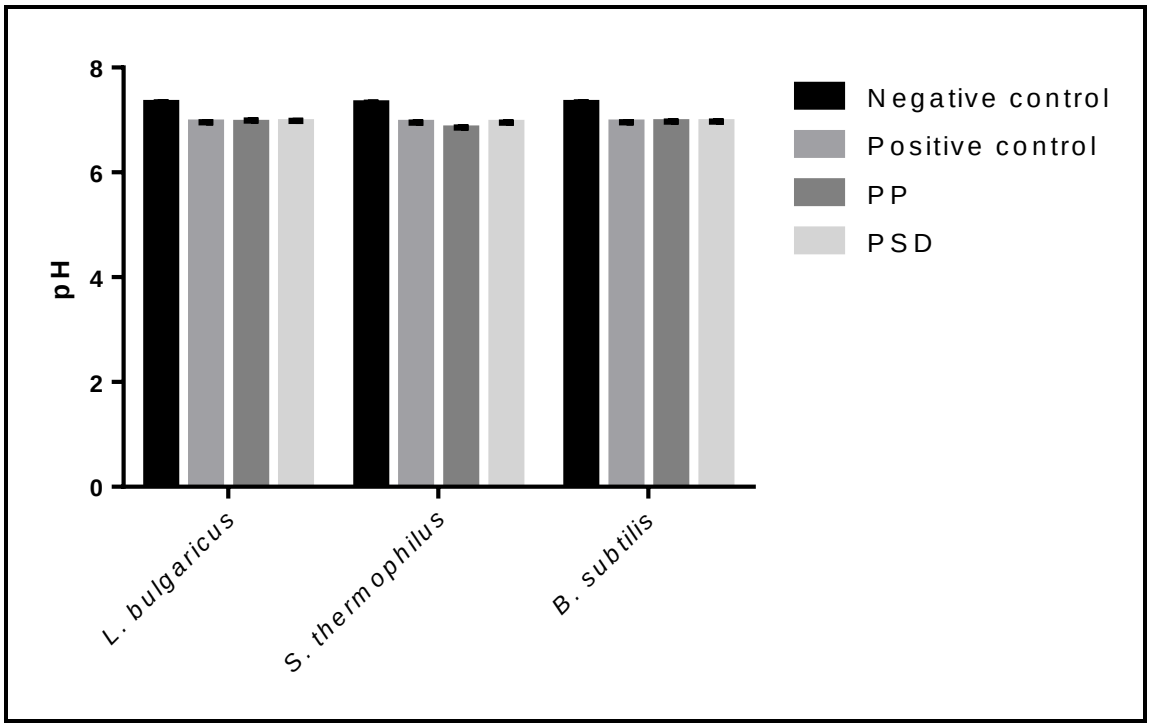

Figure C.1: Determination of pH change in growth media containing Del + PAS PP and PSD derived MOS.